METABOLISM OF ANTIRETROVIRAL DRUGS USED IN HIV PRE-EXPOSURE PROPHYLAXIS

By Elaine To

A thesis submitted to Johns Hopkins University in conformity with the requirements for the degree of Doctor of Philosophy

Baltimore, MD

June 2014

Abstract

HIV pre-exposure prophylaxis is the use of antiretroviral drugs, including dapivirine and tenofovir, in uninfected individuals to prevent the establishment of infection. Dapivirine is being developed as a topical microbicide for application to the vaginal and colorectal mucosa, and tenofovir is in clinical use as an oral formulation with a topical gel formulation for the vaginal and colorectal mucosa undergoing further clinical trials. The metabolism of dapivirine is unknown, and understanding the metabolism of tenofovir is particularly important because it is a prodrug that must be phosphorylated intracellularly to yield the active metabolite, tenofovir diphosphate. Dapivirine and tenofovir diphosphate must be present in the colorectal and vaginal mucosa for HIV prevention; tenofovir diphosphate must also be produced in white blood cells for oral HIV treatment and prevention and in hepatocytes for hepatitis B treatment. A comprehensive understanding of the metabolism that impacts drug exposure in these tissues is imperative for optimal drug use.

The metabolism of dapivirine is not yet known, nor has a full understanding of drug metabolism in the mucosal tissues been defined. The enzymes proposed to be involved in dapivirine metabolism are the cytochromes P450 (CYPs) and UDP-glucuronosyltransferases (UGTs). Immunoblotting revealed that CYP2B6, -2C19, -3A4, and -3A5were more highly expressed in vaginal tissues as compared to colorectal tissues. A liquid chromatography mass spectrometry assay was developed to identify and characterize 11 novel metabolites of dapivirine which were produced by the CYPs, UGTs, or both. In vitro metabolism assays were used to identify members of the CYP3A family as the primary enzymes responsible for dapivirine metabolism. The dapivirine

mass spectrometry assay was then used, leveraging dapivirine as a small molecule probe, to demonstrate CYP activity in both colorectal and vaginal tissues, but UGT activity only in colorectal.

While creatine kinase, adenylate kinase, and pyruvate kinase have been implicated in tenofovir's activation, these studies were carried out *in vitro* and do not investigate whether these enzymes are expressed in the tissues of clinical relevance. Immunoblots revealed that the four creatine kinases and adenylate kinase 2 are more highly expressed in colorectal tissue compared to vaginal tissue and white blood cells, whereas the two pyruvate kinases displayed the opposite trend. Additionally, adenylate kinase 2, creatine kinase muscle, and both pyruvate kinases were expressed in primary human hepatocytes. An ion pairing liquid chromatography mass spectrometry assay was utilized to directly detect tenofovir phosphorylation. This assay was used to in combination with siRNA mediated knockdowns to show that AK2, PKM, and PKLR are responsible for activating tenofovir in white blood cells and vaginal tissues, whereas AK2 and CKM perform the same function in colorectal tissues.

Collectively, these findings represent a fundamental shift in the current understanding of drug metabolism in the body. Not only are colorectal tissues and vaginal tissues able to biotransform drugs, but they do it in a tissue specific manner. I anticipate that these results lay the groundwork for future studies in tissue specific drug metabolism that can be leveraged to optimize future drug development and use in the colorectal and vaginal mucosa.

Doctoral advisor:	Dr. Namandjé N. Bumpus
Thesis readers:	Dr. Namandjé N. Bumpus
	Dr. Craig W. Hendrix
Thesis committee:	Dr. Namandjé N. Bumpus
	Dr. Craig W. Hendrix
	Dr. Susan H. Eshleman
	Dr. Robert F. Siliciano
	Dr. Heng Zhu

Copyright Disclaimer

Acknowledgements

"It takes a village to raise a child." While perhaps a cliché, this quote applies to a doctoral thesis as well. The work detailed here is due in no small part to those who have supported me throughout these many years.

First and foremost I thank my doctoral advisor, Dr. Namandjé Bumpus. She was a highly supportive and encouraging mentor even while I was rotating in different labs, and she continued this guidance after I joined hers. It is because of her that I learned how to be rigorous, to analyze information beyond the surface level, and to tie together information from different sources. In my time here I have grown not only as a scientist, but also as an individual, and Namandjé's high standards and patience are the cause.

Secondly, I thank my thesis committee, especially Dr. Craig Hendrix, whose assistance with obtaining samples through the Drug Development Unit and editing my publications and thesis was invaluable. Dr. Robert Siliciano is another individual who supported me from my very first year beginning with my rotation in his laboratory. Dr. Susan Eshleman's and Dr. Heng Zhu's perspectives and advice on my research project were greatly appreciated.

The entire pharmacology department here at Johns Hopkins is cherished and played a significant role in my accomplishments. Thank you to Dr. Philip Cole, Dr. Jun Liu, and Dr. James Stivers for overseeing the graduate program and providing a firm foundation when things got tough. Thank you to Amy, Paula, Brenda, Mimi, and Robin for organizing the various aspects of the program and being available whenever I had a question, whether it was how to send a fax or when I locked myself out of little Abel.

Thank you to my fellow members of the Bumpus lab—Lindsay Avery, Liz Hersman, Julie Lade, Phil Cox, and Jenni Van Ausdall. Your day to day companionship and encouragement kept me well-balanced and ensured my success. Thank you to the other pharmacology students, especially those who matriculated with me: Kirsten Meyers, Polina Prusevich, Sarah Head, Anne Cieniewicz, Jessica Yang, Linde Miles, and Robert Hsiao. It has been wonderful getting to know everyone, and I look forward to hearing about your successes.

Thank you to my undergraduate research advisor, Dr. Paul Patterson. You and Ali Khoshnan were my introduction to the excitement of research in the biomedical sciences, thus inspiring my career path. Thank you for the opportunity to learn (and fumble) in your research program. In this vein I also thank Dr. Nathan Dalleska for his patience with my freshman antics and our relationship which has developed from employer/mentor to friend/mentor. Dr. Jared Leadbetter was an additional valuable source of perspective and support in both my academic and personal endeavors.

I thank my family for not disowning me for moving to the east coast. I jest, I know that would never be the case. Nevertheless, I am aware that it was a tough situation and I cannot show them enough gratitude for their love and support from afar. Thank you for your guidance, advice, and pride in me and my accomplishments. I loved that during every annual family vacation, it seemed that no time had passed since the last one. More hiking and camping adventures are yet to come!

Of my friends, Ali Ebrahim is the absolute best. Words are not enough to describe how much you mean to me. Our 7 year friendship has been fulfilling in the greatest ways

possible and while it has been put to the test in recent years, I am thrilled that it has survived. Let me take the time now to apologize for being stubborn and not always listening to your advice. Thank you for being straightforward with my shortcomings and unfailing in your crisis management. Always remember that you're awesome, and don't you dare forget it.

Michael Woods is another amazing individual. Thank you for listening to my rants and musings on a near daily basis, and providing the right perspective when I was too agitated to see it. The long conversations arguing about fantasy, sharing life stories, and doing math puzzles are among my most treasured memories. Frankly, it is amazing how close our friendship has grown, despite being primarily online.

From here on out, the rest of my friends that I am grateful for are too many to list. I treasure each and every one of you and look forward to sharing in your accomplishments as you have shared in my own. Here I list the categories of friends I cherish—it should be easy to find yourself! Thank you to my Caltech family, high school buddies, the Settlers junkies, the DC/PAX gaming crew, chemistry bros, BME Wolfpack, immunology friends, the Hopkins marathon team, Incentive Mentoring Program, and all others who may not fit in a category but are no less prized.

This is the village it took to raise my doctoral thesis. Without further ado, the following pages detail the results of our shared success.

Table of Contents

List of Tables

List of Figures

Chapter 1: Introduction

HIV Pre-exposure Prophylaxis

There are multiple routes for transmission of HIV-1, but the most prevalent is through vaginal or anal intercourse [1]. Through efforts including male circumcision and increased condom use, the amount of new human immunodeficiency virus (HIV) infections decreased from 3.4 million in 2001 to 2.3 million in 2013 [2]. The use of antiretroviral therapy in conjunction is predicted to further accelerate the decline of infection rates. It is already known that antiretroviral therapy in the infected individual reduces viral load and therefore chance of HIV-1 transmission [2]. Pre-exposure prophylaxis (PrEP) is a promising new prevention strategy that uses antiretrovirals to interrupt the viral life cycle before infection is established in newly exposed individuals [3]. Evidence supporting the potential efficacy of PrEP comes from postnatal transmission prophylaxis and macaque model studies [4, 5].

In July 2012, Truvada® became the first antiretroviral drug to be approved for use in HIV PrEP by the United States Food and Drug Administration [6]. Truvada® is a once daily oral coformulation of emtricitabine and a prodrug of tenofovir. Tenofovir and emtricitabine are also coformulated with the non-nucleoside reverse transcriptase inhibitor efavirenz into Atripla®, a highly effective once daily pill that is now prescribed to 80% of treatment naïve HIV patients in the United States [7]. Tenofovir and emtricitabine are nucleoside/nucleotide analog reverse transcriptase inhibitors (NRTIs) that require intracellular phosphorylation to yield their active metabolites: tenofovir diphosphate and emtricitabine triphosphate [8]. Advantages include the lack of mitochondrial toxicity that is typical of NRTI drugs, drug action early in the viral life

cycle, and long intracellular half lives of their active metabolites [9]. Tenofovir and emtricitabine are strongly synergistic, most likely because tenofovir is a purine analog while emtricitabine is a pyrimidine analog [10]. When given orally, tenofovir's poor oral bioavailability necessitates use of the prodrug tenofovir disoproxil fumarate [9]. Despite these advantages, however, the clinical trials examining tenofovir use for HIV PrEP have not been unequivocally successful.

Out of six completed PrEP clinical trials testing oral tenofovir alone or in conjunction with emtricitabine, four demonstrated a significant reduction in HIV transmission. Of the successful trials, iPrEx, TDF2, and Partners PrEP used once daily oral tenofovir/emtricitabine to demonstrate 44%, 62%, and 75% reduction in HIV infectivity, respectively [11-13]. Partners PrEP also and the Bangkok Tenofovir study tested oral tenofovir alone, and found it to yield 67% and 48.9% reduction in infectivity, respectively, nearly as effective as the tenofovir/emtricitabine combination [13, 14]. The unsuccessful trials were FEM-PrEP, using once daily oral tenofovir/emtricitabine dosing and two subsets of VOICE using once daily oral tenofovir or tenofovir/emtricitabine [15, 16]. Analysis of drug levels in plasma indicate that adherence was relatively low in the FEM-PrEP, VOICE, and iPrEx trials, but iPrEx showed 44% reduction in HIV infectivity among homosexual men whereas FEM-PrEP and VOICE could not demonstrate similar protection for heterosexual women [11, 15, 17]. This may be due to the fact that orally dosed tenofovir results in drug levels that are 100 fold higher in rectal than in vaginal tissue [18, 19], leading to greater forgiveness of nonadherence in iPrEx. Pharmacologic reasons for this differential distribution remain to be determined.

Many of the trials demonstrated a strong correlation between detectable drug levels in blood plasma and increased protection from HIV infection. However, in patients infected despite PrEP, systemic drug levels could select for drug resistant mutations. Topically applied microbicides have the potential to overcome this disadvantage of oral dosage since the systemic concentrations achieved are lower and put less selective pressure on resistant virus mutants. In addition, topical dosing yields higher concentrations of antiretroviral drugs in mucosal tissues [20]. This has recently been demonstrated for both vaginally and rectally applied tenofovir microbicides [21, 22]. Formulations using tenofovir or dapivirine have progressed farthest in microbicide development, with a completed phase III trial for tenofovir (CAPRISA 004) and an ongoing phase III trials for dapivirine [23]. In the CAPRISA 004 trial, 1% tenofovir gel was applied to the vagina 12 hours pre and post intercourse, resulting in 39% protection overall and up to 54% protection from HIV infection in the high adherence participants [24]. Additionally, the CAPRISA trial demonstrated no selection for viral strains with enhanced fitness, no impact on the number of viruses transmitted in seroconverted individuals, and protection from herpes simplex virus infection [25, 26]. The unanticipated protection from herpes simplex virus is likely due to the higher tenofovir levels in cerviovaginal tissue that result from topical dosing [27]. In contrast, the daily 1% tenofovir gel subset of VOICE was stopped early because there was no discernable protection, likely due to poor adherence [16]. Current phase III clinical trials following up on the success of CAPRISA 004 include CAPRISA 008, which aims to develop a model for tenofovir gel distribution through family planning and analyze gel safety, and FACTS 001, a larger scale repetition of CAPRISA 004 [28, 29].

As stated above, dapivirine is another antiretroviral drug that has made significant progress in HIV PrEP trials. Dapivirine is one of the diarylpyrimidine non-nucleoside reverse transcriptase inhibitors (NNRTI), which inhibit HIV reverse transcriptase through allosteric binding. First generation NNRTIs were known for their low genetic barriers to resistance [30, 31]. Diarylpyrimidine NNRTIs such as dapivirine are conformationally flexible, resulting in higher genetic barriers without compromising anti-HIV activity [32]. While the oral bioavailability of dapivirine is an ongoing debate [23], many conclude that dapivirine does not have good oral bioavailability [20], leading to its development as primarily a topical microbicide. Current trials using dapivirine include ASPIRE (MTN 020) and The Ring Study (IPM 027), both of which aim to test the safety and efficacy of a monthly dapivirine vaginal ring [33, 34]. Multiple phase I and II trials using dapivirine formulated in gels and a phase I trial of a vaginal ring (MTN 013/IPM 026) testing a coformulation of dapivirine with the entry inhibitor maraviroc have been completed [35]. MTN 013 showed that dapivirine penetrated the cervicovaginal tissues and was able to prevent HIV infection of vaginal biopsies obtained from study participants [36]. Maraviroc, on the other hand, had poor vaginal tissue penetration, which is an interesting contrast with a previous study showing effective vaginal tissue penetration from oral maraviroc administration [37].

Drug Metabolism

The majority of drugs are taken orally, due to the ease of administration thus leading to high patient compliance. Orally administered drugs must bypass several barriers before reaching the systemic circulation for delivery to their targeted tissues. Upon ingestion, a drug will proceed to the intestines where it can be absorbed into the

bloodstream through intestinal villi. While lipophilic compounds may readily diffuse across the intestinal epithelium, others may require the assistance of transport enzymes [38]. The uptake of drugs is referred to as phase 0 transport or absorption [39]. Some chemical modification, known as metabolism, may occur during this stage. Blood from the intestinal villi is carried through the hepatic portal vein to the liver, which is the primary organ for drug metabolism and detoxification. Enzymes within the liver's hepatocytes metabolize compounds present in the blood; this stage is known as phase I and phase II metabolism. Metabolites formed in the liver and their parent drugs may proceed to the heart through the hepatic vein or be returned to the gastrointestinal system via the enterohepatic circulation, where they will join intestinally formed metabolites and unabsorbed drug to be excreted via the rectum. Once within the heart chambers, drugs and metabolites are a part of the systemic circulation and can proceed to their targeted tissues to exert their biological effect or be excreted through the renal system. This final excretion step is known as phase III transport [39]. The overall consequence of drug metabolism is to increase the polarity of compounds to facilitate their excretion. Figure 1 provides a summary of these processes [40]. However, the metabolites of a drug may retain pharmacologic activity, lose pharmacologic activity, or gain novel pharmacologic activity or toxicity. Drug absorption, distribution, metabolism, and excretion together determine the disposition of a drug and its metabolites, which often obstructs the progress of or eliminates drugs under clinical development [41, 42].

Phase I metabolism is primarily mediated by the cytochromes P450 (P450s), which are discussed in far greater detail below. In general, phase I metabolism serves to introduce functional groups into drugs, which can be further modified. The metabolite

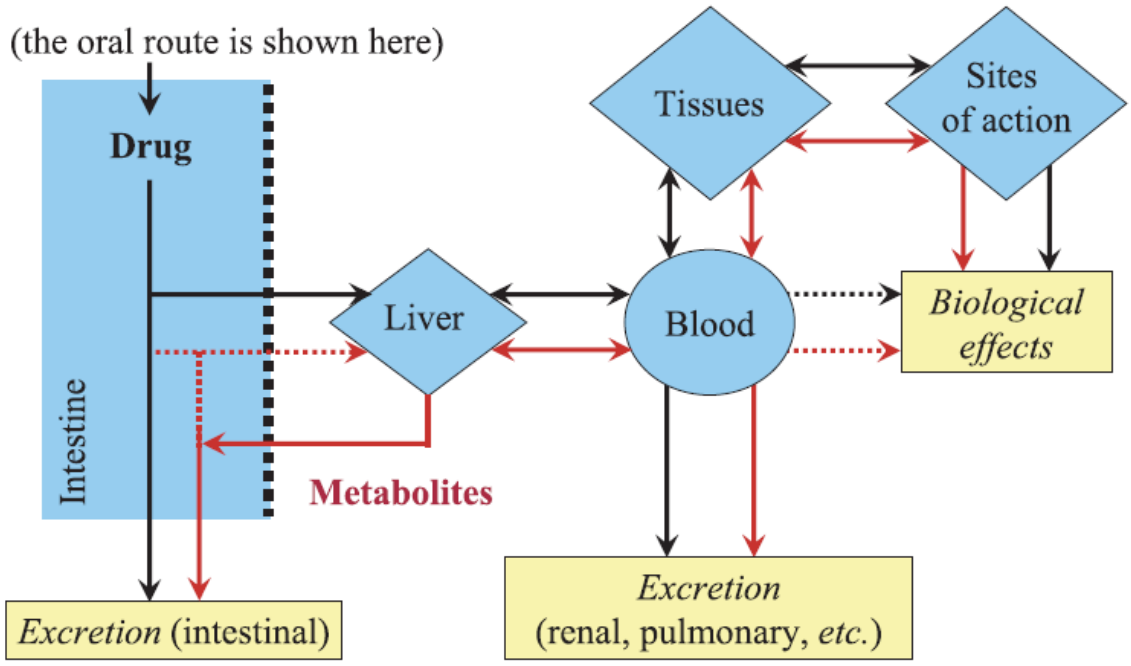

Figure 1. (Borrowed from [40]) **The fate of an orally administered drug in the human body**. Drugs must are absorbed across the intestinal membrane and arrive in the liver. The liver carries out the bulk of drug metabolism, and metabolites may return to the intestine or proceed with the parent drug into the systemic circulation. From the systemic circulation, parent drug and its metabolites may proceed to tissues and sites of action where they can exert biological effects, or be excreted through the renal or pulmonary system. Excretion also occurs rectally from the intestine; this will primarily be excretion of unabsorbed drug and metabolites that have returned from the liver.

tends to be more hydrophilic than the parent drug; an example is the reaction of a $–CH_3$ to $–CH_2OH$. In addition to oxygenations, other P450-mediated oxidation reactions that contribute to phase I metabolism are heteroatom release, epoxidation, and group migration [43]. Phase II metabolism consists of conjugation reactions that add additional hydrophilic moieties to functional groups on molecules. While these functional groups are typically introduced into the drug during phase I metabolism, phase I metabolism is not required for phase II metabolism to occur; often the functional groups are present in the parent drug [44]. Enzymes responsible for phase II metabolism include the uridine 5'-diphospho-glucuronosyltransferases (UGTs) and sulfotransferases (SULTs). Nucleophilic functional groups on drug molecules are modified by UGTs to add glucuronic acid and by SULTs to add sulfonate [45, 46]. Although glucuronidation and sulfonylation are generally considered detoxifying, there are exceptions. The most notable example is the glucuronidation of morphine to produce its 6β-glucuronide, which has 90-650 fold greater potency than morphine itself [47].

Drug metabolism varies widely across individuals, populations, and throughout an individual's life. In the generalized case where drug metabolism deactivates a drug and decreases systemic drug concentrations, individuals who are extensive metabolizers may require higher than normal doses to reach drug therapeutic windows, whereas those who are poor metabolizers may accumulate drug over time and experience negative side effects [42]. If metabolism of a particular drug serves to activate it, as in the case of prodrugs, or generate toxic metabolites, extensive metabolizers would need to be given lower doses and poor metabolizers would require higher doses to reach therapeutic windows while avoiding toxicity. Genetic variation and differential expression of drug

metabolizing enzymes account for much of the variability between individuals. For example, individuals with mutant alleles of CYP2C9, one of the P450 isozymes, display up to 60% reduced clearance of the antithrombotic warfarin [48]. In order to ensure coagulant action and minimize risk of bleeding, patients must be genotyped and the warfarin dosage decreased if one of the variant alleles is detected [49]. Drug dosing also cannot safely be assumed to be similar between pediatric and adult patients. In addition to the differences in size, pediatric and adult patients have differences in both phase I and II metabolizing enzymes. Many of the P450 isozymes are undetectable in the fetal liver and only reach adult expression levels later in maturation [50]. UGTs are similarly deficient in infancy whereas SULTs are essentially mature at birth, allowing SULTs to compensate for the lack in UGT activity [50].

An individual's drug metabolizing ability may change based on environmental and health factors as well. Grapefruit juice is known for elevating the systemic concentrations of drugs when taken concomitantly, increasing toxicity risk. This is due to the presence of bergamottin, a strong inhibitor of many P450 isozymes, in particular CYP3A4 [51]. As such, patients receiving drugs that are known to be metabolized by CYP3A4 are told to avoid grapefruit juice [52]. Patients on a long term drug regime who experience onset of inflammation are also at higher risk for drug toxicities, as seen when an influenza outbreak caused theophylline toxicity in many asthmatic children [53]. The inflammatory state is known for transcriptional inhibition of P450s in multiple tissues. It is generally accepted that this alteration is due to the increase in pro-inflammatory cytokines. Notably, however, inflammation resulting from different infectious pathogens result in differential alterations in P450 expression [54]. A thorough understanding of an

individual's drug metabolism ability and how it may change is crucial for the optimization of drug dosing.

Cytochromes P450

In 1958, Garfinkel and Klingenberg both published studies reporting the detection of a strong absorption at 450 nm when carbon monoxide reacted with reduced pig and rat liver microsomes [55, 56]. This characteristic resulted in the naming of the cytochromes P450, which we now know to be a superfamily of heme-containing [57] proteins responsible for the oxidation of both endogenous and exogenous substrates [58]. P450s are found in most organisms, with 102 genes known in mice and 57 known in humans [59]. Protein expression is primarily in the endoplasmic reticulum of the liver, though there is also significant evidence of P450 expression in the pancreas, skin, brain, and gastrointestinal tract [60]. P450s are of particular interest in drug metabolism because a small subset of approximately 12 human P450s are responsible for the biotransformation of 70-80% of all clinically used drugs [61].

The canonical reaction catalyzed by P450s is the nicotinamide adenine dinucleotide phosphate (NADPH) dependent oxidation of an organic substrate by the introduction of an oxygen: $NADPH + H^+ + O_2 + RH \rightarrow NADP^+ + H_2O + ROH$ [43]. Figure 2 depicts the generalized P450 catalytic cycle. Following substrate binding, NADPH-cytochrome P450 oxidoreductase donates an electron, reducing the ferric heme to a ferrous state. Oxygen then binds to the ferrous heme followed by a second electron that can be donated by NADPH-cytochrome P450 oxidoreductase or cytochrome b5. With the addition of a proton and the cleaving of the oxygen-oxygen bond, H_2O is generated. The remaining ferric complex abstracts a hydrogen atom from the substrate to

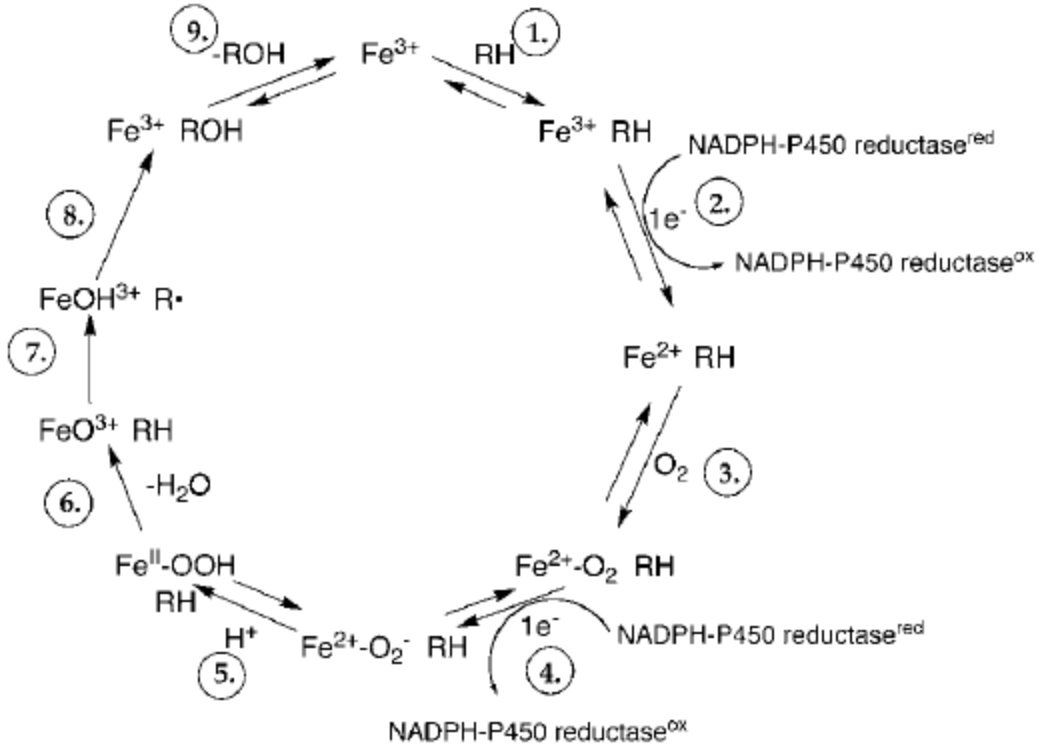

Figure 2. (Borrowed from [62]) **Cytochrome P450 catalytic cycle**. Following the donation of two electrons, a substrate RH is monooxygenated to produce ROH.

create a radical, which then reacts with $FeOH^{3+}$ to create ROH. This generalized catalytic cycle results in a variety of possible modifications to organic substrates, including carbon oxygenation, heteroatom oxygenation, heteroatom dealkylation, and epoxidation. P450 catalyzed reactions increase hydrophilicity of molecules and add functional groups for additional modification that further facilitates compound excretion. In some cases, the metabolites may retain, gain, or lose the pharmacological activity of the parent compound. Metabolites may also be toxic, thus causing the side effects experienced when using many drugs [42].

Human P450s are membrane bound 57 kDa proteins (~ 500 amino acids) containing a single heme group, which is anchored via the thiolate ligand of a conserved cysteine residue [63]. General enzyme structure is characterized by twelve highly conserved α-helices designated A through L and an N-terminal β-sheet region [64]. Helices C, D, and I-L comprise the heme and protein partner binding sites whereas F-G, B-C, and the N- and C-terminal regions form the substrate binding sites. The F-G helix in particular is known to slide over the I helix, opening and closing the active site channel [65]. P450s are primarily found in the endoplasmic reticulum, anchored by an N-terminal transmembrane peptide [66]. The NADPH-cytochrome P450 oxidoreductases that provide the requisite electrons are also located in the endoplasmic reticulum [67].

P450s have an established nomenclature that relies on amino acid sequence similarity. Individual genes are referred to by "CYP," followed by a number designating its family, a letter designating its subfamily, and a number representing the gene. Members within the same family have greater than 40% sequence identity and members within the same subfamily have greater than 55% sequence identity [68]. The enzymes

commonly associated with drug metabolism are CYP1A2, -2A6, -2B6, -2C8, -2C9, -2C19, -2D6, -2E1, -3A4, and -3A5.

Of the drug metabolizing P450s, CYP3A4 is the most abundantly expressed in the liver, comprising 14.5-37% of the total hepatic P450 content. The CYP3A family is known for metabolizing the largest proportion, 30%, of clinically used drugs [61]. Many substrates of CYP3A4 are also substrates of CYP3A5, perhaps due to the 84% amino acid similarity between the two proteins [69]. Extrapolation of an individual's relative CYP3A4 and -3A5 activity is possible due to varying levels of activity on the same substrate. For example, when the psychoactive drug midazolam is metabolized, CYP3A5 produces a greater ratio of the 1-hydroxy metabolite to the 4-hydroxy metabolite than does CYP3A4 [70]. An additional reaction catalyzed by CYP3A4/5 is the metabolism of testosterone to its 6β hydroxylated metabolite. Due to the selective production of these midazolam and testosterone metabolites by CYP3A4/5, they are known as prototypic substrates and monitoring of these reactions is commonly used to quantify CYP3A4/5 activity. The antifungal ketoconazole is a known mixed competitive-noncompetitive inhibitor of CYP3A enzymes; thus it can also be leveraged to study enzyme activity [71].

The CYP2C family is responsible for the metabolism of approximately 20% of clinically used drugs and comprise 20% of the total hepatic P450 proteins [72]. There are four members of the family in humans, CYP2C8, -2C9, -2C18, and -2C19. While CYP2C18 mRNA has been detected in multiple tissues, there is no known evidence of expression on the protein level [73]. In the liver CYP2C9 protein is found in the greatest amounts, followed by CYP2C8 then CYP2C19 [72]. Despite the high DNA and protein sequence similarity (82%) between the individual enzymes, the enzymes metabolize

markedly different substrates. Prototypic substrate reactions include the following: 6α-hydroxylation of cancer chemotherapeutic paclitaxel for CYP2C8, 4'-hydroxylation of the nonsteroidal anti-inflammatory drug diclofenac for CYP2C9, and 4'-hydroxylation of the anticonvulsant mephenytoin for CYP2C19 [61]. Inhibitors used to study CYP2C activity include the antibacterial sulfaphenazole, which competitively inhibits CYP2C9 and (+)-N-3-benzyl-nirvanol, which inhibits CYP2C19 [74, 75].

The remaining members of the CYP2 family that are involved in drug metabolism are CYP2A6, -2B6, -2D6, and -2E1. They make up 3.5-14%, 1.7-5.3%, 1.3-4.3%, and 5.5-16.5% of the total hepatic P450 protein, and metabolize 3.4%, 7.2%, 20%, and 3% of clinically used drugs, respectively [61]. CYP2A6 is well known for participating in the metabolism of nicotine and various other carcinogens, though its prototypic substrate reaction is the 7-hydroxylation of coumarin [76]. CYP2B6 catalyzes the 4-hydroxylation of the antidepressant buproprion and the 8-hydroxylation of the anti-HIV drug efavirenz [77, 78], and is inactivated in a mechanism dependent fashion by 2-phenyl-2-(1-piperidinyl)propane, an analog of the recreational drug phencyclidine [79]. CYP2D6 is required for the bioactivation of codeine into morphine by O-demethylation, causing adverse effects for patients with high CYP2D6 activity [80]. The antiarrhythmic agent quinidine is a potent competitive inhibitor of CYP2D6 activity [81]. CYP2E1 is ethanol inducible and N-hydroxylates acetaminophen to its toxic metabolite N-acetyl-p-benzoquinoneimine, making CYP2E1 is the enzyme responsible for alcohol induced acetaminophen hepatotoxicity [82].

Lastly, CYP1A2 comprises 4.4-16.3% of the hepatic P450 proteins and is responsible for metabolizing 8.9% of clinically used drugs [61]. It is best known for

being the sole enzyme responsible for catalyzing the 1-N and 3-N-demethylation of caffeine [83]. CYP1A2 also catalyzes the O-deethylation of the once widely used analgesic phenacetin to produce acetaminophen. Phenacetin was discontinued due to its association with renal and urinary tract carcinogenicity, however it has been shown that CYP1A2 carries out a primarily detoxifying role and that other P450s are responsible for production of toxic metabolites from phenacetin [84]. Furafylline, a compound that was synthesized in hopes of replacing the asthmatic drug theophylline, is a selective mechanism based inhibitor of CYP1A2 [85].

Because this small subset of enzymes is responsible for metabolizing the majority of clinically used drugs, P450s mediate many observed drug-drug interactions. Often, one drug will induce or inhibit the expression or activity of a P450 that plays a role in the metabolism of another drug [86]. A frequently cited example is the interaction between alcohol and acetaminophen, which was already described above due to its dependence on CYP2E1 induction and activity. Additionally, the anti-tuberculosis drug rifampicin has been shown to reduce systemic concentrations of the cancer drug erlotinib when administrated together [87]. Rifampicin is known to induce the expression of CYP3A4 through activation of the pregnane-X-receptor (PXR), which is a key transcriptional regulator of many drug metabolizing enzymes including CYP2A6, -2B6, -2C, and -3A members [88]. In order to predict drug-drug interactions, a sufficient understanding of the transcriptional regulation of CYPs is necessary. Other transcriptional regulators of P450 expression include the aryl hydrocarbon receptor (AhR) which regulates CYP1A, the constitutive androstane receptor (CAR) which regulates CYP2A, -2B6, -2C, and -3A, the

hepatocyte nuclear factor 1 alpha (HNF1α) which regulates CYP2E1, and hepatocyte nuclear factor 4 alpha (HNF4α) which regulates CYP2C and -2D6 [61].

While the liver is the major site of oral xenobiotic metabolism, drugs that are administered topically, such as the HIV PrEP microbicides, are unlikely to encounter hepatic tissue. Thus, local tissue metabolism will be the primary mediator of pharmacokinetics of topically applied drugs. The tissues of relevance when studying HIV PrEP are the colorectal and vaginal mucosa. Expression of CYP1A2, -2C, -2E1, -3A4, and -3A5 has been found on the mRNA level [89-91] and expression of CYP2C8, -2E1, -3A4, and -3A5 have been found on the protein level in colorectal tissues [90]. Expression of CYP1A1, -2C8, and -3A4 mRNA [92, 93] and expression of CYP1A, -2B, -2C, and -3A protein have been found in the cervicovaginal tissues [94]. However, P450 activity has not been clearly demonstrated in either mucosal tissue, nor have potential differences between hepatic and mucosal metabolism been examined.

Nucleotide Kinases

Tenofovir is a NRTI that requires two intracellular phosphorylation steps to yield its active metabolite, tenofovir-diphosphate. This is advantageous compared to nucleoside analog reverse transcriptase inhibitors, which require three phosphorylation steps with the first step often being rate limiting [95]. Tenofovir diphosphate mimics the nucleotide triphosphates that are the natural substrates of HIV reverse transcriptase and is incorporated into the growing viral DNA chain. However, due to the lack of a 3'-OH on tenofovir and its metabolites, reverse transcriptase cannot extend the chain beyond tenofovir and DNA synthesis halts [96]. In order to ensure the efficacy of tenofovir, expression and activity of the enzymes that catalyze the phosphorylation steps must be

understood in the cells of importance: $CD4^+$ T cells, systemically and within the colorectal and vaginal mucosa (HIV), and hepatocytes (Hepatitis B virus). Many studies which have identified enzymes capable of participating in tenofovir activation were performed *in vitro* with purified enzymes or subcellular fractions.

Adenylate kinases (AKs) are participants in the *de novo* and salvage pathways of nucleotide synthesis, and are known for catalyzing the reversible transfer of a phosphate group from adenosine triphosphate (ATP) to adenosine monophosphate, resulting in two molecules of adenosine diphosphate [97]. Nine individual adenylate kinases have been identified and they have been shown to have differential subcellular localizations and tissue distributions [97, 98]. AK1, AK7, and AK8 are solely found in the cytosol, AK2, AK3, and AK4 are found in the mitochondria, and AK5 and AK9 can be found in either the cytosol or nucleus. Only AK1 and AK6 are known to be expressed in all tissues, whereas AK5 is expressed only in brain and the others are found in various subsets [97]. The individual isoforms also display different donor specificities. The fact that AK2 is able to use all nucleotide triphosphates and AK3 only uses guanine triphosphate and inosine triphosphate was leveraged to show that adefovir, an analog of tenofovir, is phosphorylated by AK2 and not AK3 in an *in vitro* system using mitochondrial and cytosolic cell extracts [99]. The susceptibility of AK1 to inactivation by sulfhydryl reagents also eliminated AK1 as a candidate for adefovir phosphorylation. Additionally, AK2 isolated from both human and mouse lymphoid cell lines was shown to phosphorylate tenofovir [99, 100]. The remaining adenylate kinases have not been examined for their activity towards tenofovir or other adenine analogs.

There are two groups of guanylate kinases (GUKs), the nucleotide phosphorylating and membrane associated [98]. The membrane associated GUKs have function primarily as scaffold proteins in tissue development and differentiation [101]. Due to their lack of phosphoryl transfer activity, membrane associated GUKs are not implicated in the activation of nucleoside analog drugs. However, the nucleotide phosphorylating guanylate kinases (NPGUKs) catalyze the phosphorylation of guanosine monophosphate to guanosine diphosphate using ATP as a phosphate donor [102]. Similar to AKs, NPGUKs also participate in both the *de novo* and salvage pathways of nucleotide synthesis. There have been three isozymes of NPGUKs identified [103, 104], though only GUK1 has been cloned and therefore it is the most well studied [98]. GUK1 has been shown to phosphorylate guanosine analog antivirals such as acyclovir, ganciclovir, and cyclopropavir [105]. Adenine and guanine are highly similar nucleobases, so it is conceivable that GUK1 may also be able to phosphorylate adenine analogs, but this has ever been examined.

Nucleotide diphosphate kinases (NDPKs) catalyze the phosphorylation of nucleotide diphosphates to nucleotide triphosphates without being selective for purines or pyrimidines [97]. They play key roles in both the *de novo* and salvage pathways of nucleotide synthesis, participate in cell differentiation and development, regulate gene expression, and are implicated in tumor metastasis [106, 107]. NDPKs are commonly implicated in catalyzing the last phosphorylation step for all NRTIs [9, 108] and have been shown to activate the antivirals azidothymidine, dideoxyadenosine, and ribavirin [109, 110]. However, studies examining the NDPK activity towards tenofovir disagree,

with one study showing low efficiency production of tenofovir diphosphate [111] and the other lacking any detectable activity [112].

Creatine kinases (CKs) catalyze the reversible phosphorylation of creatine to phosphocreatine, using ATP as a phosphate donor. Phosphocreatine is an alternate source of cellular energy that can be used to create ATP when necessary [113]. The two cytosolic isoforms of creatine kinase are the brain type (CKB) and muscle type (CKM). They are expressed as homodimers or heterodimers, with CKMM being found in muscle and heart, CKMB found heart, and CKBB found in brain, kidney, retina, and various other tissues [114, 115]. The two mitochondrial CK isoforms are localized to the outer mitochondrial compartment and are known as the ubiquitously expressed isoform (CKMT1) and the sarcomeric isoform (CKMT2). They are expressed as homodimers and homooctamers, with CKMT1 expressed in a wide variety of cells and tissues and CKMT2 primarily expressed in muscle tissue [114]. Serum mitochondrial CK levels are known to increase in response to tenofovir administration, which is possibly linked to the renal tubulopathy that is sometimes associated with tenofovir [116]. Although creatine is not structurally similar to nucleotides, the reverse reaction used to generate ATP can be leveraged to phosphorylate adenine analog drugs. Human CKBB, CKMM, and CKMB have been shown to efficiently phosphorylate tenofovir monophosphate to yield tenofovir diphosphate in *in vitro* systems [111, 112].

Pyruvate kinases (PKs) are key rate-limiting enzymes in the glycolytic pathway that can only act in one direction [117]. They catalyze the transfer of a phosphate group from phosphoenolpyruvate to ADP, thus producing pyruvate and ATP [118]. There are two PK genes which translate into four isozymes. The muscle PK gene (PKM) can be

differentially spliced to yield PKM1, expressed in skeletal muscle, heart, and brain, and PKM2, expressed in early fetal tissues and most adult tissues. The liver and red blood cell gene (PKLR) encodes both PKR, which is expressed in red blood cells, and PKL, which is primarily found in the liver [119]. Many diseases are associated with PKs; examples include PMK2's role in promoting the Warburg effect in cancer [120] and PKR deficiency leading to anemia [121]. Rabbit PKM has been shown to phosphorylate tenofovir monophosphate *in vitro*, but studies have not been carried out with human enzymes [111, 112].

Summary

It is evident that metabolism by the P450s has potential to result in adverse events which cannot be predicted without understanding how P450s act on every drug that is administered. Dapivirine is one drug whose metabolism is yet unknown. However, because all other NNRTIs have shown themselves to be metabolized by P450s, it is likely that P450s also act on dapivirine. Because dapivirine is only being given topically to the colorectal or vaginal mucosa, P450 expression and activity in these tissues must also be investigated. An understanding of local drug metabolism will help to inform the use of many drugs in the colorectal and vaginal tissues, including contraceptives, spermicides, and the HIV drug maraviroc which is also being developed for microbicide use.

While multiple kinases have been shown to phosphorylate tenofovir in *in vitro* assays, these studies do not account for the presence of other potentially competing nucleotide kinases or the differences in enzyme expression and activity within the cells of clinical relevance. Thus the pathway for tenofovir activation is not yet understood in white blood cells, vaginal tissues, colorectal tissues, and liver tissues. The possibility of

tissue specific activation differences may be an intriguing explanation for the clinical observation that tenofovir-diphosphate is found in greater quantities in colorectal versus vaginal tissues. Such an understanding would allow pharmacogenetic investigation to explore potential inter-individual differences in NRTI activation and inform the use of NRTI use in these various cell types.

References

1. Cohen MS, Hellmann N, Levy JA, et al. The spread, treatment, and prevention of HIV-1: evolution of a global pandemic. J Clin Invest **2008**; 118:1244-54.

2. UNAIDS. UNAIDS report on the global AIDS epidemic 2013, **2013**.

3. Baeten J, Celum C. Systemic and topical drugs for the prevention of HIV infection: antiretroviral pre-exposure prophylaxis. Annu Rev Med **2013**; 64:219-32.

4. Chasela CS, Hudgens MG, Jamieson DJ, et al. Maternal or infant antiretroviral drugs to reduce HIV-1 transmission. N Engl J Med **2010**; 362:2271-81.

5. Nakasone T, Murakami T, Yamamoto N. Double oral administration of emtricitabine/tenofovir prior to virus exposure protects against highly pathogenic simian/human immunodeficiency virus infection in macaques. Jpn J Infect Dis **2012**; 65:345-9.

6. CDER-USFDA. Approval Package for: 021752Orig1s030. Available at: http://www.accessdata.fda.gov/drugsatfda_docs/nda/2012/021752Orig1s030Approv.pdf. Published **2012**, Accessed 2014.

7. Hughes B. Tapping into combination pills for HIV. Nat Rev Drug Discov **2009**; 8:439-40.

8. Piacenti FJ. An update and review of antiretroviral therapy. Pharmacotherapy **2006**; 26:1111-33.

9. Anderson PL, Kiser JJ, Gardner EM, et al. Pharmacological considerations for tenofovir and emtricitabine to prevent HIV infection. J Antimicrob Chemother **2011**; 66:240-50.

10. Borroto-Esoda K, Vela JE, Myrick F, et al. In vitro evaluation of the anti-HIV activity and metabolic interactions of tenofovir and emtricitabine. Antivir Ther **2006**; 11:377-84.

11. Grant RM, Lama JR, Anderson PL, et al. Preexposure chemoprophylaxis for HIV prevention in men who have sex with men. N Engl J Med **2010**; 363:2587-99.

12. Thigpen MC, Kebaabetswe PM, Paxton LA, et al. Antiretroviral preexposure prophylaxis for heterosexual HIV transmission in Botswana. N Engl J Med **2012**; 367:423-34.

13. Baeten JM, Donnell D, Ndase P, et al. Antiretroviral prophylaxis for HIV prevention in heterosexual men and women. N Engl J Med **2012**; 367:399-410.

14. Choopanya K, Martin M, Suntharasamai P, et al. Antiretroviral prophylaxis for HIV infection in injecting drug users in Bangkok, Thailand (the Bangkok Tenofovir Study): a randomised, double-blind, placebo-controlled phase 3 trial. Lancet **2013**; 381:2083-90.

15. Van Damme L, Corneli A, Ahmed K, et al. Preexposure prophylaxis for HIV infection among African women. N Engl J Med **2012**; 367:411-22.

16. NIAID. Daily-Use HIV Prevention Approaches Prove Ineffective Among Women in NIH Study, **2013**.

17. Marrazzo J, Ramjee G, Nair G, et al. Pre-exposure prophylaxis for HIV in women: daily oral tenofovir, oral tenofovir/emtricitabine, or vaginal tenofovir gel in the VOICE study (MTN 003). In: 20th Conference on Retroviruses and Opportunistic Infections. (Atlanta).Abstract # 26LB.

18. Patterson KB, Prince HA, Kraft E, et al. Penetration of tenofovir and emtricitabine in mucosal tissues: implications for prevention of HIV-1 transmission. Sci Transl Med **2011**; 3:112re4.

19. Louissaint NA, Cao YJ, Skipper PL, et al. Single Dose Pharmacokinetics of Oral Tenofovir in Plasma, Peripheral Blood Mononuclear Cells, Colonic and Vaginal Tissue. AIDS Res Hum Retroviruses **2013**.

20. Adams JL, Kashuba AD. Formulation, pharmacokinetics and pharmacodynamics of topical microbicides. Best Pract Res Clin Obstet Gynaecol **2012**; 26:451-62.

21. Anton PA, Cranston RD, Kashuba A, et al. RMP-02/MTN-006: A phase 1 rectal safety, acceptability, pharmacokinetic, and pharmacodynamic study of tenofovir 1% gel compared with oral tenofovir disoproxil fumarate. AIDS Res Hum Retroviruses **2012**; 28:1412-21.

22. Hendrix CW, Chen BA, Guddera V, et al. MTN-001: randomized pharmacokinetic cross-over study comparing tenofovir vaginal gel and oral tablets in vaginal tissue and other compartments. PLoS One **2013**; 8:e55013.

23. Lewi P, Heeres J, Arien K, et al. Reverse transcriptase inhibitors as microbicides. Curr HIV Res **2012**; 10:27-35.

24. Abdool Karim Q, Abdool Karim SS, Frohlich JA, et al. Effectiveness and safety of tenofovir gel, an antiretroviral microbicide, for the prevention of HIV infection in women. Science **2010**; 329:1168-74.

25. Chopera DR, Mann JK, Mwimanzi P, et al. No evidence for selection of HIV-1 with enhanced gag-protease or Nef function among breakthrough infections in the CAPRISA 004 tenofovir microbicide trial. PLoS One **2013**; 8:e71758.

26. Valley-Omar Z, Sibeko S, Anderson J, et al. CAPRISA 004 tenofovir microbicide trial: no impact of tenofovir gel on the HIV transmission bottleneck. J Infect Dis **2012**; 206:35-40.

27. Andrei G, Lisco A, Vanpouille C, et al. Topical tenofovir, a microbicide effective against HIV, inhibits herpes simplex virus-2 replication. Cell Host Microbe **2011**; 10:379-89.

28. FACTS. FACTS Consortium: FACTS 001 Study. Available at: http://www.facts-consortium.co.za/?page_id=83. Published **2014**, Accessed 2014.

29. CAPRISA. Current Studies. Available at: http://www.caprisa.org/Pages/Current-Studies. Published **2014**, Accessed 2014.

30. Michaud V, Bar-Magen T, Turgeon J, et al. The dual role of pharmacogenetics in HIV treatment: mutations and polymorphisms regulating antiretroviral drug resistance and disposition. Pharmacol Rev **2012**; 64:803-33.

31. De Clercq E. Emerging anti-HIV drugs. Expert Opin Emerg Drugs **2005**; 10:241-73.

32. Das K, Clark AD, Jr., Lewi PJ, et al. Roles of conformational and positional adaptability in structure-based design of TMC125-R165335 (etravirine) and related non-nucleoside reverse transcriptase inhibitors that are highly potent and effective against wild-type and drug-resistant HIV-1 variants. J Med Chem **2004**; 47:2550-60.

33. MTN. MTN-020 - ASPIRE | Microbicide Trials Network. Available at: http://www.mtnstopshiv.org/news/studies/mtn020. Published **2013**, Accessed 2014.

34. IPM. The Ring Study | IPM | International Partnership for Microbicides. Available at: http://www.ipmglobal.org/the-ring-study. Published **2011**, Accessed 2014.

35. IPM. IPM Clinical Trials | IPM | International Partnership for Microbicides. Available at: http://www.ipmglobal.org/our-work/research/clinical-trial. Published **2013**, Accessed 2014.

36. Chen BA, Panther L, Hoesle, C, Hendrix C, van der Straten A, Husnik M, Soto-Torres LE, Nel A, Johnson S, Dezzutti CS. Safety and Pharmacokinetics/Pharmacodynamics of Dapivirine and Maraviroc Vaginal Rings. Conference on Retroviruses and Opportunistic Infections. Boston, MA, USA, **2014**.

37. Dumond JB, Patterson KB, Pecha AL, et al. Maraviroc concentrates in the cervicovaginal fluid and vaginal tissue of HIV-negative women. J Acquir Immune Defic Syndr **2009**; 51:546-53.

38. Chan LM, Lowes S, Hirst BH. The ABCs of drug transport in intestine and liver: efflux proteins limiting drug absorption and bioavailability. Eur J Pharm Sci **2004**; 21:25-51.

39. Doring B, Petzinger E. Phase 0 and phase III transport in various organs: Combined concept of phases in xenobiotic transport and metabolism. Drug Metab Rev **2014**.

40. Testa B, Kramer SD. The biochemistry of drug metabolism--an introduction: part 1. Principles and overview. Chem Biodivers **2006**; 3:1053-101.

41. Ionescu C, Caira MR, SpringerLink (Online service). Drug Metabolism Current Concepts. Dordrecht: Springer, **2005**.

42. Guengerich FP. Cytochrome P450s and other enzymes in drug metabolism and toxicity. AAPS J **2006**; 8:E101-11.

43. Guengerich FP. Common and uncommon cytochrome P450 reactions related to metabolism and chemical toxicity. Chem Res Toxicol **2001**; 14:611-50.

44. David Josephy P, Peter Guengerich F, Miners JO. "Phase I and Phase II" drug metabolism: terminology that we should phase out? Drug Metab Rev **2005**; 37:575-80.

45. Rowland A, Miners JO, Mackenzie PI. The UDP-glucuronosyltransferases: their role in drug metabolism and detoxification. Int J Biochem Cell Biol **2013**; 45:1121-32.

46. Runge-Morris M, Kocarek TA, Falany CN. Regulation of the cytosolic sulfotransferases by nuclear receptors. Drug Metab Rev **2013**; 45:15-33.

47. Paul D, Standifer KM, Inturrisi CE, et al. Pharmacological characterization of morphine-6 beta-glucuronide, a very potent morphine metabolite. J Pharmacol Exp Ther **1989**; 251:477-83.

48. Wadelius M, Pirmohamed M. Pharmacogenetics of warfarin: current status and future challenges. Pharmacogenomics J **2007**; 7:99-111.

49. USFDA. Coumadin (warfarin sodium) drug label. Available at: http://www.accessdata.fda.gov/drugsatfda_docs/label/2010/009218s108lbl.pdf. Published **2010**, Accessed 2014.

50. Strolin Benedetti M, Baltes EL. Drug metabolism and disposition in children. Fundam Clin Pharmacol **2003**; 17:281-99.

51. Guo LQ, Yamazoe Y. Inhibition of cytochrome P450 by furanocoumarins in grapefruit juice and herbal medicines. Acta Pharmacol Sin **2004**; 25:129-36.

52. Wilkinson GR. Drug metabolism and variability among patients in drug response. N Engl J Med **2005**; 352:2211-21.

53. Kraemer MJ, Furukawa CT, Koup JR, et al. Altered theophylline clearance during an influenza B outbreak. Pediatrics **1982**; 69:476-80.

54. Morgan ET. Impact of infectious and inflammatory disease on cytochrome P450-mediated drug metabolism and pharmacokinetics. Clin Pharmacol Ther **2009**; 85:434-8.

55. Garfinkel D. Studies on pig liver microsomes. I. Enzymic and pigment composition of different microsomal fractions. Arch Biochem Biophys **1958**; 77:493-509.

56. Klingenberg M. Pigments of rat liver microsomes. Arch Biochem Biophys **1958**; 75:376-86.

57. Omura T, Sato R. The Carbon Monoxide-Binding Pigment of Liver Microsomes. I. Evidence for Its Hemoprotein Nature. J Biol Chem **1964**; 239:2370-8.

58. Grogan G. Cytochromes P450: exploiting diversity and enabling application as biocatalysts. Curr Opin Chem Biol **2011**; 15:241-8.

59. Nelson DR, Zeldin DC, Hoffman SM, et al. Comparison of cytochrome P450 (CYP) genes from the mouse and human genomes, including nomenclature recommendations for genes, pseudogenes and alternative-splice variants. Pharmacogenetics **2004**; 14:1-18.

60. Seliskar M, Rozman D. Mammalian cytochromes P450--importance of tissue specificity. Biochim Biophys Acta **2007**; 1770:458-66.

61. Zanger UM, Schwab M. Cytochrome P450 enzymes in drug metabolism: Regulation of gene expression, enzyme activities, and impact of genetic variation. Pharmacol Ther **2013**; 138:103-41.

62. Guengerich FP. Mechanisms of Cytochrome P450 Reactions. Acta Chim Slov **2008**; 55:7-19.

63. Ortiz de Montellano PR, SpringerLink (Online service). Cytochrome P450 Structure, Mechanism, and Biochemistry. Third edition. ed. Boston, MA: Kluwer Academic/Plenum Publishers, New York, **2005**.

64. Johnson EF, Stout CD. Structural diversity of eukaryotic membrane cytochrome p450s. J Biol Chem **2013**; 288:17082-90.

65. Poulos TL. Cytochrome P450 flexibility. Proc Natl Acad Sci U S A **2003**; 100:13121-2.

66. Black SD. Membrane topology of the mammalian P450 cytochromes. FASEB J **1992**; 6:680-5.

67. Werck-Reichhart D, Feyereisen R. Cytochromes P450: a success story. Genome Biol **2000**; 1:REVIEWS3003.

68. Nelson DR, Koymans L, Kamataki T, et al. P450 superfamily: update on new sequences, gene mapping, accession numbers and nomenclature. Pharmacogenetics **1996**; 6:1-42.

69. Emoto C, Iwasaki K. Enzymatic characteristics of CYP3A5 and CYP3A4: a comparison of in vitro kinetic and drug-drug interaction patterns. Xenobiotica **2006**; 36:219-33.

70. Gorski JC, Hall SD, Jones DR, et al. Regioselective biotransformation of midazolam by members of the human cytochrome P450 3A (CYP3A) subfamily. Biochem Pharmacol **1994**; 47:1643-53.

71. Greenblatt DJ, Zhao Y, Venkatakrishnan K, et al. Mechanism of cytochrome P450-3A inhibition by ketoconazole. J Pharm Pharmacol **2011**; 63:214-21.

72. Chen Y, Goldstein JA. The transcriptional regulation of the human CYP2C genes. Curr Drug Metab **2009**; 10:567-78.

73. Klose TS, Blaisdell JA, Goldstein JA. Gene structure of CYP2C8 and extrahepatic distribution of the human CYP2Cs. J Biochem Mol Toxicol **1999**; 13:289-95.

74. Suzuki H, Kneller MB, Haining RL, et al. (+)-N-3-Benzyl-nirvanol and (-)-N-3-benzyl-phenobarbital: new potent and selective in vitro inhibitors of CYP2C19. Drug Metab Dispos **2002**; 30:235-9.

75. Bourrie M, Meunier V, Berger Y, et al. Cytochrome P450 isoform inhibitors as a tool for the investigation of metabolic reactions catalyzed by human liver microsomes. J Pharmacol Exp Ther **1996**; 277:321-32.

76. Raunio H, Rautio A, Gullsten H, et al. Polymorphisms of CYP2A6 and its practical consequences. Br J Clin Pharmacol **2001**; 52:357-63.

77. Faucette SR, Hawke RL, Lecluyse EL, et al. Validation of bupropion hydroxylation as a selective marker of human cytochrome P450 2B6 catalytic activity. Drug Metab Dispos **2000**; 28:1222-30.

78. Ward BA, Gorski JC, Jones DR, et al. The cytochrome P450 2B6 (CYP2B6) is the main catalyst of efavirenz primary and secondary metabolism: implication for HIV/AIDS therapy and utility of efavirenz as a substrate marker of CYP2B6 catalytic activity. J Pharmacol Exp Ther **2003**; 306:287-300.

79. Chun J, Kent UM, Moss RM, et al. Mechanism-based inactivation of cytochromes P450 2B1 and P450 2B6 by 2-phenyl-2-(1-piperidinyl)propane. Drug Metab Dispos **2000**; 28:905-11.

80. Gasche Y, Daali Y, Fathi M, et al. Codeine intoxication associated with ultrarapid CYP2D6 metabolism. N Engl J Med **2004**; 351:2827-31.

81. von Moltke LL, Greenblatt DJ, Cotreau-Bibbo MM, et al. Inhibition of desipramine hydroxylation in vitro by serotonin-reuptake-inhibitor antidepressants, and by quinidine

and ketoconazole: a model system to predict drug interactions in vivo. J Pharmacol Exp Ther **1994**; 268:1278-83.

82. Lee SS, Buters JT, Pineau T, et al. Role of CYP2E1 in the hepatotoxicity of acetaminophen. J Biol Chem **1996**; 271:12063-7.

83. Kot M, Daniel WA. The relative contribution of human cytochrome P450 isoforms to the four caffeine oxidation pathways: an in vitro comparative study with cDNA-expressed P450s including CYP2C isoforms. Biochem Pharmacol **2008**; 76:543-51.

84. Peters JM, Morishima H, Ward JM, et al. Role of CYP1A2 in the toxicity of long-term phenacetin feeding in mice. Toxicol Sci **1999**; 50:82-9.

85. Racha JK, Rettie AE, Kunze KL. Mechanism-based inactivation of human cytochrome P450 1A2 by furafylline: detection of a 1:1 adduct to protein and evidence for the formation of a novel imidazomethide intermediate. Biochemistry **1998**; 37:7407-19.

86. Preissner S, Kroll K, Dunkel M, et al. SuperCYP: a comprehensive database on Cytochrome P450 enzymes including a tool for analysis of CYP-drug interactions. Nucleic Acids Res **2010**; 38:D237-43.

87. Hamilton M, Wolf JL, Drolet DW, et al. The effect of rifampicin, a prototypical CYP3A4 inducer, on erlotinib pharmacokinetics in healthy subjects. Cancer Chemother Pharmacol **2014**; 73:613-21.

88. Shukla SJ, Sakamuru S, Huang R, et al. Identification of clinically used drugs that activate pregnane X receptors. Drug Metab Dispos **2011**; 39:151-9.

89. Ding X, Kaminsky LS. Human extrahepatic cytochromes P450: function in xenobiotic metabolism and tissue-selective chemical toxicity in the respiratory and gastrointestinal tracts. Annu Rev Pharmacol Toxicol **2003**; 43:149-73.

90. Bergheim I, Bode C, Parlesak A. Distribution of cytochrome P450 2C, 2E1, 3A4, and 3A5 in human colon mucosa. BMC Clin Pharmacol **2005**; 5:4.

91. Thorn M, Finnstrom N, Lundgren S, et al. Cytochromes P450 and MDR1 mRNA expression along the human gastrointestinal tract. Br J Clin Pharmacol **2005**; 60:54-60.

92. Zhou T, Hu M, Cost M, et al. Short communication: expression of transporters and metabolizing enzymes in the female lower genital tract: implications for microbicide research. AIDS Res Hum Retroviruses **2013**; 29:1496-503.

93. Sarkar MA, Vadlamuri V, Ghosh S, et al. Expression and cyclic variability of CYP3A4 and CYP3A7 isoforms in human endometrium and cervix during the menstrual cycle. Drug Metab Dispos **2003**; 31:1-6.

94. Patel KR, Astley S, Adams DJ, et al. Expression of cytochrome P450 enzymes in the cervix. An immunohistochemical study. Int J Gynecol Cancer **1993**; 3:159-63.

95. Ray AS, Hostetler KY. Application of kinase bypass strategies to nucleoside antivirals. Antiviral Res **2011**; 92:277-91.

96. Gotte M, Wainberg MA. Biochemical mechanisms involved in overcoming HIV resistance to nucleoside inhibitors of reverse transcriptase. Drug Resist Updat **2000**; 3:30-8.

97. Panayiotou C, Solaroli N, Karlsson A. The many isoforms of human adenylate kinases. Int J Biochem Cell Biol **2014**; 49C:75-83.

98. Van Rompay AR, Johansson M, Karlsson A. Phosphorylation of nucleosides and nucleoside analogs by mammalian nucleoside monophosphate kinases. Pharmacol Ther **2000**; 87:189-98.

99. Robbins BL, Greenhaw J, Connelly MC, et al. Metabolic pathways for activation of the antiviral agent 9-(2-phosphonylmethoxyethyl)adenine in human lymphoid cells. Antimicrob Agents Chemother **1995**; 39:2304-8.

100. Krejcova R HK, Votruba I & Holy A. Phosphorylation of purine (phosphonomethoxy)alkyl derivatives
by mitochondrial AMP kinase (AK2 type) from
L1210 cells. Collection of Czechoslovak Chemical
Contributions **2000**; 65:1653-68.

101. Funke L, Dakoji S, Bredt DS. Membrane-associated guanylate kinases regulate adhesion and plasticity at cell junctions. Annu Rev Biochem **2005**; 74:219-45.

102. Stehle T, Schulz GE. Refined structure of the complex between guanylate kinase and its substrate GMP at 2.0 A resolution. J Mol Biol **1992**; 224:1127-41.

103. Jamil T, Fisher RA, Harris H. Studies on the properties and tissue distribution of the isozymes of guanylate kinase in man. Hum Hered **1975**; 25:402-13.

104. Jamil T, Fisher RA. An investigation of the homology of guanylate kinase isozymes in mammals and further evidence for multiple GUK gene loci. Biochem Genet **1977**; 15:847-58.

105. Gentry BG, Gentry SN, Jackson TL, et al. Phosphorylation of antiviral and endogenous nucleotides to di- and triphosphates by guanosine monophosphate kinase. Biochem Pharmacol **2011**; 81:43-9.

106. Postel EH. NM23-NDP kinase. Int J Biochem Cell Biol **1998**; 30:1291-5.

107. Boissan M, Dabernat S, Peuchant E, et al. The mammalian Nm23/NDPK family: from metastasis control to cilia movement. Mol Cell Biochem **2009**; 329:51-62.

108. Anderson PL, Kakuda TN, Lichtenstein KA. The cellular pharmacology of nucleoside- and nucleotide-analogue reverse-transcriptase inhibitors and its relationship to clinical toxicities. Clin Infect Dis **2004**; 38:743-53.

109. Bourdais J, Biondi R, Sarfati S, et al. Cellular phosphorylation of anti-HIV nucleosides. Role of nucleoside diphosphate kinase. J Biol Chem **1996**; 271:7887-90.

110. Gallois-Montbrun S, Chen Y, Dutartre H, et al. Structural analysis of the activation of ribavirin analogs by NDP kinase: comparison with other ribavirin targets. Mol Pharmacol **2003**; 63:538-46.

111. Koch K, Chen Y, Feng JY, et al. Nucleoside diphosphate kinase and the activation of antiviral phosphonate analogs of nucleotides: binding mode and phosphorylation of tenofovir derivatives. Nucleosides Nucleotides Nucleic Acids **2009**; 28:776-92.

112. Varga A, Graczer E, Chaloin L, et al. Selectivity of kinases on the activation of tenofovir, an anti-HIV agent. Eur J Pharm Sci **2013**; 48:307-15.

113. Sahlin K, Harris RC. The creatine kinase reaction: a simple reaction with functional complexity. Amino Acids **2011**; 40:1363-7.

114. Wallimann T, Tokarska-Schlattner M, Schlattner U. The creatine kinase system and pleiotropic effects of creatine. Amino Acids **2011**; 40:1271-96.

115. Bong SM, Moon JH, Nam KH, et al. Structural studies of human brain-type creatine kinase complexed with the ADP-Mg2+-NO3- -creatine transition-state analogue complex. FEBS Lett **2008**; 582:3959-65.

116. Watanabe D, Yoshino M, Yagura H, et al. Increase in serum mitochondrial creatine kinase levels induced by tenofovir administration. J Infect Chemother **2012**; 18:675-82.

117. Weber G, Singhal RL, Stamm NB, et al. Synchronous behavior pattern of key glycolytic enzymes: glucokinase, phosphofructokinase, and pyruvate kinase. Adv Enzyme Regul **1966**; 4:59-81.

118. Munoz ME, Ponce E. Pyruvate kinase: current status of regulatory and functional properties. Comp Biochem Physiol B Biochem Mol Biol **2003**; 135:197-218.

119. van Wijk R, Huizinga EG, van Wesel AC, et al. Fifteen novel mutations in PKLR associated with pyruvate kinase (PK) deficiency: structural implications of amino acid substitutions in PK. Hum Mutat **2009**; 30:446-53.

120. Yang W, Lu Z. Regulation and function of pyruvate kinase M2 in cancer. Cancer Lett **2013**; 339:153-8.

121. Zanella A, Bianchi P, Fermo E. Pyruvate kinase deficiency. Haematologica **2007**; 92:721-3.

Chapter 2: Dissimilarities in the metabolism of antiretroviral drugs used in HIV pre-exposure prophylaxis in colon and vagina tissues

Abstract:

Attempts to prevent HIV infection through pre-exposure prophylaxis (PrEP) include topical application of anti-HIV drugs to the mucosal sites of infection; however, a potential role for local drug metabolizing enzymes in modulating the exposure of the mucosal tissues to these drugs has yet to be explored. Here we present the first report that enzymes belonging to the cytochrome P450 (P450) and UDP-glucuronosyltransferase (UGT) families of drug metabolizing enzymes are expressed and active in vaginal and colorectal tissue using biopsies collected from healthy volunteers. In doing so, we discovered that dapivirine and maraviroc, a non-nucleoside reverse transcriptase inhibitor and an entry inhibitor currently in development as microbicides for HIV PrEP, are differentially metabolized in colorectal tissue and vaginal tissue. Taken together, these data should help to guide the optimization of small molecules being developed for HIV PrEP.

Introduction

Pre-exposure prophylaxis (PrEP) is a promising new strategy to prevent the spread of human immunodeficiency virus (HIV) by using antiretroviral (ARV) therapy to interrupt the viral life cycle before infection is established in newly exposed individuals [1]; however, oral ARV drugs may select for drug resistant viral strains in patients who become infected while on the prophylactic regimen. Topically applied microbicides may overcome this disadvantage by preventing the establishment of infection within the mucosal tissues without resulting in significant systemic exposure [2]. A pharmacokinetics study of tenofovir, which is one of the two drugs that comprise the therapy Truvada®, currently the only antiretroviral therapy FDA approved for HIV PrEP, corroborates this by demonstrating lower systemic and higher mucosal concentrations of tenofovir and its active metabolite when dosed vaginally versus orally [3].

Dapivirine is a non-nucleoside reverse transcriptase inhibitor (NNRTI) currently undergoing phase III clinical trials for use in HIV PrEP [4]; however, due to its poor oral bioavailability and remarkable inhibitory activity against both cell-associated and cell-free virions [2], dapivirine is in development solely as a topical microbicide. Maraviroc is an entry inhibitor co-formulated into a vaginal ring with dapivirine that is currently undergoing phase I clinical trials [5]. The factors that might modulate dapivirine and maraviroc exposure, including a role for metabolism of dapivirine in mucosal tissues, are unknown. A small subset of P450 isozymes are responsible for the phase I metabolism of 70-80% of all clinically used drugs, including maraviroc and other antiretrovirals used to treat HIV [6]. The P450 superfamily of enzymes are heme-containing monooxygenases that increase the hydrophilicity of their substrates, facilitating their clearance [7]. Further,

P450-dependent metabolism plays a major role in drug-drug interactions and can result in the formation of metabolites that exhibit toxicity. Phase II drug metabolism that is mediated by the UGT family of enzymes transfers a glucuronic acid moiety onto the substrate, further facilitating their elimination.

P450 enzymes are primarily expressed in the liver, which is the major site of oral xenobiotic metabolism; however, it is unknown whether drugs applied topically to vaginal and colorectal tissues, such as topical microbicides used in HIV PrEP, are metabolized locally. Topically applied drugs are unlikely to encounter the liver, and as such local metabolism would likely be a primary mediator of the pharmacokinetics of these drugs. Further, it is unclear whether a drug would be metabolized similarly if it were administered orally versus topically. In the present study, we demonstrate for the first time that P450 isozymes are expressed and active in vagina and colon. In addition, our findings indicate that metabolism of dapivirine and maraviroc differs between colorectal and vaginal tissues, potentially resulting in differential drug exposure. Collectively, these data provide novel insight that can be leveraged in interpreting HIV PrEP clinical pharmacology data and in developing drugs that will be administered topically to vaginal and/or colorectal tissue including antiretrovirals to be used in HIV PrEP.

Materials and Methods

Materials

Dapivirine, dapivirine-d11, sulforaphane, and maraviroc were obtained from Toronto Research Chemical (Toronto, Ontario, Canada). Furafylline, sulfaphenazole, (+)-N3-

benzylnirvanol, quinidine, and ketoconazole were obtained from Sigma-Aldrich (St. Louis, MO) and 2-phenyl-2-(1-piperidenyl) propane (PPP) purchased from Santa Cruz Biotechnology, Inc (Santa Cruz, CA). Optima liquid chromatography/mass spectrometry grade water, acetonitrile, and formic acid were obtained from Thermo Fisher Scientific (Pittsburg, PA).

Metabolism Assays

All experiments were performed in Fisherbrand Siliconized Low-Retention Microcentrifuge Tubes (Thermo Fisher Scientific). Dapivirine (10 μM) was incubated with human liver microsomes (50 donor pool, Xenotech, LLC, Lenexa, KS), cDNA-expressed individual human CYPs (Supersomes™, BD Biosciences, San Jose, CA, CYP -1A2, -2A6, -2B6, -2C8, -2C9, -2C19, -2D6, -3A4, -3A5) or UGTs (Supersomes™, BD Biosciences, UGT1A1, -1A3, -1A4, -1A6, -1A7, -1A8, -1A9, -1A10, -2B4, -2B7, -2B15, -2B17). Final concentrations were as follows: human liver microsomes at 1 mg/mL, P450s at 10 pmol/mL, and UGTs at 0.2 mg/mL. Human liver microsomes or CYPs were combined with dapivirine in 100 mM potassium phosphate buffer, pH 7.4, and incubated for 5 min in a 37 °C water bath. Reactions were initiated by the addition of a NADPH-regenerating system (BD Biosciences) and allowed to proceed for 30 min at 37 °C. For inhibition studies, small molecule inhibitors were prepared as 500x solutions in DMSO and preincubated with the human liver microsomes in potassium phosphate buffer with the NADPH-regenerating system for 5 min at 37 °C. Inhibitors used were: furafylline (20 μM) for CYP1A2, 2-phenyl-2-(1-piperidenyl) propane (30 μM) for CYP2B6, sulfaphenazole (20 μM) for CYP2C9, (+)-N3-benzylnirvanol (10 μM) for CYP2C19, quinidine (1 μM) for CYP2D6, and ketoconazole (1 μM) for CYP3A4/5. After the

addition of dapivirine, the reactions were allowed to proceed for 30 min at 37 °C. For reactions containing UGTs, the enzymes were combined with dapivirine in UGT reaction mix (Tris buffer, pH 7.5, alamethicin, and $MgCL_2$; BD Biosciences) and incubated for 5 min in a 37 °C water bath before initiating the reaction with 2 mM UDPGA. Reactions were allowed to proceed for 60 min at 37 °C and the total reaction volumes were 100 µL. After incubations, reactions were quenched with 100 µL acetonitrile, incubated for 10 min at 4 °C, and the proteins removed by centrifugation at 3000g for 10 min at 4 °C. The supernatant was dried at 65 °C under vacuum pressure and the resulting residue reconstituted in 100 µL methanol for uHPLC-MS/MS analysis. Reactions carried out with liver microsomes from different species were carried out similar to reactions using human liver microsomes. Microsomes from BALB/C mice (male, pool of 800), CD-1 mice (male, pool of 1,000), Sprague-Dawley rat (male, pool of 433), New Zealand rabbit (male, pool of 8), rhesus monkey (male, pool of 6), cynomolgus monkey (male, pool of 800), Sinclair minipig (male, pool of 3), Hartley albino guinea pig (male, pool of 50), golden Syrian hamster (male, pool of 100), and beagle dog (male, pool of 8) were obtained from Xenotech.

Ultra high performance liquid chromatography mass spectrometry (uHPLC-MS)

A uHPLC-MS assay was developed for the quantification and identification of dapivirine metabolites, using a Dionex Ultimate 3000 uHPLC system coupled to a TSQ Vantage Triple Stage Quadrupole mass spectrometer (Thermo Fisher Scientific). Compounds were separated using a Polaris 5 C18-A column (5 µm, 100 x 2.0 mm, Agilent Technologies, Santa Clara, CA) at a flow rate of 0.4 mL/min. Solvent A was 0.1% formic acid in H_2O and solvent B was 0.1% formic acid in acetonitrile. The gradient used is as follows: from

0% B to 50% B from 0.0-9.0 min, 50% B to 100% B from 9.0 min to 9.3 min, held at 100% B until 12.3 min, from 100% B to 0% B from 12.3 to 13.3 min, and held at 0% B until 16.3 min. In MS/MS mode, metabolites were detected in positive ion mode as m/z = 346.4 (monohydroxy dapivirine), 362.4 (dihydroxy dapivirine), 506.4 (glucuronidated dapivirine), and 522.4 (glucuronidated monohydroxy dapivirine). In selected reaction monitoring mode, fragment ions were detected in positive ion mode using the following transitions (Q1→Q3): dapivirine (m/z 330.4→158.4); M1 (m/z 346.4→316.0); M2 (m/z 346.4→185.0); M3 (m/z 346.4→174.0); M4 (m/z 346.4→119.0); M5 (m/z 362.4→171.0); M6 (m/z 362.4→332.0); M7 (m/z 506.4→330.4); M8 (m/z 522.4→316.0); M9 (m/z 522.4→346.4); M10 (m/z 522.4→312.0); and M11 (m/z 522.4→346.6).

The assay used to detect maraviroc metabolites used the same uHPLC and mass spectrometer system as the dapivirine assay and a uHPLC BEH C8 column (1.7 μm, 2.1 x 100 mm, Waters, Milford, MA). Solvent A was 0.1% formic acid, 5% acetonitrile, and 95% H_2O and solvent B was 0.1% formic acid, 95% acetonitrile, and 5% H_2O. The gradient started at 0% B and increased to 10% B over 1.1 min, 14.3% B at 10.0 min, 25% B at 15.0 min, held at 25% B for 1 min, then brought down to 0% B at 16.1 min and held at 0% B for 0.9 min. Transitions for selected reaction monitoring were identical to those used in a previously reported assay [8].

Tissue Biopsy Culture

Healthy subjects were recruited for tissue donation after providing written informed consent for participation in a protocol approved by the institutional review board of Johns Hopkins Medical Institutions. Each colorectal tissue donor provided 30 biopsies

(approximately 25 mg each) and each vaginal donor provided 5 biopsies (approximately 25 mg each). Donor information is presented as sex and age: colorectal donors were female 49 years old, male 24 years old, and female 28 years old (denoted as colon 1, colon 2 and colon 3, respectively) while vaginal donors were female 27 years old, female 27 years old, and female 28 years old (vagina 1, vagina 2 and vagina 3, respectively). The third colon and third vagina samples were obtained from the same individual. Upon collection, biopsies were placed into RPMI 1640 medium (Corning Life Sciences, Tewksbury, MA) supplemented with 10% heat inactivated fetal bovine serum, penicillin-streptomycin, and L-glutamine and stored on ice for transport. The medium was replaced with fresh medium containing the appropriate treatment: methanol (vehicle control, 0.1%), dapivirine (10 μM), sulforaphane (25 μM), or maraviroc (10 μM). After incubation for 6, 12, or 24 hours at 37 °C in a 5% CO_2 humidified environment, culture medium was collected, dried at 65 °C under vacuum, and the residue reconstituted in 100 μL methanol for uHPLC-MS/MS analysis.

Primary Human Hepatocyte Culture

Primary human hepatocytes were obtained from Xenotech. Donor information is presented as lot number, viability, sex, and age: 1152, 79.9%, female, 69; 1155, 74.7%, female, 43; 1157, 77.9%, female, 59 (denoted as hepatocyte 1, hepatocyte 2, and hepatocyte 3, respectively). Upon arrival, the shipment medium was aspirated and replaced with William's medium E (Invitrogen) supplemented with 10% fetal bovine serum, 1% penicillin-streptomycin, and 1% L-glutamine. Hepatocytes were incubated overnight at 37 °C in a 5% CO_2 humidified environment. The medium was replaced with fresh medium containing the appropriate treatment: methanol (vehicle control, 0.1%) or

dapivirine (10 μM) and cells were incubated for 6, 12, or 24 hours 37 °C in a 5% CO_2 humidified environment. RNA was isolated as described below.

RNA Isolation, Endpoint PCR, and qRT-PCR Analysis

Immediately after culture medium was removed, tissue biopsies or hepatocytes were immersed in TRIzol® (Life Technologies, Grand Island, NY) and RNA isolated following the manufacturer's instructions. RNA was quantitated spectrophotometrically, and 2 μg of each used to synthesize cDNA using a Maxima First-Strand cDNA Synthesis Kit (Thermo Fisher Scientific) for use in endpoint reverse transcriptase PCR or qRT-PCR. For qRT-PCR, a standard curve was generated using glyceraldehyde-3-phosphate dehydrogenase (GAPDH) PCR products cloned into pJET1.2/blunt cloning vectors (Thermo Fisher Scientific). Primers used are presented in Table 1. Endpoint reverse transcriptase PCR was run using PCR Master Mix (2X) (Thermo Fisher Scientific), with the following thermal cycling conditions: 95 °C for 1 min, followed by 30 cycles of 95 °C for 30 s, 60 °C for 30 s, and 72 °C for 1 min, and a final extension step of 72 °C for 5 min. Products were analyzed via 1% agarose gel electrophoresis and visualized with SYBR® Safe DNA Gel Stain (Life Technologies). qRT-PCR was run using Maxima SYBR Green qPCR Master Mix (Thermo Fisher Scientific), with the following thermal cycling conditions: 95 °C for 10 min, followed by 40 cycles of 95 °C for 15 s, 60 °C for 30 s, and 72 °C for 30 s. GAPDH was used for normalization of mRNA levels.

Protein Isolation and Immunoblotting Analysis

Biopsies were washed once in 500 μL phosphate buffered saline (PBS) and homogenized on ice in cell lysis buffer (Cell Signaling Technology, Danvers, MA) containing Halt Protease + Phosphatase Inhibitor Cocktail (Thermo Fisher Scientific) and 1 mM

Table 1:

Primer	Accession Number	Role	Primers (5'→3')	Coordinates
GAPDH	NM_002046.3	Forward	CTTCTTTTGCGTCGCCAGCCGA	62-83
		Reverse	CACGACGTACTCAGCGCCAGC	390-370
CYP1A1	NM_000499.3	Forward	GTACCTCAGCCACCTCCAAGAT	88-109
		Reverse	GCTCCTGCAACGTGCTTATC	632-651
CYP1A2	NM_000761.3	Forward	CATCCCCCACAGCACAACAAGGG	1219-1241
		Reverse	CAGTTGATGGAGAAGCGCAGCC	1593-1614
CYP2B6	NM_000767.4	Forward	GTCGACCCATTCTTCCGGGGAT	317-338
		Reverse	GAAGAGCTCAAACAGCTGGCCGAA	644-667
CYP2C19	NM_000769.1	Forward	TGGAGAAGGAAAAGCAAAACCAAC	812-835
		Reverse	GGTTGTGCCCTTGGGAATGAGG	1137-1158
CYP2E1	NM_000773.3	Forward	ACCCAAGGCCAGCCTTTCGAC	514-534
		Reverse	TCCACGAGCAGGCAGTCGGT	829-848

CYP3A4	NM_017460.5	Forward	GGAAAAGTGTGGGGCTTTTATGATGG	307-333
		Reverse	GCCTGTCTCTGCTTCCCGCC	589-608
CYP3A5	NM_000777.3	Forward	TTCACCATGACCCAAAGTACTGGAC	1304-1321
		Reverse	TAACTCATTCTCCACTTAGGGTTCC	1591-1615
PXR	NM_022002.2	Forward	CAAGCGGAAGAAAAGTGAACG	540-560
		Reverse	CTGGTCCTCGATGGGCAAGTC	961-981

Table 1. Primers used for qRT-PCR for P450

phenylmethanesulfonylfluoride (Sigma-Aldrich) using disposable pellet mixer pestles attached to a pestle motor (VWR International, Radnor, PA). Samples were centrifuged for 10 min at 3000 g, 4 °C and the resulting supernatant was stored at -20 °C. Protein concentrations were determined using a Pierce® BCA Protein Assay Kit (Thermo Scientific), following the manufacturer's instructions. For immunoblots, 10 µg of each sample were loaded onto 10% or 12% Mini-PROTEAN® TGX™ Precast Gels (Bio-Rad, Hercules, CA) for separation via SDS-polyacrylamide gel electrophoresis. Proteins were transferred onto 0.2 µm pore nitrocellulose membranes (Life Technologies) and blotted with commercially available antibodies. Antibodies for CYP -2B6, -2C9, -2C19, -3A4, and -3A5 were obtained from BD Biosciences, anti-CYP2D6 was obtained from Xenotech. Anti-β-actin was used for normalization and was obtained from Cell Signaling. Proteins were visualized using SuperSignal West Dura Chemiluminescent Substrate (Thermo Fisher Scientific) according to the manufacturer's protocol and imaged with a Carestream 4000R system. Blots were stripped with ReBlot Plus Strong Antibody Stripping Solution (Millipore, Billerica, MA), then blotted with different antibodies following confirmation of antibody stripping.

In situ Extract Preparation

For analysis of in situ metabolite concentrations the tissue biopsies were washed with PBS 3 times prior to homogenizing in 500 µL ethyl acetate. The solution was dried at 65 °C under vacuum followed by reconstitution in 100 µL methanol for uHPLC-MS/MS analysis.

Statistical Analyses

All data presented are means ± S. E. from three independent experiments. Two-tailed unpaired *t* tests were performed to compare datasets, and $p \leq 0.05$ was considered significant. Significance was denoted as follows: *, $p \leq 0.05$; **, $p \leq 0.01$; ***, $p \leq 0.001$.

Results

Cytochrome P450 Expression in Mucosal Tissues that are Sites of HIV Infection

The ability of the colorectal and vaginal mucosa to biotransform xenobiotics has not been clearly defined; thus the expression of P450 isozymes found to metabolize HIV antiretroviral drugs was explored in these tissues. Vaginal and colorectal mRNA expression of P450s that play a prominent role in drug metabolism was examined through quantitative reverse transcriptase PCR (qRT-PCR). Expression of CYP1A1, -1A2, -2B6, -2C19, -2E1, -3A4, and -3A5 mRNA was detected in all samples (Figure 1A). Comparing the expression levels of these mRNAs in colorectal tissue to those of the vaginal tissue samples revealed that CYP3A5 mRNA levels were 4- (p-value = 0.04) fold higher in colorectal tissues. Expression was also probed on the protein level via immunoblotting using cell lysates isolated from the vaginal and colorectal biopsies (Figure 1B). Prior to screening, we verified that all of the antibodies were able to detect the cDNA expressed P450 isozymes that they were designed to target (data not shown). While CYP2B6, -2C19, -3A4, and -3A5 were readily detected in both tissue types, CYP1A2, -2A6, -2C9, and -2D6 were not. These results were consistent when comparing samples “colon 3 (C3)” and “vagina 3 (V3)” that were collected from the same

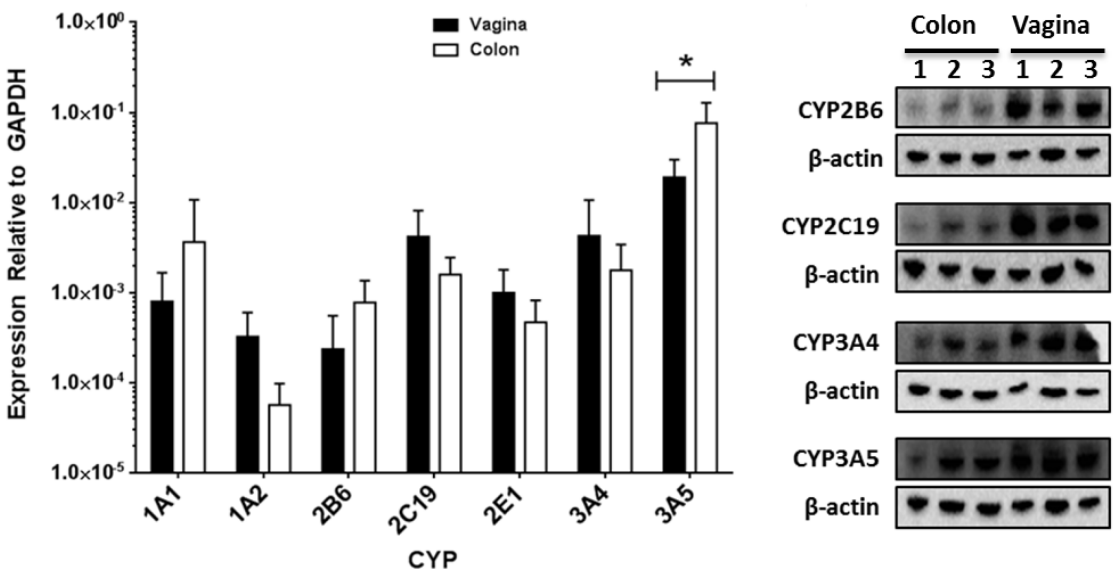

Figure 1. Expression of P450 mRNA and protein in colorectal and vaginal tissues. A. Quantification of mRNA expression levels of P450s (n=6) in colorectal and vaginal tissue. B. Immunoblots of P450 isozymes in protein lysates isolated from vaginal and colorectal tissue biopsies. C=colon donor, V=vagina donor. Colon 3 and vagina 3 are from a single individual. * = $p \leq 0.05$.

individual. Additionally, protein expression of CYP2B6, -2C19, and -3A4 was markedly higher in vaginal tissue than in colorectal.

Maraviroc Metabolism by Colorectal and Vaginal Tissues

In order to probe the P450 activity in the mucosal tissues, colorectal and vaginal biopsies were obtained from healthy human donors for maraviroc treatment, followed by metabolite detection using uHPLC-MS/MS. We have previously demonstrated that maraviroc is a substrate of CYP3A4/5 [8], identifying 6 monooxygenated metabolites (M1-M6), 4 dioxygenated metabolites (M7-M10), and 2 glucuronidated metabolites (M11, M12) in human liver microsomes, plasma, and urine. Maraviroc is also being tested for use as a topical microbicide for HIV PrEP. After 24 hours of maraviroc treatment, colon tissue from all three donors produced a monooxygenated metabolite that was detectable in both the culture medium and in situ (Figure 2A and 2B). In contrast, of the two vaginal tissue donors that were treated with maraviroc, one produced this same monooxygenated metabolite (as measured in both culture medium and in situ) while the other did not (Figure 2C-2F).

Identification of Dapivirine Metabolites

Since dapivirine is under development as a topical microbicide for HIV PrEP we sought to determine whether dapivirine is also metabolized in the mucosal tissues to which it would be applied; however, since the metabolism of dapivirine has yet to be reported, we began our studies by using human liver microsomes to identify potential metabolites of dapivirine and to develop our uHPLC-MS methods for qualitatively detecting dapivirine and dapivirine products. Dapivirine (m/z = 330.4) was incubated with human liver microsomes and the phase I- and phase II-dependent metabolites of dapivirine were

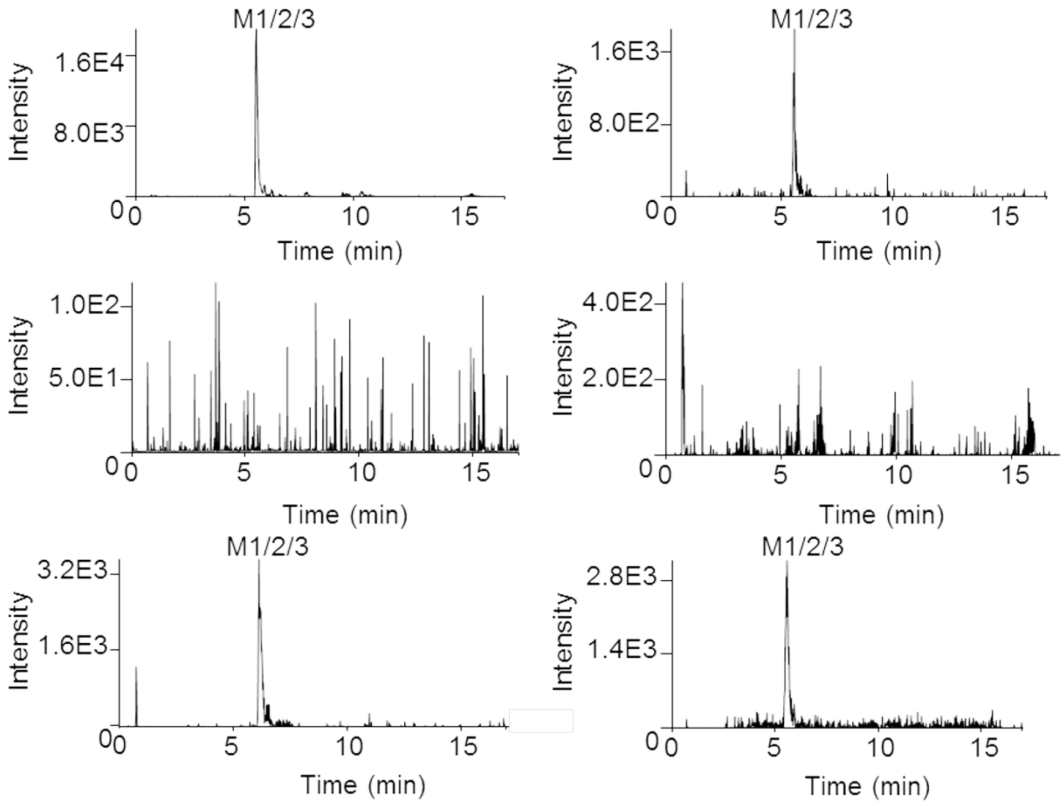

Figure 2. Representative chromatograms depicting metabolism of maraviroc by colon and vagina tissue biopsies. Biopsies were incubated with maraviroc (10 μM) for 24 hours at 37 °C. After incubation, the medium was collected and biopsies were homogenized in ethyl acetate. Medium and homogenates were analyzed via uHPLC-MS/MS in selected reaction monitoring mode. A. Colon 3 biopsy medium. B. Colon 3 biopsy in situ. C. Vagina 2 biopsy medium. D. Vagina 2 biopsy in situ. E. Vagina 3 biopsy medium. F. Vagina 3 biopsy in situ.

analyzed using uHPLC-MS/MS in product ion mode. In this manner, four monooxygenated (m/z = 346.4), two dioxygenated (m/z = 362.4), and five glucuronidated (m/z = 506.4 and m/z = 522.4) metabolites were identified. The monooxygenated metabolites were designated M1-M4, dioxygenated products M5-M6 and glucuronides M7-M11. No additional analytes corresponding to metabolites were detectable above background. Figure 3 shows the chromatograms for these metabolites that were obtained using uHPLC-MS/MS performed in selected reaction monitoring mode. Transitions for each metabolite were identified from the corresponding MS/MS fragmentation spectra and are detailed under Materials and Methods. Since NADPH is required for P450 activity and UDPGA (uridine diphosphate glucuronic acid) is required for UGT activity, it was possible to confirm which biotransformations were catalyzed by each enzyme class in the human liver microsomal system. When the reaction contained only NADPH, M1 was the most abundant metabolite and only products M1-M6 were detected. Reactions containing dapivirine in the presence of only UDPGA produced metabolite M7 as the sole detectable metabolite while formation of M8-M11 required incubation with both NADPH and UDPGA. In reactions that were performed in the absence of either NADPH or UDPGA no oxygenated or glucuronidated products, respectively, were detected. These data demonstrate that metabolites M1-M6 are CYP-dependent, M7 is UGT-dependent, and that the formations of M8-M11 are catalyzed by both P450s and UGTs acting in concert. Of the glucuronides, M7 and M11 are the most abundant metabolites.

In order to elucidate the chemical structures of each metabolite, the MS/MS spectra were analyzed. Potential structures and proposed origins of fragment ions for the mono- and di- oxygenated metabolites are presented in Figure 4. The fragments 316.2, 173.1, and

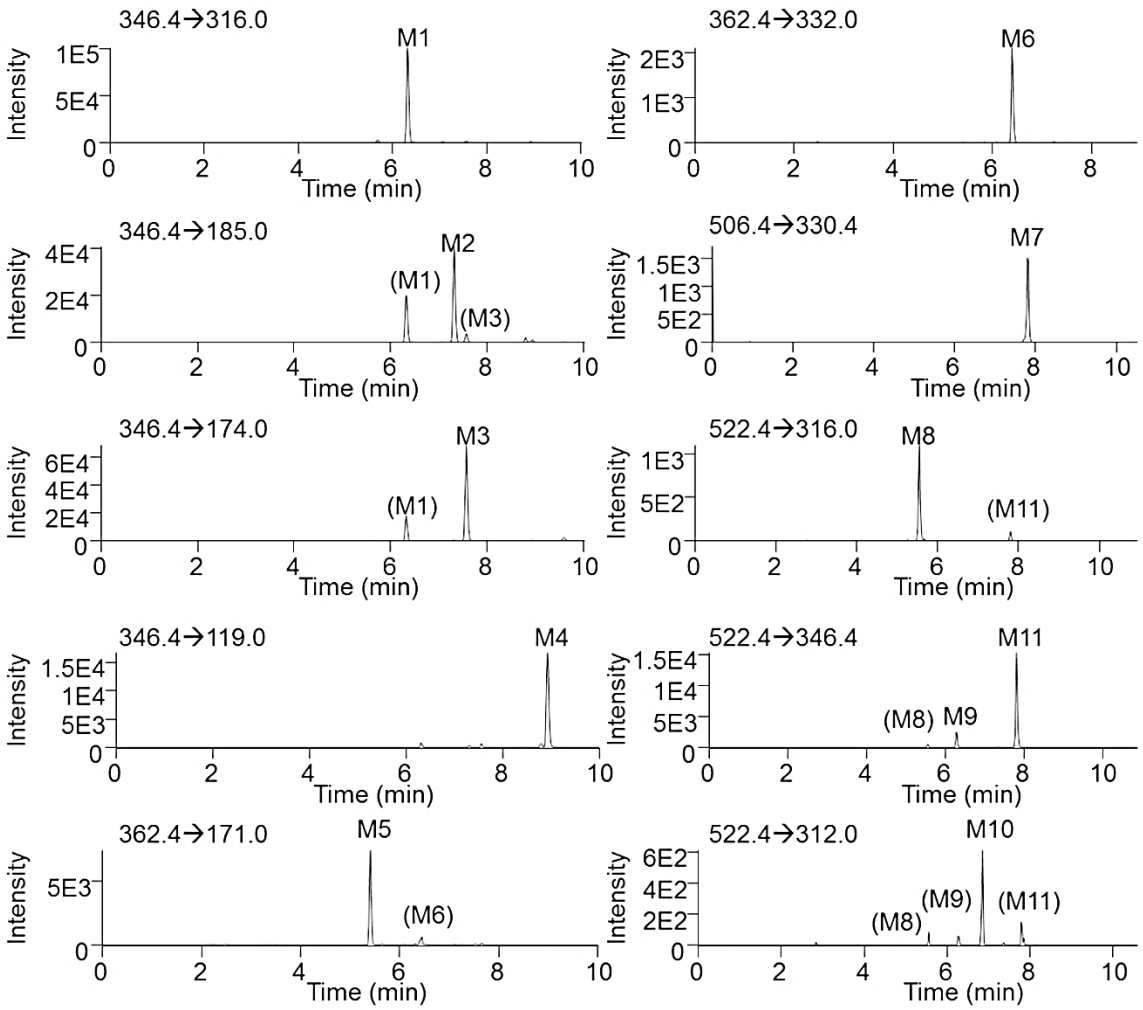

Figure 3. Extracted ion chromatograms showing the transitions used to monitor dapivirine metabolite formation. Dapivirine (10 μM) was incubated with human liver microsomes (1 mg/mL) for 30 min at 37 °C in the presence of a NADPH-regenerating system. Fragmentation spectra were used to derive the following transitions (Q1→Q3): M1 (m/z 346.4→316.0); M2 (m/z 346.4→185.0); M3 (m/z 346.4→174.0); M4 (m/z 346.4→119.0); M5 (m/z 362.4→171.0); M6 (m/z 362.4→332.0); M7 (m/z 506.4→330.4); M8 (m/z 522.4→316.0); M9 (m/z 522.4→346.4); M10 (m/z 522.4→312.0); and M11 (m/z 522.4→346.6).

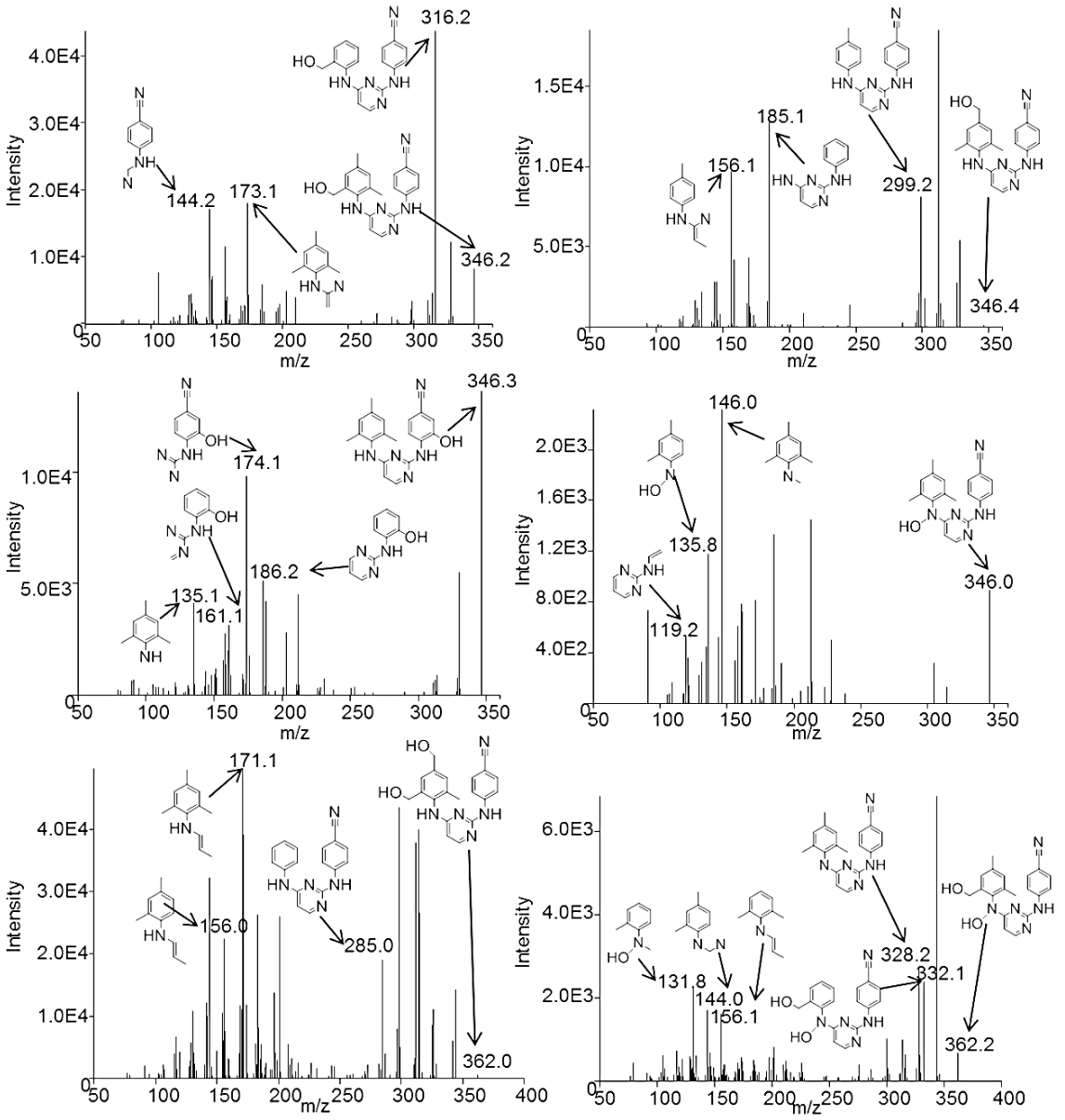

Figure 4. Fragmentation analysis of MS/MS spectra for M1-M6. Human liver microsomes (1 mg/mL) were incubated with 10 μM dapivirine for 30 min at 37 °C in the presence of a NADPH-regenerating system. Metabolites were detected and fragmented using uHPLC-MS/MS in product ion mode. From left to right, then top to bottom are M1, M2, M3, M4, M5, and M6.

144.2 *m/z* found in the spectrum of metabolite M1 are proposed to originate from the loss of C_2H_6, $C_9H_7N_3O$, and $C_{12}H_{14}N_2O$, respectively. Fragments of 299.2, 185.1, and 156.1 *m/z* in MS/MS spectrum collected for product M2 are due to the loss of C_2H_7O, $C_{10}H_{11}NO$, and $C_{10}H_{12}N_3O$, respectively. For M3, we propose that fragments 186.2, 174.1, 161.1, and 135.1 *m/z* derive from the loss of $C_{10}H_{12}N_2$, $C_{12}H_{14}N$, $C_{12}H_{13}N_2$, and $C_{11}H_7N_4O$, respectively. The spectrum of M4 has fragments 146.0, 135.8, and 119.2 *m/z*, corresponding to losses of $C_{10}H_8N_4O$, $C_{12}H_{10}N_4$, and $C_{14}H_{15}N_2O$, respectively. Metabolite M5 has ions of 285.0, 171.1, and 156.0 *m/z*, proposed to result from losses of $C_3H_9O_2$, $C_8H_7N_4O_2$, and $C_9H_{10}N_4O_2$, respectively. Lastly, the fragmentation spectrum of M6 shows ions of 332.1, 328.2, 156.1, 144.0, and 131.8 *m/z,* which are proposed to originate from the loss of H_2O_2, C_2H_6, $C_9H_{10}N_4O_2$, $C_{11}H_{12}N_3O_2$, and $C_{12}H_{14}N_4O$. Quality spectra were difficult to obtain for M7-M11, as for each of these products the glucuronic acid dissociated from the parent ion in the mass spectrometer; however, the remainder of the molecule did not fragment to detectable ions. Since M7 is only dependent on UDPGA, it must be the result of the direct glucuronidation of dapivirine. It is known that *O*- and *N*-glucuronidation are the most common glucuronidation reactions [9], thus the glucuronic acid moiety of M7 is most likely located on one of the secondary amines or a nitrogen atom within the pyrimidine ring. The other four glucuronides result from glucuronidation of monooxygenated metabolites M1-M4, although it remains to be determined whether the glucuronide conjugation to these metabolites occurs on the oxygen inserted by the CYP or on a nitrogen atom already present in dapivirine.

In order to further probe which sites of dapivirine were oxygenated by P450 enzymes metabolism assays were carried out using deuterated dapivirine, with 11 deuteriums

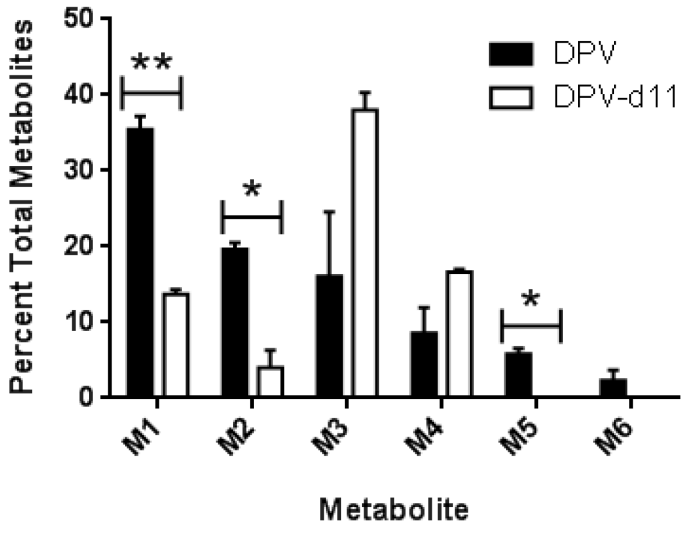

Figure 5. Determining which dapivirine metabolites are modified on the mesitylene ring. Relative contributions to total metabolite profile when dapivirine or dapivirine-d11 are incubated with human liver microsomes (1 mg/mL) for 60 min at 37 °C in the presence of an NADPH-regenerating system and UDPGA. All metabolites were detected in product ion mode. The experiment was carried out in triplicate. ** = $p \leq 0.01$.

replacing the 11 hydrogens on the mesitylene ring. Due to the isotope effects, oxygen insertions occurring at the deuterated locations proceed at a slower rate, resulting in decreased abundance of the oxygenated metabolites as compared to parallel assays performed using the non-isotopically labeled dapivirine. As can be seen in Figure 5, the relative abundances of M1 (p-value = 0.003), M2 (p-value = 0.014), and M5 (p-value = 0.018) were decreased when the deuteriums are present. Taken together, the fragmentation analyses and dapivirine-d11 studies indicate that M1 and M2 each result from monooxygenation of one of the three methyl groups of the mesitylene ring while M3 appears to be oxygenated on one of the four carbons of the benzene ring, M4 is oxygenated at the nitrogen connecting the mesitylene to the pyrimidine, M5 is oxygenated on two of the mesitylene carbons, and M6 is oxygenated on one mesitylene carbon and a secondary amine.

Enzymes Responsible for Dapivirine Metabolism

In order to determine which P450 isozymes were responsible for producing the observed dapivirine metabolites, metabolism assays were carried out using individual cDNA-expressed CYP1A2, -2A6, -2B6, -2C8, -2C9, -2C19, -2D6, -3A4, and -3A5 (Figure 6A). M1 was primarily produced by CYP1A2, -2B6, -2D6, -3A4, and -3A5 and to a lesser extent by CYP2C8 and -2C19. M2 had a similar profile, although CYP2A6 and -2D6 were minor contributors to the formation of this metabolite. M3 was primarily produced by CYP3A4 and -3A5, with minor production by CYP1A2, -2C8, -2C19, and -2D6. Formation of M4 was primarily catalyzed by CYP1A2 with all of other CYP isozymes tested being minor contributors. M5 was produced solely by CYP3A5 and M6 was most

abundant in the incubations containing CYP3A4 with CYP2D6 and -3A5 as lesser contributors.

The relative contributions of each P450 to overall formation of these metabolites in vitro was explored by performing human liver microsome metabolism assays in the presence and absence of small molecule inhibitors of the individual P450 isozymes (Figure 6B). There were no statistically significant differences in the formation of any of the metabolites when furafylline, which inhibits CYP1A2, nor sulfaphenazole, which inhibits CYP2C9, nor when quinidine, which inhibits CYP2D6, were present. When a CYP2B6 inhibitor, 2-phenyl-2-(1-piperidenyl), was present, the production of M2, M3, and M4 was decreased. An inhibitor for CYP2C19, benzylnirvanol, resulted in decreased production of M3 and M6. The greatest decreases in M2-M6 production were observed when ketoconazole, an inhibitor of CYP3A4/5, was present. In addition, M1 production was also decreased in the incubations containing ketoconazole.

Relative contributions of UGT isozymes to the formation of glucuronides M7-M11 were also probed (Figure 7). Dapivirine was incubated with human liver microsomes in the presence of a NADPH-regenerating system, so that all P450-mediated metabolites were produced. The reaction product was then incubated with individual cDNA-expressed UGT1A1, -1A3, -1A4, -1A6, -1A7, -1A8, -1A9, -1A10, -2B4, -2B7, -2B15, and -2B17. M7 was primarily produced by UGT1A4 and -2B7, with UGT1A1 as a minor producer. UGT1A1 was the major contributor to M8 formation and UGT1A3, -1A4, -2B7, and -2B15 were minor contributors. M9 was most abundant in the incubations containing UGT1A7, -1A9, and -2B7 while UGT1A6, -1A8, -1A10, and -2B4 were minor producers. M10 formation was primarily catalyzed by UGT2B7 and to a lesser

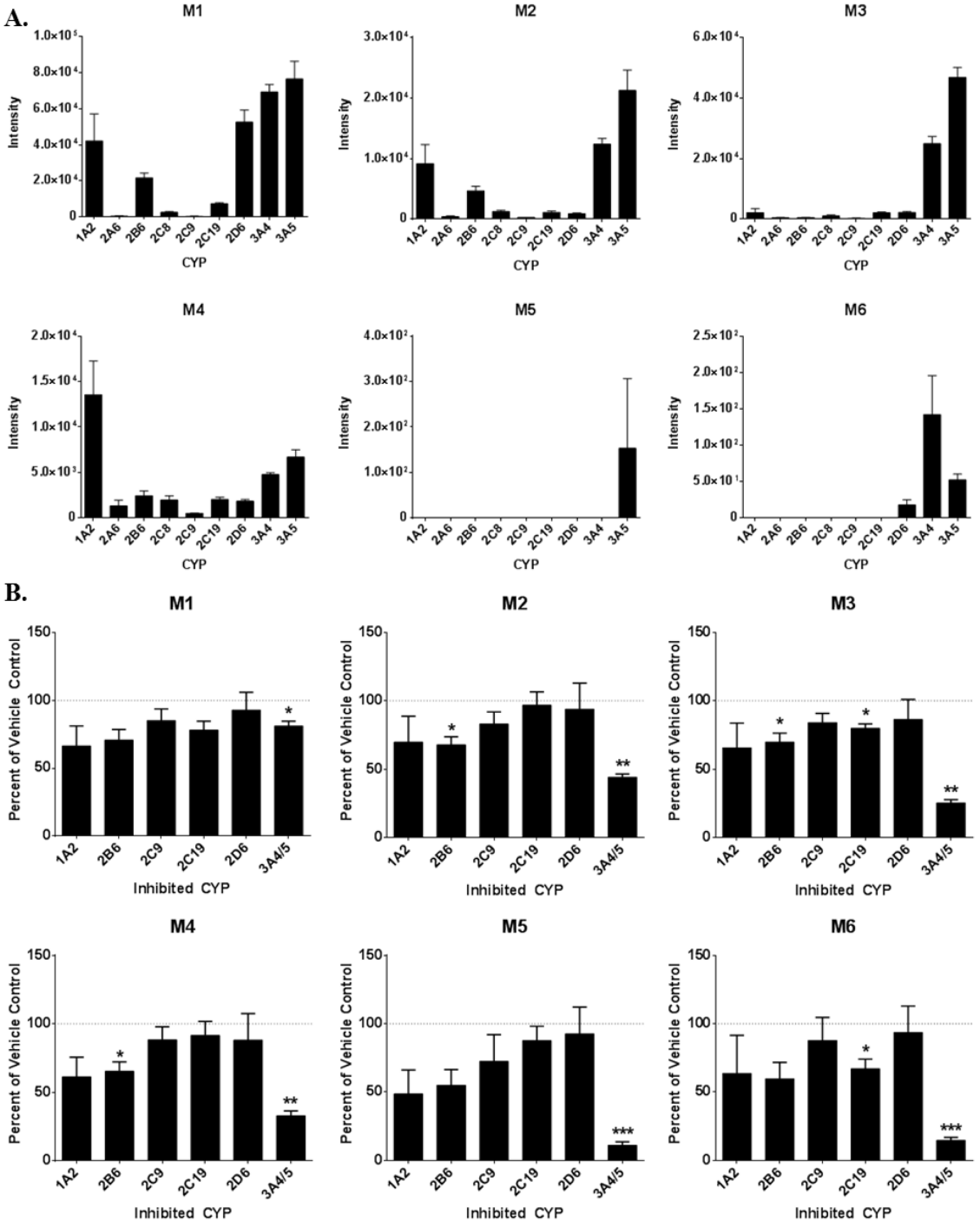
A.
M1
M2
M3
M4
M5
M6
Intensity
CYP
1A2
2A6
2B6
2C8
2C9
2C19
2D6
3A4
3A5
B.
Percent of Vehicle Control
Inhibited CYP
2B6
2C9
2C19
2D6
3A4/5

Figure 6. Formation of dapivirine metabolites by P450 isozymes. A. Ability of individual cDNA-expressed P450s to produce dapivirine metabolites. P450 isozymes (10 pmol/mL) were incubated individually with dapivirine (10 μM) for 30 min at 37 °C in the presence of an NADPH-regenerating system. B. Inhibition of individual P450s in order to examine dapivirine metabolite production when multiple P450 isozymes are present. Human liver microsomes (1 mg/mL) were preincubated with small molecule P450 inhibitors in the presence of a NADPH-regenerating system for 5 min at 37 °C prior to the addition of dapivirine (10 μM), then incubated for 30 min at 37°C. Dapivirine metabolites were detected via uHPLC-MS/MS in selected reaction monitoring mode. The experiments were performed in triplicate. * = $p \leq 0.05$; ** = $p \leq 0.01$; *** = $p \leq 0.001$.

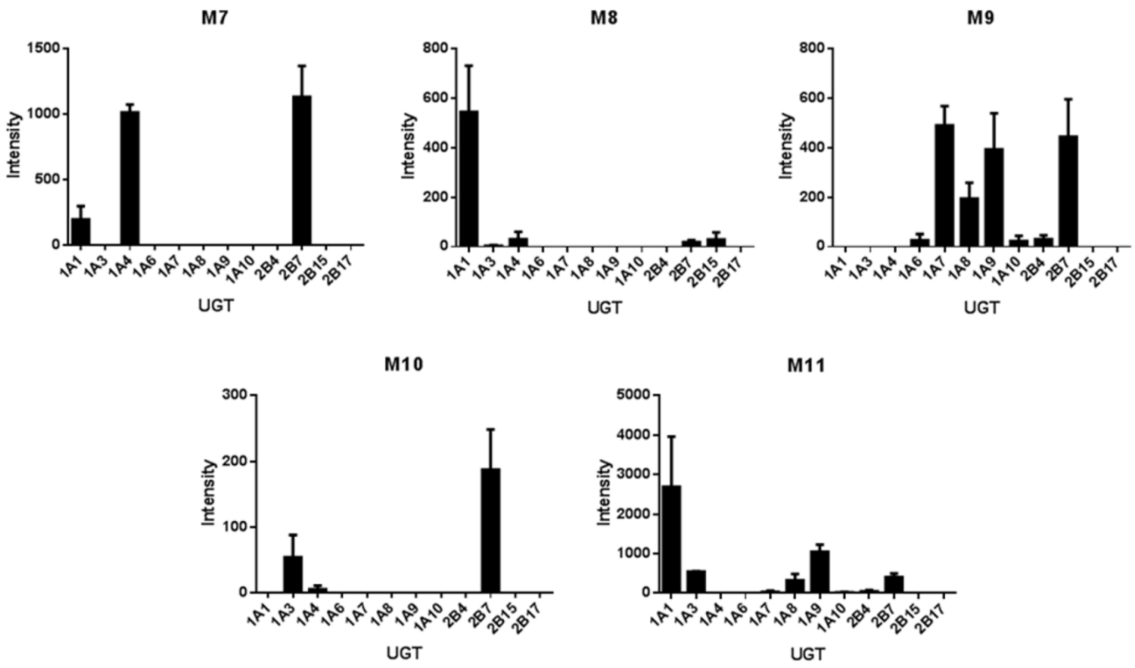

Figure 7. Ability of individual UGTs to produce dapivirine metabolites. For the UGT incubations, dapivirine (10 μM) was incubated with human liver microsomes (2 mg/mL) for 30 min at 37 °C in the presence of NADPH-regenerating system, the reactions were quenched and dried under vacuum followed by resuspension of the residue in methanol for use as a substrate for UGTs. UGT (0.2 mg/mL) incubations were for 60 min at 37 °C in the presence of UDPGA. Dapivirine metabolites were detected using uHPLC-MS/MS in selected reaction monitoring mode. Experiments were carried out in triplicate.

extent by UGT1A3 and -1A4. Lastly, UGT1A1 was the major contributor to M11 production and UGT1A3, -1A7, -1A8, -1A9, -2B4, and -2B7 were minor contributors.

Dapivirine Metabolism by Vaginal and Colorectal Tissues

Following the identification of the metabolites that result from dapivirine metabolism and the demonstration that mucosal tissues produce maraviroc metabolites, dapivirine was similarly used as a probe for enzymatic activity in mucosal tissues (Figure 8). The biopsies were submerged in culture medium and following 24 hours of dapivirine treatment, monooxygenated metabolites M1 and M4 as well as glucuronides M7 and M11 were consistently detected in medium that was incubated with colorectal biopsies. However, only monooxygenated metabolites M1, M2, and M4 could be detected in the medium used to treat vaginal biopsies. Tissue biopsies were also homogenized in ethyl acetate in order to detect metabolites in situ. M1, M2, M3, M4, M7, and M11 were all detected within colon tissues while only M1, M2, M3, and M4 were present in vagina tissue. These differences were consistent in the matched colon and vagina biopsy samples from the same donor. In addition, no metabolites were identified following incubation with colorectal or vaginal tissue that were not present in the human liver microsome or cDNA-expressed enzyme systems. Taken together, these data are a demonstration of P450 activity in both colon and vagina tissues, whereas UGTs that catalyze the formation of dapivirine and dapivirine metabolite glucuronic acid conjugates may be active in colon but not vagina.

Since drug-induced changes in P450 expression are a major mechanism of drug-drug interactions, dapivirine treatment dependent P450 mRNA changes were explored in colorectal tissue (Figure 9). Such analysis could not be performed in vaginal tissue due to

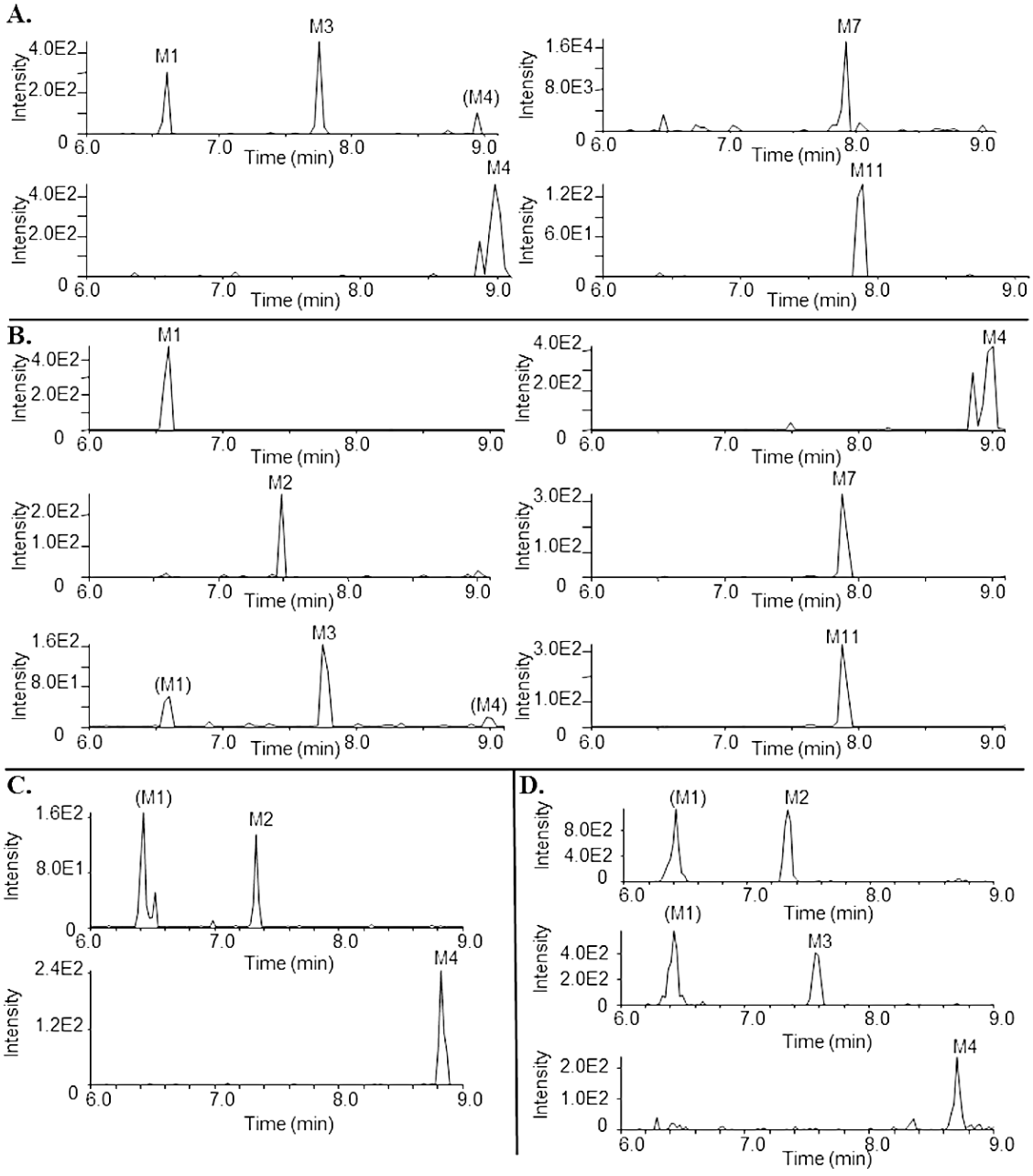
A.
M1
M3
(M4)
M4
M7
M11
B.
M1
M4
M2
M7
(M1)
M3
M11
C.
(M1)
M2
M4
D.
(M1)
M2
(M1)
M3
M4
Intensity
Time (min)

Figure 8. Representative chromatograms depicting metabolism of dapivirine by colon and vagina tissue biopsies. Biopsies were incubated with dapivirine (10 μM) for 24 hours at 37 °C. After incubation, the medium was collected and biopsies were homogenized in ethyl acetate. Medium and homogenates were analyzed via uHPLC-MS/MS in selected reaction monitoring mode. A. Colon 3 biopsy medium. B. Colon 3 biopsy in situ. C.Vagina 3 biopsy medium. D. Vagina 3 biopsy in situ.

limited tissue availability as a result of the marked difference in the maximum amount of tissue that could reasonably be collected from the colon versus the vagina. Colon donor 1 (age 49, female) demonstrated a 3-fold decrease of CYP2B6 and a 4-fold decrease in CYP2E1 mRNA levels following 24 hours of dapivirine treatment and no changes in CYP1A1, -1A2, -2C19, -3A4, nor -3A5 mRNA, as compared to the vehicle-treated control tissue that was cultured in parallel with the drug-treated samples. The second colon donor (age 24, male) exhibited a 4-fold, 5-fold, 5-fold and 7-fold increase in CYP1A2, CYP2C19, CYP2E1 and CYP3A4 mRNA levels, respectively, after 24 hours, and no changes in mRNA levels of CYP1A1, -2B6, nor -3A5.The third donor (age 28, female) demonstrated a 2.5-fold increase in CYP3A4 mRNA levels with no other changes. It was previously reported that etravirine modulates CYP3A4 expression in a pregnane x receptor (PXR)-dependent manner [10]. When biopsies from the third donor were incubated in the presence of both dapivirine and sulforaphane, a PXR inhibitor, the 2.5-fold increase in CYP3A4 mRNA observed with dapivirine alone was abrogated (Fig 9D). With this in mind, PXR mRNA expression in the colon tissues was measured and showed positive correlation with the observed changes in CYP3A4 mRNA, indicating that there may be a relationship between PXR levels and dapivirine-treatment dependent CYP3A4 mRNA expression changes in colon tissue (Figure 9E).

Dapivirine dependent induction of CYP3A4 mRNA in primary human hepatocytes

The potential for dapivirine to induce CYP3A4 expression was further explored by incubating primary human hepatocytes with dapivirine for increasing amounts of time (Fig 10). Hepatocyte donors 1 and 3 showed no significant change in CYP3A4 mRNA level whereas hepatocyte donor 2 showed 5.3-fold, 4.8-fold, and 16.9-fold induction at 6,

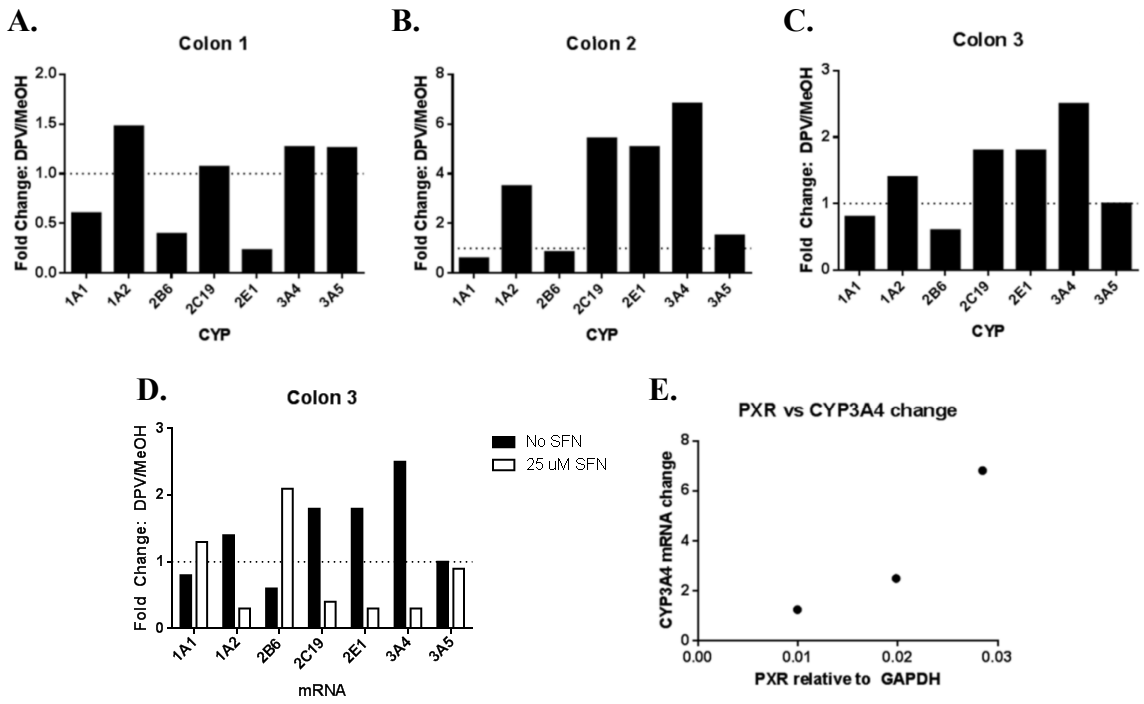

Figure 9. **Dapivirine-treatment mediated changes in colon P450 mRNA levels and the relationship to basal PXR expression**. Colon biopsies (A-C) were incubated with dapivirine (10 μM) for 24 hours at 37 °C. Biopsies from colon 3 were also incubated in the presence of 25 μM sulforaphane (D). After incubation, RNA was isolated and used in qRT-PCR to quantify P450 and PXR mRNA levels (E).

Figure 10. Dapivirine dependent induction of CYP3A4 mRNA in one out of three hepatocyte donors. Dapivirine (10 μM) was incubated with primary human hepatocytes for 6, 12, and 24 hours at 37 °C. After incubation, RNA was isolated and used in qRT-PCR to quantify P450 mRNA levels.

12, and 24 hours, respectively. Hepatocyte donor 1 demonstrated 5-fold decrease in CYP2B6 mRNA at 6 hours, but the trend did not continue through extended incubation. Lastly, hepatocyte donor 3 showed 11.9-fold, 14.6-fold, and 14.1-fold decrease in CYP1A1 mRNA and 2.1-fold, 5.6-fold, and 7.3-fold decrease in CYP1A2 mRNA over 6, 12, and 24 hours, respectively.

Dapivirine metabolism by multiple animal species

In order to determine which animal species would be the ideal model system for examining dapivirine metabolism, metabolism assays were carried out using liver microsomes from the following species: BALB/c mouse, Sprague-Dawley rat, New Zealand rabbit, rhesus monkey, cynomolgous monkey, CD-1 mouse, Sinclair minipig, Hartley albino guinea pig, golden Syrian hamster, and beagle dog. Reactions were carried out in the presence and absence of NADPH regenerating system (Figure 11). BALB/c mouse, Sprague-Dawley rat, and New Zealand rabbit displayed significantly greater production of M1 than humans (p-values 0.028, 0.001, and 0.035, respectively). Golden Syrian hamster deviated from the other animals in that there was no production of monohydroxylates M1-M3 in the presence of NADPH, but M1-M3 were all produced in the absence of NADPH. The rat, guinea pig, and beagle produced significantly larger amounts of M2 than humans (p-values 0.008, 0.014, and 0.049, respectively) and cynomolgous monkey and golden Syrian hamster produced significantly less M3 than humans (p-values 0.0009 and 0.0040, respectively). M4 production varied greatly, with rabbit, cynomolgous monkey, minipig, and hamster producing less than humans (p-values 0.0010, 0.0004, 0.0340, and 0.0002, respectively) and guinea pig and beagle producing greater amounts (p-values 0.0359 and 0.0446, respectively). There were no

Figure 11. Dapivirine metabolism by microsomes from multiple animal species. Dapivirine was incubated with liver microsomes (1 mg/mL) for 30 min at 37 °C in the presence or absence of a NADPH-regenerating system. Experiment performed in triplicate. Two-tailed unpaired student's t tests were carried out to compare each animal to humans. * = $p \leq 0.05$; ** = $p \leq 0.01$; *** = $p \leq 0.001$.

statistically significant differences in M5 production. Lastly, rabbit produced less M6 than humans (p-value 0.013) whereas rat, rhesus monkey, and cynomolgous monkey produced more (p-values 0.012, 0.022, and 0.010, respectively). Overall, CD-1 mouse is the only animal that did not display any statistically significant differences in dapivirine metabolism when compared to humans.

Discussion

Through an examination of dapivirine and maraviroc metabolism in colon and vagina tissues, the present study demonstrates, for the first time, P450 activity in both colon and vagina and UGT activity in colon. While dapivirine metabolism was consistent across donors, and maraviroc was metabolized in all colon donors, maraviroc was only metabolized in one of the two vagina biopsies treated. This hints at inter-individual differences in antiretroviral drug metabolism and disposition which will have to be explored further. While the relatively small number of samples employed in the current study is a potential limitation, these data lay the groundwork for future studies of drug metabolism in the vaginal and colorectal mucosa. Analyses of larger study populations will be required to gain a comprehensive understanding of tissue-specific biotransformation in these compartments.

While the liver is the primary organ responsible for xenobiotic metabolism, when drugs are dosed orally, mucosal tissues may be important to the local metabolism of topical drugs used as microbicides. Previous studies have examined colorectal P450 mRNA expression [11, 12]. These studies found that multiple members of the CYP2C, CYP2E, and CYP3A families are expressed on the mRNA and protein level in human

colon biopsy tissue, and that this expression may vary in different parts of the colon. There have also been studies that detect protein or mRNA expression of CYP1A, CYP2B, CYP2C, and CYP3A in cervical tissue [13-15]. However, enzymatic activity of P540s and other metabolizing enzymes in the colon and vagina has not yet been reported. Using qRT-PCR, the present study demonstrates differences in P450 mRNA expression levels between colon and vagina tissues, finding higher CYP1A2 and -2B6 mRNA in vagina and greater expression of CYP3A5 mRNA in colon. Immunoblots also revealed that protein expression of CYP2B6, -2C19, and -3A4 is higher in the vagina than in the colon. Interestingly, in colon samples, dapivirine stimulated increases in CYP3A4 mRNA levels that appeared to be positively correlated with basal PXR mRNA expression. PXR is a nuclear receptor that contributes to the transcriptional regulation of CYP3A4 [6] and we have previously demonstrated that etravirine, which is structurally similar to dapivirine, upregulates CYP3A4 mRNA expression in a PXR-dependent manner [10]. As such, PXR may play a role in mediating the dapivirine-dependent increases in CYP3A4 mRNA levels in colorectal tissue that were observed here.

The proposed scheme for P450-mediated metabolism of dapivirine is presented in Figure 12. Both colon and vagina tissues were able to metabolize dapivirine, producing metabolites that were determined to be P450-mediated using human liver microsomes. This is a definitive demonstration of P450 activity in colorectal and vaginal tissues. Metabolites M1-M4 were produced by colon and vagina tissue biopsies, and the P450 isozymes that we determined were responsible for the formation of these dapivirine metabolites were all found to be expressed in these same biopsies using immunoblotting. Dapivirine oxygenations occurred on the mesitylene and phenyl rings but not the pyridine

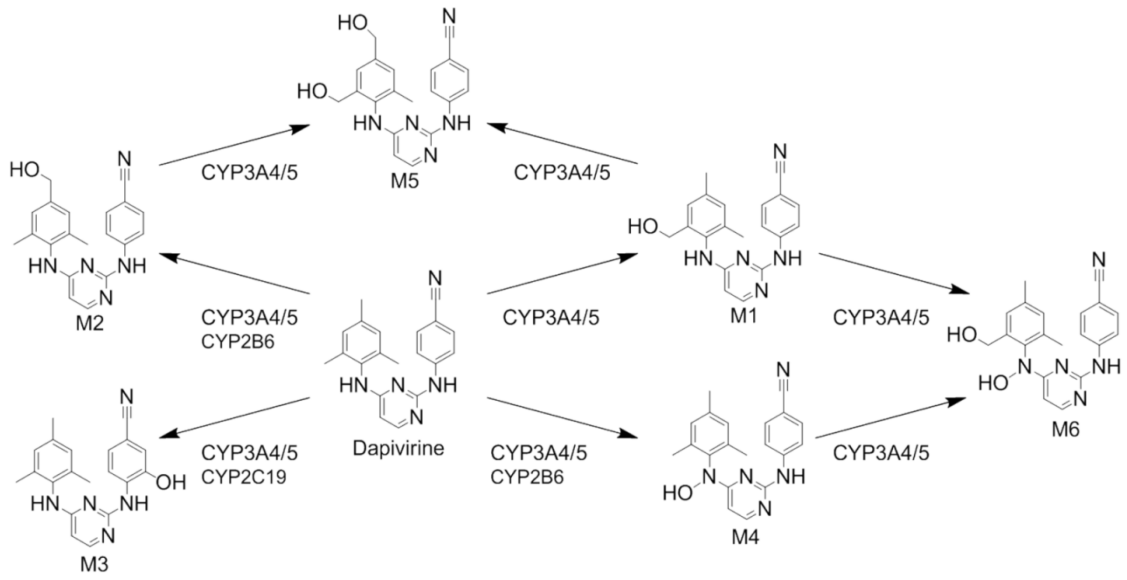

Figure 12. Proposed P450-mediated metabolism of dapivirine.

ring. This may be due to constraints on substrate positioning within the active site of the P450 isozymes, which can be further examined through the use of molecular docking.

Incubations of dapivirine with individual cDNA-expressed P450s or human liver microsomes with small molecule inhibitors of individual P450s established which P450 isozymes produce the observed metabolites of dapivirine. There is strong evidence for major contributions from CYP3A4 and -3A5, since human liver microsomes pre-incubated with the CYP3A inhibitor ketoconazole exhibited significantly lower production of all oxygenated metabolites with the exception of M1. Production of M1 was shown to be catalyzed by cDNA expressed CYP1A2, -2B6, -2D6, -3A4, and -3A5. Thus, even in the presence of chemical inhibition of CYP3A4/5 activity in human liver microsomes this metabolite may be formed by other microsomal P450 isozymes. It was also noted that CYP1A2 appeared to be able to produce metabolite M4 in our cDNA-expressed P450 assays; however, incubation of human liver microsomes with the CYP1A2 inhibitor furafylline did not result in a significant decrease in M4 levels. These data indicate that, while CYP1A2 may have the ability to form M4, this enzyme may not be a major contributor to the formation of this metabolite in a system where all hepatic microsomal P450 isozymes are present. Interestingly, while P450-dependent metabolites of dapivirine were detected in the culture medium collected following incubation with both vaginal and colorectal tissue as well as in situ in both tissues the UGT-dependent metabolites of this compound were only produced by colorectal tissue. This difference in metabolism may lead to differential rates of clearance between the two tissues.

Further, our data indicate that metabolism of dapivirine and maraviroc by vaginal and colorectal tissue may vary from hepatic metabolism of these drugs. The ideal

comparison to examine differences in hepatic and mucosal metabolism would be to compare human liver microsomes to microsomes isolated from the colorectal and vaginal mucosa. However, due to constraints on the amount of tissue that can be collected from living donors, neither colorectal nor vaginal microsomes were able to be isolated in large enough quantities to facilitate metabolism assays. Additionally, it is not feasible to collect liver tissue from living donors to be used as a direct comparison to the mucosal biopsies we have studied. A potential difference in metabolism of a drug dosed orally versus topically is particularly evident in the case of maraviroc since in the present study we observed a marked difference in metabolite formation by colorectal and vaginal tissues as compared to the metabolite profiles that we have previously described in plasma and urine of human subjects following oral administration of maraviroc [8]. As such, both tissue and hepatic biotransformation may need to be examined in working to gain a complete understanding of the clearance of antiretrovirals and other drugs being developed for both oral and topical administration. Since dapivirine is being developed for topical use only, metabolism by the tissue upon which dapivirine would be administered is likely to be the most relevant in understanding the biotransformation of this compound.

In order to facilitate the success of HIV PrEP while concurrently avoiding selection for resistant strains of virus it is crucial that the factors that regulate the exposure to individual antiretrovirals be understood. While dapivirine is highly potent with an IC_{50} in the nanomolar range for both cell-free and cell-associated virus [16, 17], it has been shown that suboptimal concentrations of dapivirine can still lead to resistance [18]. Patient non-adherence is the most widely cited factor for lower than intended

concentrations of drugs, but drug metabolism must also be taken into account. If the metabolites are not pharmacologically active against HIV, individuals with high metabolic activity may experience decreased efficacy and select for resistant strains of virus. For instance, CYP3A5 which we have demonstrated here to be a major contributor to dapivirine metabolism, is highly polymorphic [19] and as such CYP3A5 genotype could potentially influence the vaginal and colorectal tissue exposure to dapivirine. Biotransformation of drugs may also produce toxic metabolites, as is the case with the 8-hydroxy metabolite of efavirenz, another NNRTI [20]. Toxic metabolites formed locally by the vaginal and colorectal tissues have the potential to stimulate inflammation in the mucosa, whether from mucosal cell death or pathogenic bacteria displacing the commensal species, which may initiate the recruitment of immune cells and make establishment of HIV infection more likely [21]. While studies have already shown that dapivirine is not toxic to commensal vaginal *Lactobacillus* [22] this testing has not been performed for the dapivirine metabolites. To this end, now that the metabolites of dapivirine have been identified, future studies should include an analysis of the toxicity and pharmacologic activity of these compounds. Such studies will help to understand how inter-individual differences in metabolizing enzyme activity may contribute to differences in toxicity and efficacy across populations. Because these dapivirine metabolites were previously unreported, reference standards were unavailable for development of a quantitative assay. The current qualitative assay serves the desired purpose of metabolite identification and preliminary characterization, and could be developed into a quantitative assay which would be required for studying the in vivo pharmacokinetics of dapivirine metabolites.

In summary, the studies described here examine the metabolism in vaginal and colorectal tissues of dapivirine and maraviroc, a NNRTI and an entry inhibitor, respectively, being developed for use as topical microbicides for HIV PrEP. P450 activity was demonstrated for the first time in vaginal and colorectal mucosal tissues and potential differences in P450 and UGT expression and activity between these two tissues were revealed. We anticipate that these data can be leveraged in order to inform the development of antiretroviral drugs as topical microbicides for HIV PrEP as well as a broader spectrum of drugs that may be developed for administration to vaginal and colorectal tissues for other indications.

References

1. Baeten J, Celum C. Systemic and topical drugs for the prevention of HIV infection: antiretroviral pre-exposure prophylaxis. Annu Rev Med **2013**; 64:219-32.

2. Adams JL, Kashuba AD. Formulation, pharmacokinetics and pharmacodynamics of topical microbicides. Best Pract Res Clin Obstet Gynaecol **2012**; 26:451-62.

3. Hendrix CW, Chen BA, Guddera V, et al. MTN-001: randomized pharmacokinetic cross-over study comparing tenofovir vaginal gel and oral tablets in vaginal tissue and other compartments. PLoS One **2013**; 8:e55013.

4. Lewi P, Heeres J, Arien K, et al. Reverse transcriptase inhibitors as microbicides. Curr HIV Res **2012**; 10:27-35.

5. Fetherston SM, Boyd P, McCoy CF, et al. A silicone elastomer vaginal ring for HIV prevention containing two microbicides with different mechanisms of action. Eur J Pharm Sci **2012**; 48:406-15.

6. Zanger UM, Schwab M. Cytochrome P450 enzymes in drug metabolism: Regulation of gene expression, enzyme activities, and impact of genetic variation. Pharmacol Ther **2013**; 138:103-41.

7. Guengerich FP. Common and uncommon cytochrome P450 reactions related to metabolism and chemical toxicity. Chem Res Toxicol **2001**; 14:611-50.

8. Lu Y, Hendrix CW, Bumpus NN. Cytochrome P450 3A5 plays a prominent role in the oxidative metabolism of the anti-human immunodeficiency virus drug maraviroc. Drug Metab Dispos **2012**; 40:2221-30.

9. Kaivosaari S, Finel M, Koskinen M. N-glucuronidation of drugs and other xenobiotics by human and animal UDP-glucuronosyltransferases. Xenobiotica **2011**; 41:652-69.

10. Yanakakis LJ, Bumpus NN. Biotransformation of the antiretroviral drug etravirine: metabolite identification, reaction phenotyping, and characterization of autoinduction of cytochrome P450-dependent metabolism. Drug Metab Dispos **2012**; 40:803-14.

11. Thorn M, Finnstrom N, Lundgren S, et al. Cytochromes P450 and MDR1 mRNA expression along the human gastrointestinal tract. Br J Clin Pharmacol **2005**; 60:54-60.

12. Bergheim I, Bode C, Parlesak A. Distribution of cytochrome P450 2C, 2E1, 3A4, and 3A5 in human colon mucosa. BMC Clin Pharmacol **2005**; 5:4.

13. Patel KR, Astley S, Adams DJ, et al. Expression of cytochrome P450 enzymes in the cervix. An immunohistochemical study. Int J Gynecol Cancer **1993**; 3:159-63.

14. Farin FM, Bigler LG, Oda D, et al. Expression of cytochrome P450 and microsomal exposide hydrolase in cervical and oral epithelial cells immortalized by human papillomavirus type 16 E6/E7 genes. Carcinogenesis **1995**; 16:1670.

15. Yokose T, Doy M, Taniguchi T, et al. Immunohistochemical study of cytochrome P450 2C and 3A in human non-neoplastic and neoplastic tissues. Virchows Arch **1999**; 434:401-11.

16. Van Herrewege Y, Michiels J, Van Roey J, et al. In vitro evaluation of nonnucleoside reverse transcriptase inhibitors UC-781 and TMC120-R147681 as human immunodeficiency virus microbicides. Antimicrob Agents Chemother **2004**; 48:337-9.

17. Fletcher P, Harman S, Azijn H, et al. Inhibition of human immunodeficiency virus type 1 infection by the candidate microbicide dapivirine, a nonnucleoside reverse transcriptase inhibitor. Antimicrobial agents and chemotherapy **2009**; 53:487-95.

18. Schader SM, Oliveira M, Ibanescu RI, et al. In vitro resistance profile of the candidate HIV-1 microbicide drug dapivirine. Antimicrobial agents and chemotherapy **2012**; 56:751-6.

19. Guengerich FP. Cytochrome P450s and other enzymes in drug metabolism and toxicity. AAPS J **2006**; 8:E101-11.

20. Bumpus NN. Efavirenz and 8-hydroxyefavirenz induce cell death via a JNK- and BimEL-dependent mechanism in primary human hepatocytes. Toxicol Appl Pharmacol **2011**; 257:227-34.

21. Eade CR, Cole AL, Diaz C, et al. The anti-HIV microbicide candidate RC-101 inhibits pathogenic vaginal bacteria without harming endogenous flora or mucosa. Am J Reprod Immunol **2013**; 69:150-8.

22. Moncla BJ, Pryke K, Rohan LC, et al. Testing of viscous anti-HIV microbicides using Lactobacillus. J Microbiol Methods **2012**; 88:292-6.

Chapter 3: Identification and expression profiling of nucleoside kinases that activate tenofovir in tissues targeted by human immunodeficiency and hepatitis B virus

Abstract

Nucleoside reverse transcriptase inhibitors such as tenofovir are used to treat and prevent human immunodeficiency virus infections and to treat hepatitis B infections. These drugs must be phosphorylated intracellularly in order to become active within the tissue types targeted by these viruses; however the enzymes that modulate the activation of these drugs are unknown. Here we probed the expression of candidate nucleotide kinases in peripheral blood mononuclear cells, $CD4^+$ cells, colorectal tissue, vaginal tissue, and liver tissue. We found that expression of adenylate kinase 2 and creatine kinases was markedly higher in colon tissues versus white blood cells and vaginal tissue. Knockdown of candidate nucleotide kinases also shows that adenylate kinase 2 and pyruvate kinases activate tenofovir in white blood cells and vaginal tissues whereas adenylate kinase 2 and creatine kinase muscle carry out the activation in colorectal tissues. Taken together, these data form an understanding of which enzymes are responsible for the activation of nucleoside reverse transcriptase inhibitors in these tissues and cells.

Introduction

Antiretroviral therapies such as tenofovir (TFV) are used to decrease viral counts in individuals infected with human immunodeficiency virus (HIV), hepatitis B (HBV), or both [1]. These compounds are nucleoside based reverse transcriptase inhibitors (NRTIs) that require intracellular phosphorylation to their active forms, which are analogous to the natural nucleotide triphosphate substrates of viral reverse transcriptase [2]. However, HBV targets hepatocytes within the liver while HIV targets $CD4^+$ cells. Drugs that are taken orally are subject to the first-pass effect, whereby a drug may be extensively metabolized in the liver and gastrointestinal tract before reaching the systemic circulation. While hepatic metabolism of drugs meant to treat HBV may result in drug activation within hepatocytes, drugs meant to treat HIV must proceed beyond the liver and gastrointestinal tract to be activated within $CD4^+$ cells in the systemic circulation. Attempts to prevent the establishment of HIV infection have included topical application of antiretroviral therapies to the mucosal tissues of infection, which allows drugs to bypass the liver in order to reach the targeted $CD4^+$ cells within the colon and vagina mucosa [3]. As such, the expression and activity of the endogenous kinases that phosphorylate tenofovir, thus influencing the efficacy of therapy, must be understood in the liver (HBV) and $CD4^+$ T cells in circulation, in the colon and in the lower female genital tract (HIV).

TFV is an analogue of adenosine 5'-monophosphate that needs to undergo two phosphorylation steps to achieve its active form, tenofovir diphosphate (TFV-DP) [4]. While TFV-DP has an exceptionally long intracellular half-life of ≥ 60 h, TFV itself is not orally bioavailable and must be given as the prodrug tenofovir disoproxil fumarate

[5]. Tenofovir disoproxil fumarate contains two ester groups to enhance oral bioavailability. These esters are believed to be removed as the prodrug is absorbed by the intestines and within the liver [6]. TFV can then be phosphorylated to tenofovir monophosphate (TFV-MP) and subsequently TFV-DP in hepatocytes or in $CD4^+$ T cells. It has been shown that treating primary human hepatocytes and peripheral blood mononuclear cells (PBMCs), which contain $CD4^+$ cells, in vitro with TFV can produce TFV-DP [7, 8].

The adenylate kinase (AK) enzyme family is proposed to be responsible for the first phosphorylation step of TFV. Using subcellular fractions from a human T lymphoblast cell line, AK2 was shown to have potent kinase activity towards adefovir, a structural analogue of TFV, in vitro while AK1 and AK3 were shown to have no demonstrable activity [9]. This study also showed phosphorylation of TFV in the same system, but only reported kinetic parameters for the phosphorylation of adefovir (K_M = 14.0 ± 2.8 mM and k_{cat} = 6.8 ± 1.2 s^{-1}). The remaining AK isozymes have not been tested. While the nucleotide diphosphate kinase enzyme family is proposed to be responsible for the second phosphorylation step [5], in vitro studies using purified enzymes disagree on the ability of NDPK to perform this step [10, 11]. Koch, *et al.,* showed low activity towards TFV-MP (K_M = 0.29 ± 0.03 mM and k_{cat} = 0.12 ± 0.01 s^{-1}), but Varga, *et al.,* could not detect any NDPK activity towards TFV-MP. However, both studies demonstrate potent TFV-MP phosphorylation activity by the creatine kinase (CK) enzyme family and lower yet efficient activity by the pyruvate kinase (PK) enzyme family. The CK family consists of a brain isoform (CKB), a muscle isoform (CKM), and two mitochondrial isoforms (CKMT1 and CKMT2) while the PK family has a liver/red

blood cell isoform (PKLR) and a muscle isoform (PKM). Koch, *et al.,* reported kinetic parameters for CKB activity towards TFV-MP and indicated that CKM activity was similar (K_M = 1.2 ± 0.20 mM, k_{cat} = 400 ± 30 s^{-1}), whereas Varga *et al.* only tested CKM and found lower activity (K_M = 0.24 mM, k_{cat} = 1.9 s^{-1}). Both studies monitor activity by directly detecting TFV-DP using high performance liquid chromatography, and the CKB and CKM isoforms display 81% amino acid similarity, so the discrepancy likely arises from the higher assay temperature and presence of enzyme activators in Koch *et al.*'s CK assays. The mitochondrial CK isoforms, which show 63-67% amino acid similarity with the brain and muscle isoforms, have never been examined for activity towards tenofovir. Studies examining PK activity towards TFV-MP have only used rabbit PKM, with Koch *et al.* obtaining the kinetic parameters K_M = 11 ± 3 mM and k_{cat} = 6.8 ± 2.3 s^{-1}. Varga *et al.* were unable to calculate K_M, but assuming K_M = 11 mM were able to calculate k_{cat} = 1.35 s^{-1} from the obtained reaction velocity of 0.112 s^{-1}. Rabbit PKM has 97% amino acid identity with human PKM, thus the observed activity of rabbit PKM towards TFV is likely to be recapitulated with human PKM. However, this is less likely when considering human PKLR due to the 66% amino acid similarity between human PKM and human PKLR. Lastly, *in vitro* studies using purified enzymes show that guanylate kinase 1 (GUK1) can activate amdoxovir, a guanine analogue anti-HIV drug in phase II clinical studies, but its potential to activate TFV is unknown [12]. The primary limitation of these in vitro studies is that they do not account for the presence of other potentially competing nucleotide kinases or the presence of enzyme expression and activity within the cells of clinical relevance.

Crystal structures and docking studies endeavored to provide explanation for the observed activity towards TFV [10, 11]. Co-crystallization and docking of TFV-MP with NDPK from the amoeba *dictyostelium discoideum* (60% sequence identity with human NDPK) showed that while TFV-MP binds in the natural substrate site, fewer Van der Waals and polar interactions are made as compared to the natural substrate. This may account for the significantly lower affinity of NDPK for TFV-MP versus ADP. Additionally, NDPK is known to act through a 3'-OH dependent mechanism, and since TFV-MP lacks this moiety, the near absence of NDPK activity towards TFV-MP appears supported. Co-crystallizations have not been carried out for the remaining enzymes. However, it is known that binding of the natural substrate ADP to rabbit CKM results in quenching of the protein's intrinsic tryptophan fluorescence. Similar studies carried out on human CKM show that there is 5-fold less fluorescence quenching upon TFV-MP binding as compared to ADP binding. Docking of TFV-MP to *Torpedo californicum* CK shows that a key interaction between W228 and the magnesium-substrate complex is missing. Overall, these data support the observed weaker binding of TFV-MP versus ADP to CK enzymes. Lastly, docking of TFV-DP into a crystal structure of rabbit PKM co-crystallized with ATP shows that many of the identified enzyme-substrate interactions are preserved, supporting the observed PK activity towards TFV-MP.

Transport proteins are also expected to impact intracellular concentrations of TFV and its metabolites [6]. Organic anion transport family 1 and 3 (OAT1, OAT3) have been shown to mediate the uptake of tenofovir when overexpressed in human cell lines [13, 14] and the prodrug of TFV interacts with the organic cation transporters (OCT) [15]. Multiple drug resistance-associated protein 4 (MRP4) mediates the efflux of tenofovir in

a human ovarian carcinoma cell lines [16, 17]. Additional members of the multiple drug resistance-associated protein family (MRP), p-glycoprotein (MDR1), breast cancer resistance protein (BCRP), and the equilibrative nucleoside transporters (ENT) have also been implicated in efflux of other nucleoside monophosphate analogues [18-20].

An understanding of the enzymes that modulate intracellular concentrations of TFV-DP is necessary for optimal use of the drugs in treating and preventing HBV and HIV infection. Knowledge of which enzymes activate the drugs in which tissues enables better modeling of the activity of TFV and may help to explain the clinical observation that TFV-DP is found in greater concentrations in colorectal than in vaginal tissues [21]. With this in mind, we aimed to determine whether each of the candidate nucleotide kinases are expressed in the tissues of relevance and use these data to examine which kinases are responsible for the activation of NRTIs in whole cell systems. Transport enzyme expression was also investigated in PBMCs, colon tissue, and vaginal tissue. PBMCs, colon tissue, vaginal tissue, and liver protein lysates were obtained from healthy human donors and probed via immunoblotting for protein expression to show that AK2, CKB, CKM, CKMT1, and CKMT2 are expressed in greater amounts in colon tissues versus vagina tissues and ENT1 and BCRP are expressed in colon and vagina tissues, but not in PBMCs. A direct liquid chromatography mass spectrometry assay was developed to simultaneously detect TFV, TFV-MP, and TFV-DP, was used with siRNA knockdowns to determine which kinases are responsible for TFV phosphorylation in whole cell systems. We show that, in PBMCs and vaginal tissues, AK2 and the two PKs are responsible for TFV activation, whereas colorectal tissue phosphorylation of TFV depend on AK2 and CKM.

Materials and Methods

Materials

Bovine serum albumin (BSA), NH_4Cl and $NaHCO_3$ were obtained from Sigma-Aldrich (St Louis, MO). Phosphate buffered saline (PBS) and ethylenediaminetetraacetic acid (EDTA) were obtained from Life Technologies (Carlsbad, CA). Molecular Biology Grade Water, Nuclease and Endotoxin Free, was purchased from Quality Biological, Inc. (Gaithersburg, MD). TFV was provided through the NIH AIDS Reagent Program (Germantown, MD), TFV-13C and TFV-MP were purchased from Moravek Biochemicals (Brea, CA) and TFV-DP was purchased from Toronto Research Chemical (Toronto, Ontario, Canada). Optima liquid chromatography/mass spectrometry grade water, acetonitrile, acetic acid, and ammonium hydroxide and high performance liquid chromatography grade ammonium acetate were purchased from Thermo Fisher Scientific (Waltham, MA).

Isolation of RNA from PBMCs

Healthy subjects were recruited for blood donation after providing written informed consent for participation in a protocol approved by the institutional review board of Johns Hopkins Medical Institutions. Whole blood was collected and subjected to PBMC isolation via Ficoll-Paque (GE Healthcare, Pittsburgh, PA), following the manufacturer's instructions. Cells were them immersed in TRIzol® (Life Technologies) and the RNA isolated following the manufacturer's instructions. RNA was quantitated spectrophotometrically.

Quantitative reverse transcriptase PCR (qRT-PCR) analysis

Total RNA from the descending colon and vagina were purchased from Biochain (Newark, CA). From each RNA sample, 2 μg was used to synthesize cDNA using a Maxima First-Strand cDNA Synthesis Kit (Thermo Fisher Scientific) for use in qRT-PCR. A standard curve was generated using glyceraldehyde-3-phosphate dehydrogenase (GAPDH) PCR products cloned into pJET1.2/blunt cloning vectors (Thermo Fisher Scientific). Primers used are presented in Table 1. qRT-PCR was run using Maxima SYBR Green qPCR Master Mix (Thermo Fisher Scientific), with the following thermal cycling conditions: 95 °C for 10 min, followed by 40 cycles of 95 °C for 15 s, 60 °C for 30 s, and 72 °C for 30 s. GAPDH was used for normalization of mRNA levels. Statistical analysis was carried out using two-tailed unpaired t-tests, and $p \leq 0.05$ was considered significant. Significance was denoted as follows: *, $p \leq 0.05$; **, $p \leq 0.01$; ***, $p \leq 0.001$.

Mucosal tissue samples

Healthy subjects were recruited for tissue donation after providing written informed consent for participation in a protocol approved by the institutional review board of Johns Hopkins Medical Institutions. Each colorectal tissue donor provided 30 biopsies (approximately 25 mg each) and each vaginal donor provided 5 biopsies (approximately 25 mg each). Donors are denoted by 1, 2, and 3; colon 3 and vagina 3 were obtained from the same individual. These same subjects were used in a previously published study [22]. Upon collection, biopsies were placed into RPMI 1640 medium (Corning Inc, Corning, NY) supplemented with 10% heat inactivated fetal bovine serum, penicillin-streptomycin, and L-glutamine and stored on ice for transport. Biopsies were washed

Table 1:

Primer	Accession Number	Role	Primers (5'→3')	Coordinates
GAPDH	NM_002046.3	Forward	CTTCTTTTGCGTCGCCAGCCGA	62-83
		Reverse	CACGACGTACTCAGCGCCAGC	390-370
NDPKA	NM_198175.1	Forward	AAACCTAAGCAGCTGGAAGGG	85-105
		Reverse	AGTTGGCCATGGTTCCTGTAT	318-338
AK2	NM_001625.3	Forward	GATGCTGGGAAACTGGTGAGT	288-308
		Reverse	GCCTGTCCTATCATTCCCACC	869-849
AK7	NM_152327.3	Forward	TTGGATTCCTACAGCAGCGG	117-136
		Reverse	TCAGAATCCTCGGGGTCCAG	553-534
GUK1	NM_001242840.1	Forward	GCCGACATGGAGAGCAGAAAT	598-618
		Reverse	CCCTGGGTCCAGAGTGAGAG	860-841
CKB	NM_001823.4	Forward	GGCCTCACCCAGATTGAAACTC	872-893
		Reverse	ACTGCCCAGGCAATAAGTTAGG	1309-1288
CKM	NM_001824.4	Forward	TTGACGTGTCCAACGCTGATC	1176-1196

		Reverse	TCAATGGACTGGCCTTTCTCC	1296-1276
CKMT1	NM_001015001.1	Forward	GGCCTCAAAGAGGTGGAGAG	1257-1276
		Reverse	GCTGGCGATGGGGAGTTAAT	1661-1642
CKMT2	NM_001825.2	Forward	CACACTAAACGGGTTGGGGA	90-109
		Reverse	GTCTGGGTAGTCTGCGCTTG	410-391
PKM	NM_002654.4	Forward	CAGAGGCTGCCATCTACCAC	1438-1457
		Reverse	CCAGACTTGGTGAGGACGAT	1588-1569
PKLR	NM_181871.3	Forward	CTGGTGATTGTGGTGACAGG	1690-1709
		Reverse	TGGGCTGGAGAACGTAGACT	1839-1820
OAT1	NM_001145946.1	Forward	TGTGGCCTTAAACTTGCAGC	86-105
		Reverse	CAAGGCACACAAGAACACCTTT	502-481
OAT3	NM_004254.3	Forward	CTTCCTATCATCCTGGTGGAC	889-909
		Reverse	TAGAGGAAGAGGCAGCTGAAG	1417-1437
MDR1	NM_000927.4	Forward	CATTCAGTCAATCCGGGCCGGG	234-255
		Reverse	TCCATTCCGACCTCGCGCTCCTT	498-476

MRP1	NM_004996.3	Forward	AACCTCAGTGTCGGGCAGCG	4460-4479
		Reverse	CTGGGGCTCACACCAAGCCG	4778-4759
MRP3	NM_003786.3	Forward	TTCCTCTGGCAGAACCTAGGTCCCT	1407-1431
		Reverse	GACACAAAGGCCTTCTCGGCGTC	1792-1770
MRP4	NM_005845.3	Forward	TCTCTGTGGCTGTGGCCGTGAT	2680-2701
		Reverse	AACCTGCCCGGCATCCAGAGTTTT	3056-3033
MRP5	NM_005688.2	Forward	TCGTGCGGTCTTGGTCGCTTG	854-874
		Reverse	AGCCGTGATGCAAACATCATTGCTG	1181-1157
MRP8	NM_032583.3	Forward	GCTGAAAGAATTGGCAGGAACT	39-60
		Reverse	ATGCCCAGAAGTGCATCGAA	557-576
ENT1	NM_001078174.1	Forward	ACTCCAAAGTCTCAGCAGCAGGCC	261-284
		Reverse	AGAGTTCCGCTCAGGCAAGGGT	557-536
ENT2	NM_001532.2	Forward	CGCATTCTGGGCAGCCTGCT	521-540
		Reverse	CACGCCACTGGCCATGGACA	787-768
BCRP	NM_004827.2	Forward	TGGCTGTCATGGCTTCAGTA	2183-2202

		Reverse	GCCACGTGATTCTTCCACAA	2388-2369
OCT1	NM_003057.2	Forward	ACGGTGGCGATCATGTACC	808-826
		Reverse	CCCATTCTTTTGAGCGATGTGG	1035-1014
OCT2	NM_003058.3	Forward	AGACAGTGTAGGCGCTACGA	433-452
		Reverse	GTTAAACTCGGTGACGATGGAC	594-573

Table 1. Primers used in qRT-PCR for nucleotide kinases and transporters.

twice in 500 µL PBS and homogenized on ice in cell lysis buffer (Cell Signaling Technology, Danvers, MA) containing Halt Protease + Phosphatase Inhibitor Cocktail (Thermo Fisher Scientific) and 1 mM phenylmethanesulfonylfluoride (Sigma-Aldrich) using disposable pellet mixer pestles attached to a pestle motor (VWR International, Radnor, PA).

Separation of $CD4^+$ and $CD4^-$ populations from total PBMCs and lysis

LeukoMAX™ Source Leukopaks were obtained from Bioreclamation (Westbury, NY) and subjected to several rounds of red blood cell lysis. To prepare the red blood cell lysis buffer, NH_4Cl (0.35 g) and $NaHCO_3$ (0.0036 g) were dissolved in 50 mL Molecular Biology Grade Water and the solution filtered through 0.22 µm Steriflip-GV filter units (Millipore, Billerica, MA). Cells were suspended in the lysis solution, incubated at room temperature for 10 min, then collected via centrifugation for 5 min at 400 g, 4 °C. If the resulting pellet was not white, the cells were resuspended in a fresh batch of lysis solution and the incubation and collection repeated. After the final collection, cells were washed twice with PBS and resuspended in cold MACS™ buffer (PBS with 0.5% BSA and 2 mM EDTA). The $CD4^+$ and $CD4^-$ populations were then separated using human anti-CD4 microbeads (Miltenyi Biotec, Auburn, CA) on a LS Column (Miltenyi Biotec) attached to a MidiMACS™ Separator (Miltenyi Biotec) following the manufacturer's instructions. Cells were washed twice with PBS and lysed on ice in cell lysis buffer (Cell Signaling Technology, Danvers, MA) containing Halt Protease + Phosphatase Inhibitor Cocktail (Thermo Fisher Scientific) and 1 mM phenylmethanesulfonylfluoride (Sigma-Aldrich). Samples were centrifuged for 10 min at 3000 g, 4 °C and the resulting supernatant was stored at -20 °C.

Primary human hepatocyte culture and lysis

Primary human hepatocytes with Matrigel overlay were obtained from Xenotech, LLC (Lenexa, Kansas). Donor was a 42 year old male, lot number 1168, and viability was 82.7%. Upon receipt of the hepatocytes, shipping medium was replaced with William's E medium (Life Technologies) containing 10% fetal bovine serum (Life Technologies), penicillin-streptomycin (Sigma-Aldrich), and L-Glutamine (Life Technologies). Hepatocytes were incubated overnight at 37 °C in a 5% CO_2 humidified environment then collected with a cell scraper (Corning Inc.), washed twice with PBS, and lysed as described above.

HepG2 cell culture

HepG2 cells were obtained from the American Type Culture Collection. Upon receipt, the cells were thawed at 37 °C and seeded into Minimum Essential Medium with L-Glutamine (Quality Biological) containing 10% fetal bovine serum (Life Technologies), penicillin-streptomycin (Sigma-Aldrich), and 1 mM sodium pyruvate (Sigma-Aldrich). Cells were grown at 37 °C in a 5% CO_2 humidified environment.

Immunoblotting

Human total PBMC protein lysate was purchased from Biochain and human liver tissue lysates were obtained from Abcam (Cambridge, MA). Protein concentrations were determined using a Pierce® BCA Protein Assay Kit (Thermo Scientific), following the manufacturer's instructions. For immunoblots, 10 µg of each sample were loaded onto 10% or 12% Mini-PROTEAN® TGX™ Precast Gels (Bio-Rad, Hercules, CA) for separation via SDS-polyacrylamide gel electrophoresis. Proteins were transferred onto 0.2 µm pore nitrocellulose membranes (Life Technologies) and blotted with

commercially available antibodies. Antibodies for BCRP, ENT1, NDPKA, AK2, GUK1, CKB, CKM, CKMT1, CKMT2, PKLR, and PKM were obtained from Thermo Fisher Scientific and antibody for AK7 was obtained from Sigma-Aldrich. Anti-β-actin was used for normalization and was obtained from Cell Signaling. Proteins were visualized using SuperSignal West Dura Chemiluminescent Substrate (Thermo Fisher Scientific) according to the manufacturer's protocol and imaged with a Carestream 4000R system. Blots were stripped with ReBlot Plus Strong Antibody Stripping Solution (Millipore), then blotted with different antibodies following confirmation of antibody stripping.

Targeting of nucleotide kinases using siRNA

Nucleotide kinases were knocked down in PBMC, vaginal tissue and colorectal tissue using siGENOME siRNA (Dharmacon, GE Healthcare Life Sciences) delivered via electroporation. PBMC and vaginal tissue were transfected with siRNA targeted to AK2, GUK, PKM and PKLR while siRNA targeted to AK2, GUK and CKM were delivered to colorectal tissue. PBMCs and tissues transfected with non-targeting siGENOME siRNA were used as controls. For transfection of PBMC a Neon™ Transfection System (Life Technologies) was used and the cells were prepared for transfection according to manufacturer instructions for the 100 μL tip transfection kit. Electroporation conditions for PBMC were as follows: pulse voltage 2100 v, pulse width 15 ms, 1 pulse, 1 x 106 cells and 500 nM siRNA. For tissue electroporation, vaginal and colorectal tissues were washed twice with serum-free DMEM followed by washing with OptiMEM (Life Technologies) a total of 5 mg of tissue was used for a single electroporation. The tissues were then electroporated in 0.4 cm cuvettes (Bio-Rad, Hercules, CA) using a Gene Pulser Xcell™ electroporater (Bio-Rad). A square waveform (500 V and 10 ms) and 500 nM of

siRNA was used. Following electroporation, tissues were cultured for 24 hr in DMEM supplemented with 10% FBS prior to homogenization for immunoblotting. To examine the impact of nucleotide kinase knockdowns on phosphorylation of TFV, TFV (10 μM) was added to the culture medium 24 hr (for vaginal and colorectal tissues) or 48 hr (for PBMC) after electroporation. Following 12 hr of incubation with TFV, the tissues and cells were harvested and homogenized in 70% methanol. The samples were then centrifuged for 10 min at 1,500 x g at 4ºC and the supernatant was dried under vacuum in preparation for analysis using ultra high performance liquid chromatography tandem mass spectrometry (uHPLC-MS/MS).

Ultra high performance liquid chromatography mass spectrometry (uHPLC-MS)

A uHPLC-MS assay was developed for the quantification of TFV, TFV-MP, and TFV-DP using a Dionex Ultimate 3000 uHPLC system coupled to a TSQ Vantage Triple Stage Quadrupole mass spectrometer (Thermo Fisher Scientific). For the weak anion exchange assay, compounds were separated using a BioBasic AX column (5 μm, 50 mm x 2.1 mm, Thermo Fisher Scientific) at a flow rate of 0.25 mL/min. Solvent A was 10 mM ammonium acetate in 30% acetonitrile in water, pH 6.0 and solvent B was 1 mM ammonium acetate in 30% acetonitrile in water, pH 10.5. The pH of solvents was adjusted using acetic acid and ammonium hydroxide. The gradient used is as follows: 10% B from 0.0 to 0.5 min, 50% B from 0.51 to 1.75 min, 100% B from 1.76 to 4.5 min, 10% B from 4.6 to 6.6 min. For the ion pairing assay, compounds were separated using a Hypersil GOLD-C18 column (3 μm, 100 mm x 1 mm, Thermo Fisher Scientific) at a flow rate of 0.05 mL/min. Solvent A was 2 mM ammonium phosphate (Thermo Fisher Scientific) and 3 mM hexylamine (Thermo Fisher Scientific) in water, pH 9.2, and

solvent B was acetonitrile. The pH of solvent A was adjusted using ammonium hydroxide. The gradient used is as follows: 9% B from 0-0.5 min, 9% B to 60% B from 0.5 to 15.5 min, 60% B to 9% B from 15.5-15.6 min, and held at 9% B until 29.6 min. In selected reaction monitoring mode, fragment ions were detected in positive ion mode using the following transitions (Q1→Q3): TFV (m/z 288 → 176); TFV-MP (m/z 3668 → 270); and TFV-DP (m/z 448 → 270). The sample tray was kept at 4 °C and solvents were refreshed weekly. Dried cell and tissue extracts were reconstituted in 100 μL mobile phase A for injection.

Statistical Analyses

All data presented are means ± S. E. from three independent experiments. Two-tailed unpaired *t* tests were performed to compare datasets, and $p \leq 0.05$ was considered significant. Significance was denoted as follows: *, $p \leq 0.05$; **, $p \leq 0.01$; ***, $p \leq 0.001$.

Results

Nucleotide Kinase and Transporter mRNA Expression in PBMCs, Colorectal Tissues, and Vaginal Tissues

It is yet unknown which nucleotide kinases are expressed in the tissues of relevance. We probed for mRNA expression of nucleotide kinases that may play a role in the activation of TFV in PBMCs, colorectal tissue, and vaginal tissue via qRT-PCR (Fig 1). The colorectal tissues showed higher mRNA levels of CKB as compared to both PBMCs (p-value = 0.014) and vaginal tissues (p-value = 0.006). On the contrary, vaginal tissue demonstrated higher mRNA levels of CKMT2 than colon tissue (p-value = 0.041).

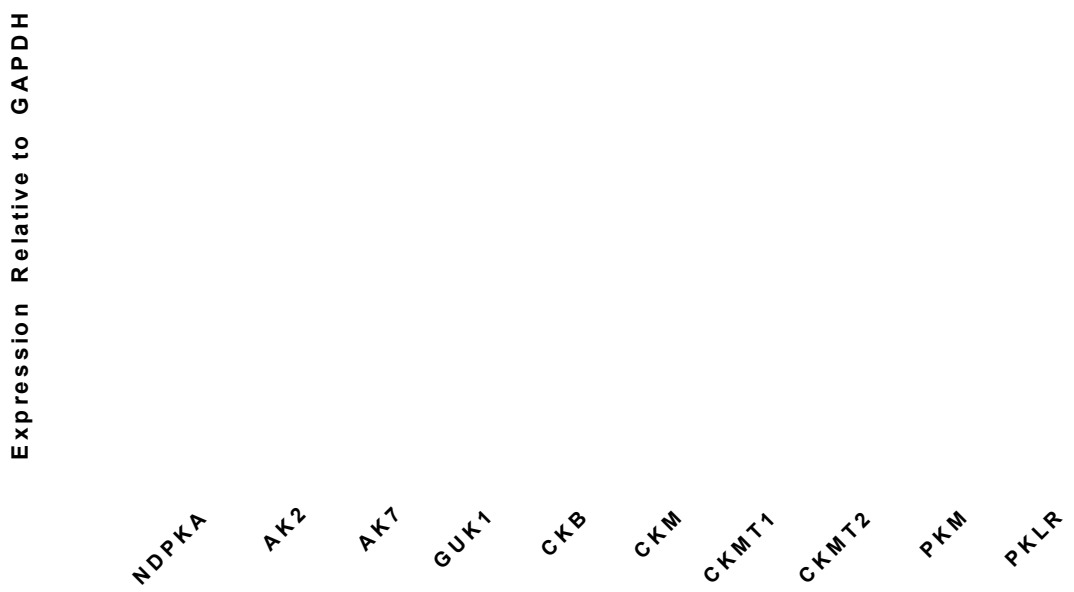

Figure 1. **Expression of nucleotide kinase mRNA in PBMCs, colorectal tissues, and vaginal tissues**. Quantification of mRNA expression levels of candidate nucleotide kinases using qRT-PCR in PBMCs, colorectal tissue, and vaginal tissue (n=3). Statistical analyses were performed via two-tailed unpaired student's t-tests to compare expression between all three tissue types; * = $p \leq 0.05$; ** = $p \leq 0.01$; *** = $p \leq 0.001$.

Figure 2. **Expression of transporter mRNA in PBMCs, colorectal tissues, and vaginal tissues**. Quantification of mRNA expression levels of transporters using qRT-PCR in PBMCs, colorectal tissue, and vaginal tissue (n=3). Statistical analyses were performed via two-tailed unpaired student's t-tests to compare expression between all three tissue types; * = $p \leq 0.05$; ** = $p \leq 0.01$; *** = $p \leq 0.001$.

Colorectal tissues also showed lower mRNA levels of PKM as compared to PBMCs (p-value = 0.038) and vaginal tissues (p-value = 0.002).

The expression of drug transport enzymes in these tissues has also not been thoroughly examined. We investigated mRNA expression of transporters that may participate in the influx or efflux of TFV in PBMCs, colorectal tissue, and vaginal tissue via qRT-PCR (Fig 2). Expression for OAT3 was not detected despite using primers validated in a previously published study [23]. Colorectal tissues exhibited higher mRNA levels of MRP3, MRP8, and OCT1 versus PBMCs (p-value = 0.032, 0.035, and 0.028 respectively) and vaginal tissues (p-value = 0.031, 0.034, and 0.012 respectively). The mRNA level of ENT2 was also higher in colorectal tissues than vaginal tissues (p-value = 0.044). Vaginal tissues displayed higher mRNA levels of MDR1 versus both PBMCs (p-value = 0.041) and colorectal tissues (p-value = 0.042) and higher mRNA levels of MRP5 and ENT1 versus PBMCs (p-value = 0.011 and 0.005, respectively).

Nucleotide Kinase and Transport Protein Expression in PBMCs, Colorectal Tissues, and Vaginal Tissues

Nucleotide kinase expression was also examined on the protein level via immunoblotting using cell lysates (Fig 3). Protein expression of NDPKA was not detected in any samples despite evidence of mRNA expression. Of the adenylate kinases, expression of AK2 was detected in all three tissues with greater expression in colorectal tissue than vaginal, and AK7 was detected only in colorectal tissue. The AK7 antibody also detected a band at approximately 90 kDa in vaginal tissue that did not match the molecular weight of AK7 (83 kDa). Meanwhile, protein expression of PKLR and PKM was detected in all three samples with greater expression in PBMCs and vaginal tissue than in colorectal. GUK1

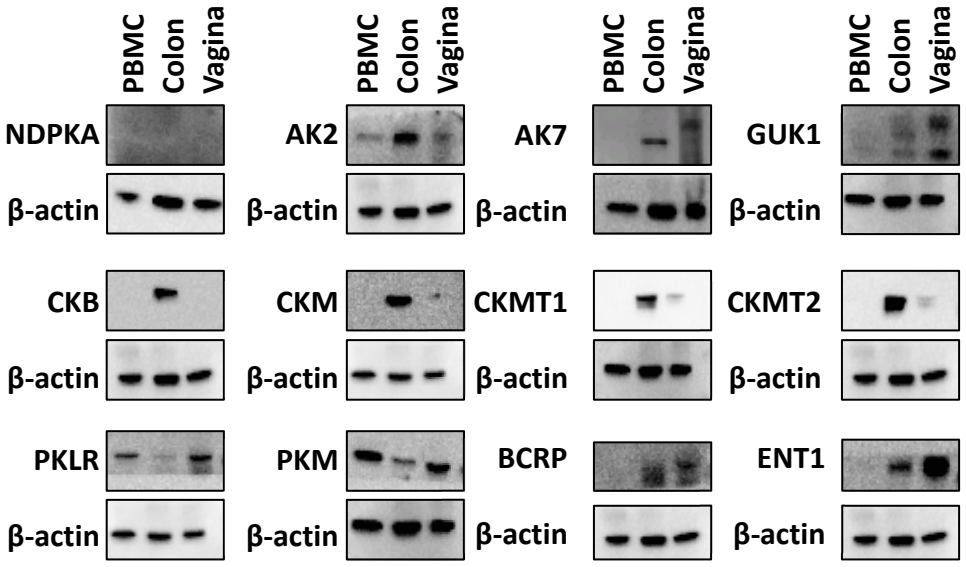

Figure 3. Protein expression of nucleotide kinases and transporters in PBMCs, colorectal tissues, and vaginal tissues. Immunoblots of nucleotide kinases in protein lysates isolated from PBMCs and colorectal and vaginal biopsies. After imaging, blots were stripped and re-probed with different antibodies.

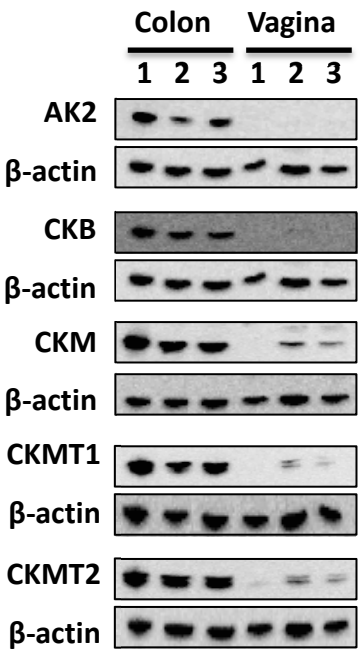

Figure 4. Immunoblots of nucleotide kinases in protein lysates isolated from colorectal tissue and vaginal tissue biopsies from multiple donors. Colon 3 and vagina 3 are from a single individual.

was detected most strongly in vaginal tissue, less strongly in colorectal tissue, and was undetected in PBMCs. The source of the multiple bands detected by the anti-GUK1 antibody is unknown as their migration does not match the expected migration from known splice variants of GUK1 [24]. Lastly, CKB, CKM, CKMT1, and CKMT2 all showed significantly higher protein expression in colorectal tissue over PBMCs and vaginal tissue. The greater expression of AK2, CKB, CKM, CKMT1, and CKMT2 in colorectal versus vaginal tissue was further confirmed through immunoblots using cell lysates from three individual colorectal and vaginal tissue donors (Fig 4). The markedly higher expression in colorectal versus vaginal tissue is consistent across multiple donors including the third colon and third vagina sample that are from the same individual.

The expression of transport proteins shown or proposed to demonstrate activity towards TFV was also examined in these tissues (Fig 3). Expression of equilibrative nucleoside transporter 1 and breast cancer resistance protein was observed in colorectal and vaginal tissues, with no expression detected in PBMCs. Other transporters that could not be detected in any of the three tissues were multiple drug resistance-associated proteins 1, 4, and 5, and organic anion transport protein 1.

Differences in Nucleotide Kinase Protein Expression between Circulating $CD4^+$ and $CD4^-$ Cells

While PBMCs are often used to study HIV drug anabolism, it is only the $CD4^+$ T cells that are susceptible to infection. However, potential differences in nucleotide kinase expression between the $CD4^+$ T cells and the $CD4^-$ expressing cells that are present in PBMC isolations are unknown. In order to explore these expression patterns, PBMCs were obtained from three individual donors, the $CD4^+$ population and $CD4^-$ populations

were separated and lysed, and nucleotide kinase expression examined via immunoblotting (Fig 5). Because only AK2, GUK1, PKLR, and PKM were previously detected in PBMCs (Fig 3), only these nucleotide kinases were examined here. All kinases were detected in both cell populations, but no consistent differences in expression levels were evident. However, two bands are detected in $CD4^+$ cells when immunoblotting for GUK1, whereas only one is detected in the $CD4^-$ population (Fig 5). The migration and separation of the two GUK1 bands seen in $CD4^+$ cells match those observed in the previously screened colon tissue.

Expression of Nucleotide Kinase Protein in Liver Tissues, Hep-G2 Cells, and Primary Human Hepatocytes

Next, we examined the expression of kinases that may activate TFV in the liver via immunoblotting of liver tissue lysates (Fig 6A). Protein expression of AK2, GUK1, PKLR, PKM, and CKM is detected in all 3 human liver lysates. Expression was also compared between primary human hepatocytes and the HepG2 hepatocellular carcinoma cell line in order to assess the feasibility of using HepG2 as a model in subsequent studies (Fig 6B). AK2, GUK1, PKLR, and PKM are highly expressed in HepG2 cells. The CKM antibody detects two proteins in HepG2 cells that migrate faster and slower than the CKM protein detected in human hepatocytes.

A uHPLC-MS Assay to Simultaneously Detect TFV, TFV-MP, and TFV-DP

Further studies to determine which nucleotide kinases exhibit activity towards TFV intracellularly require an assay that quantitates TFV, TFV-MP, and TFV-DP, thus an uHPLC-MS assay was developed using weak anion exchange. While the chromatography column and buffers are similar to a previously published assay [25], the elution gradient

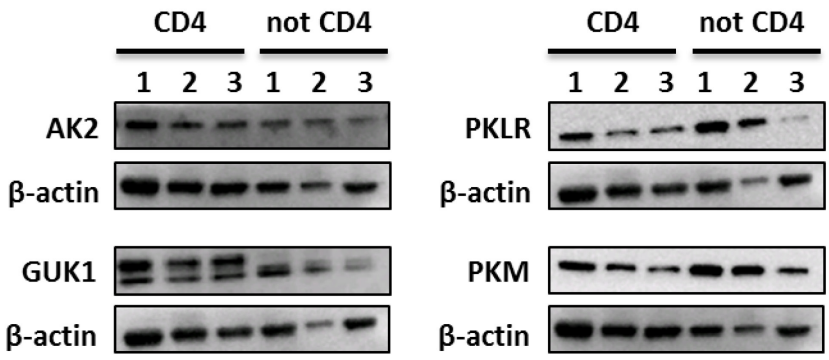

Figure 5. Protein expression of nucleotide kinases in $CD4^+$ cells and $CD4^-$ cells in total PBMC population. PBMCs were obtained from healthy donors and the $CD4^+$ and $CD4^-$ cell populations were isolated via magnetic separation. Protein lysates were then obtained and immunoblotted to probe for nucleotide kinase expression. Individual donors are indicated by 1, 2, and 3.

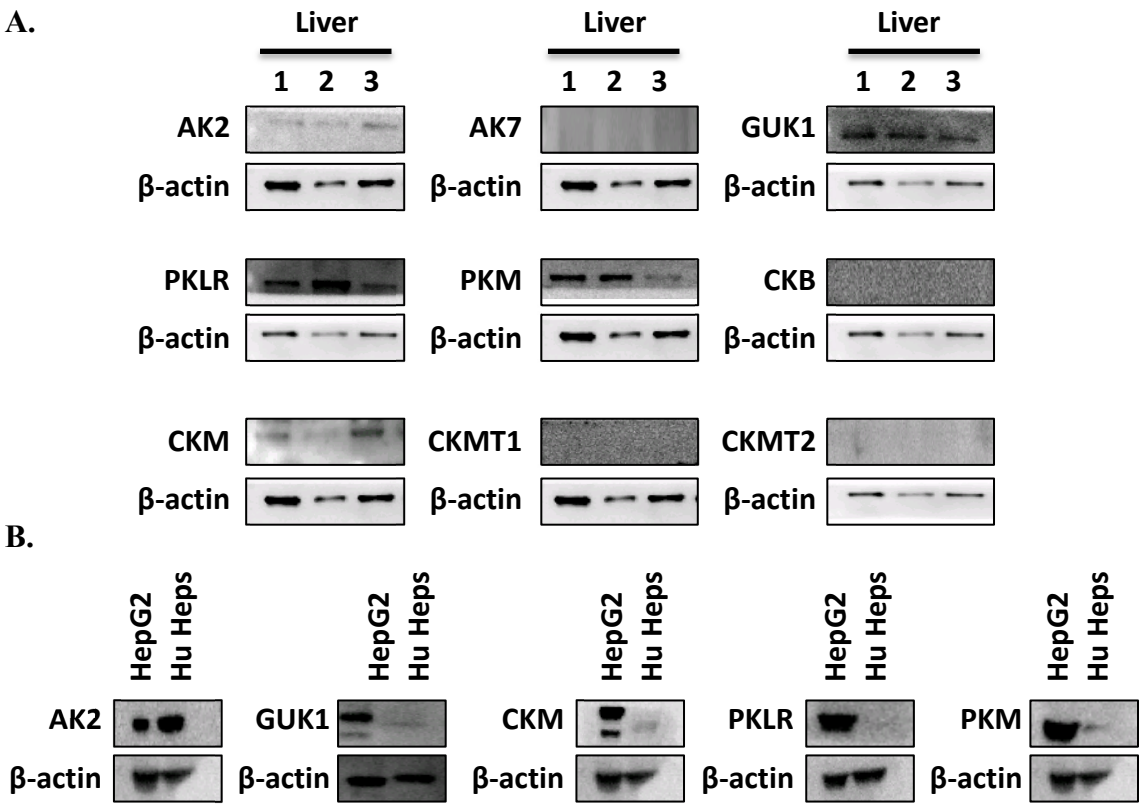

Figure 6. Protein expression of nucleotide kinases in human liver tissue, primary human hepatocytes, and HepG2 cells. A. Immunoblots of nucleotide kinases in human liver tissue lysates. Individual donors are indicated by L1, L2, and L3. B. Immunoblots comparing expression of nucleotide kinases between primary human hepatocytes and HepG2 cells.

and mass spectrometer settings are novel. Samples of each analyte were commercially obtained and detected using the following mass transitions: TFV (*m/z* = 288 → 176), TFV-MP (*m/z* = 368 → 270), and TFV-DP (*m/z* = 488→270) (Fig. 7). It was noted that when injecting pure TFV-MP, ions were detected in the chromatogram of TFV at the retention time of TFV-MP, and similarly when injecting TFV-DP, ions were detected in the chromatograms of TFV and TFV-MP at the retention time of TFV-DP. Because this in source fragmentation presents a barrier to quantitation, various aspects of the mass spectrometer settings were further optimized subsequent to instrument tuning. Decreasing neither the spray voltage nor the vaporizer temperature had a significant effect, but decreasing the capillary temperature to 150 °C resulted in minimal in source fragmentation. TFV-MP was detected as low as 100 fmol while TFV and TFV-DP were detected as low as 10 fmol. TFV-MP and TFV-DP only displayed in source fragmentation at 1 pmol.

Unfortunately, the weak anion exchange chromatography displayed poor day to day reproducibility in terms of peak shape, retention times, and compound separation. The uHPLC-MS assay was redeveloped with ion pairing chromatography, using the column, solvents, and elution gradient of a previously published assay [26]. The mass spectrometry conditions with the decreased capillary temperature of 150 °C were used with the published chromatography column, buffers, and elution gradient.

Activation of TFV in PBMCs, Colorectal Tissues, and Vaginal Tissues

Leveraging the above expression data, we predicted that in PBMCs, colorectal tissues, and vaginal tissues, AK2 and GUK1 could be responsible for the first phosphorylation step of TFV. In PBMCs and vaginal tissues, PKM and PKLR could be responsible for the

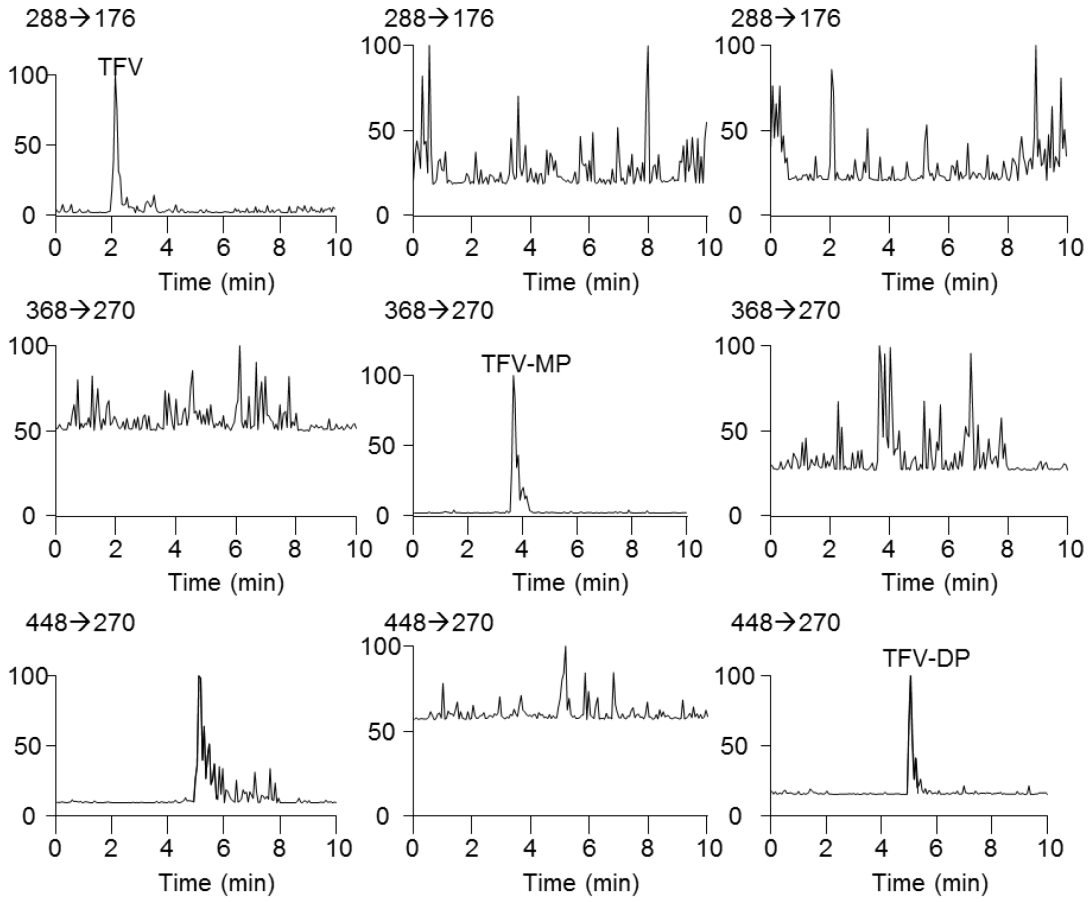

Figure 7. Lower limits of detection for TFV, TFV-MP, TFV-DP in the weak anion exchange uHPLC-MS assay. Injections of TFV (10 fmol), TFV-MP (100 fmol), and TFV-DP (10 fmol) are displayed from left to right. The following transitions are used (Q1→Q3): TFV (m/z 288→176), TFV-MP (368→270), and TFV-DP (448→270).

second phosphorylation step, and in colorectal tissues any of the CKs could perform this step. We sought to confirm this by using targeted siRNA to knock down the protein expression of the predicted kinases in each cell or tissue type. Detection of kinase expression via immunoblot showed that expression of all targeted kinases was decreased when compared to the non-targeting siRNA control (Fig 8A). Following incubation of the siRNA treated cells and tissues with TFV, the intracellular metabolites were extracted and detected using the ion pairing uHPLC-MS/MS assay (Fig 8B). When AK2 was knocked down, production of TFV-MP decreased to 17 ± 1.4%, 9.5 ± 1.1%, and 12 ± 1.5% (p-value = 3.4E-6, 3.6E-5, and 7.2E-5) of the non-targeting siRNA control in PBMCs, colorectal tissues, and vaginal tissues,

respectively. The decrease in AK2 expression also resulted in decrease of TFV-DP production to 13 ± 1.7%, 15 ± 2.3%, and 9 ± 2.2% (p-value = 3.9E-6, 4.5E-6, and 2.7E-5) of the non-targeting siRNA control in PBMCs, colorectal tissues, and vaginal tissues, respectively. Knockdown of PKM decreased TFV-DP production to 33 ± 5.8% and 27 ± 4.3% (p-value = 2.7E-5 and 8.2E-5) and knockdown of PKLR decreased TFV-DP production to 78 ± 6.6% and 81 ± 7.4% (p-value = 0.008 and 0.017) of the non-targeting control in PBMCs and vaginal tissues, respectively. When CKM was knocked down in colorectal tissues, production of TFV-DP was decreased to 8 ± 2.9% (p-value = 2.2E-5) of the non-targeting control.

Discussion

This study shows for the first time which nucleotide kinases are able to perform the phosphorylation steps required to activate TFV in PBMCs, colorectal tissues, and vaginal

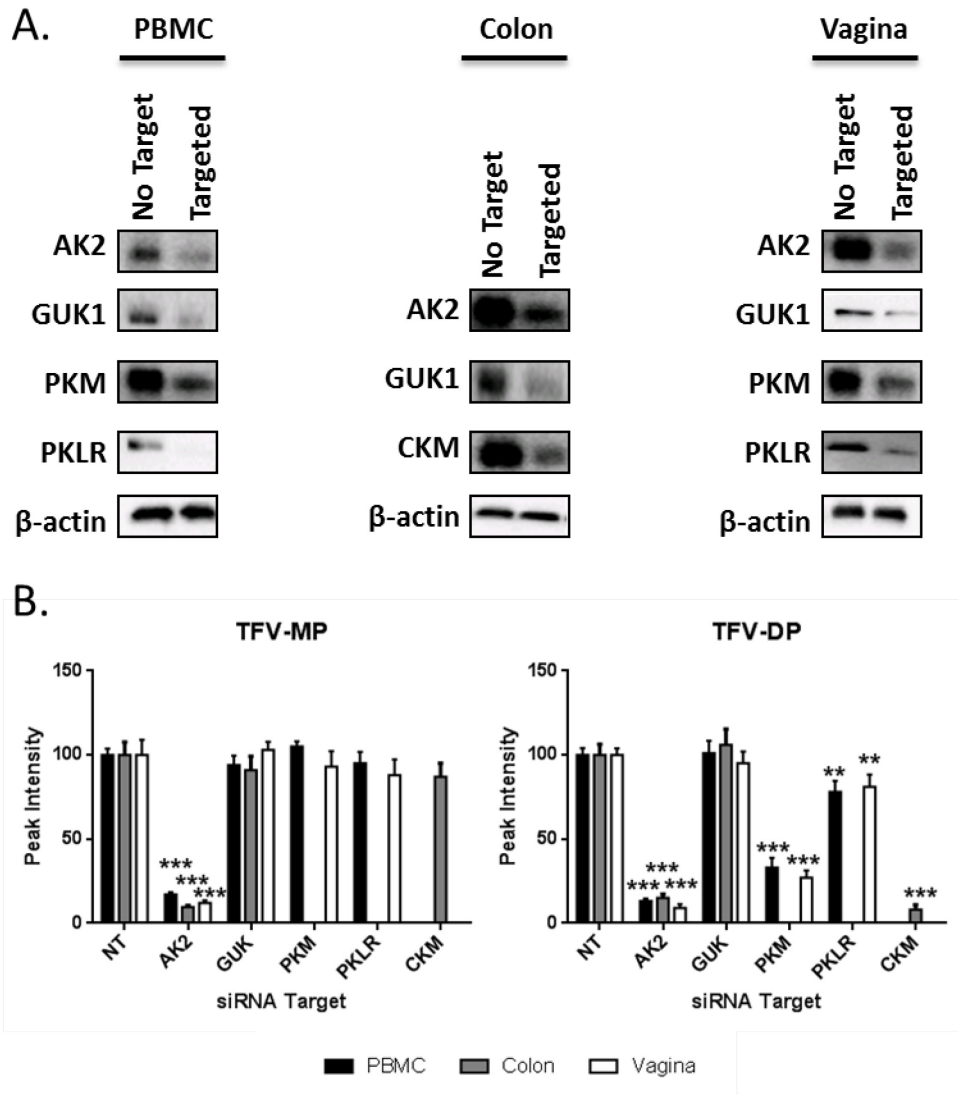

Figure 8. Knockdown of nucleotide kinases in PBMCs, colorectal tissues, and vaginal tissues, and effects on TFV metabolism. A. PBMCs, colorectal tissues, and vaginal tissues were electroporated with non-targeting siRNA or siRNA targeting nucleotide kinases. Representative immunoblots showing the extent of protein expression decrease are shown. B. SiRNA treated PBMCs, colorectal tissues, and vaginal tissues (n = 3) were incubated with 10 μM TFV for 12 hours. Intracellular metabolites were extracted and TFV-MP and TFV-DP were detected using the ion pairing uHPLC-MS/MS

assay. Statistical analyses were performed via two-tailed unpaired student's t-tests to compare metabolite production between non-targeted and targeted siRNA conditions; * = $p \leq 0.05$; ** = $p \leq 0.01$; *** = $p \leq 0.001$.

tissues. It also examines the expression patterns of candidate nucleotide kinases in tissue of interest, enabling a detailed understanding of how TFV can be activated in PBMCs, circulating $CD4^+$ cells, colon tissue, vagina tissue, and liver tissue. The expression differences observed between various tissue types may have implications on the efficacy of HIV treatment and prevention, but the small number of samples employed is a potential limitation. Nevertheless, these data lay the groundwork for future studies to gain a comprehensive understanding of NRTI activation in these tissues and leverage this knowledge to optimize the use of antiretroviral drugs.

Previous studies showing that CKs and PKs exhibit activity towards TFV-MP were carried out *in vitro* and the study identifying AK2 as the enzyme responsible for phosphorylating TFV reached its conclusions through elimination of AK1 and AK3. Lastly, GUK1 has never been examined for activity towards TFV. Here we leverage targeted siRNAs to specifically knockdown AK2 and GUK1 in PBMCs, colorectal tissues, and vaginal tissues, PKM and PKLR in PBMCs and vaginal tissues, and CKM in colorectal tissues. Subsequent incubations with TFV revealed that AK2 is responsible for the first phosphorylation step of TFV in PBMCs, vaginal tissues, and colorectal tissues. The second phosphorylation step is carried out primarily by PKM and by PKLR to a lesser extent in PBMCs and vaginal tissues. In colorectal tissues, CKM is responsible for the majority of the second phosphorylation step. Although the potential contribution of CKB, CKMT1, CKMT2, PKM, and PKLR was not examined in colorectal tissues, it is clear that their combined contributions to the second phosphorylation step are less than that of CKM.

It was observed that AK2, CKB, CKM, CKMT1, and CKMT2 are expressed at higher levels in colorectal tissue than in PBMCs and vaginal tissue. In the PBMCs and vaginal tissues which have little to no creatine kinase expression, the second phosphorylation step of TFV may be carried out by pyruvate kinases. Additionally, the muscle and brain isoforms of creatine kinase were previously shown to catalyze the phosphorylation of TFV-MP with greater efficiency than pyruvate kinase [10]. Thus, the observation that TFV-DP is found in much greater quantities in colorectal tissues over vaginal tissues after a single oral dose [21, 27] could be explained by the higher expression levels of enzymes capable of phosphorylating TFV in the colon mucosa, the greater efficiency of creatine kinases, or both. Further possibilities include differential distribution of TFV to the colon and vagina, or different absorption rates. However, when an individual is exposed to HIV through the mucosal tissues, the virus will specifically target the $CD4^+$ cells within the tissues [28]. These tissue specific $CD4^+$ cells should have the same TFV activation pathway as systemic $CD4^+$ cells, so it is not clear how increased TFV-DP levels in the surrounding colon tissue provide a higher barrier to HIV infection. Nevertheless, clinical trials support the existence of a colon advantage for prevention of HIV infection using TFV. Adherence to the drug regimen was found to be low in trials testing transmission of HIV infection in both the homosexual male population (iPrEx), who are vulnerable to infection via the colon, and to the heterosexual female population (FEM-PrEP, VOICE), who are primarily vulnerable to infection via the vagina [29-31]. Yet, the iPrEx trial showed a 44% reduction in HIV infectivity whereas FEM-PrEP and VOICE could not demonstrate similar protection. Further work may help to elucidate the

mechanism behind this colon advantage and determine whether the differential activation of TFV between the colon and vagina plays a significant role.

The most striking difference between $CD4^+$ cells and $CD4^-$ cells in the total PBMC population was the presence of two bands in $CD4^+$ cells when probing for GUK1. The ability of GUK1 to phosphorylate TFV has not been examined, though the detection of GUK1 expression in PBMCs and $CD4^+$ cells shows that GUK1 may be one of the factors that determine intracellular concentrations of amdoxovir in these cells. Otherwise, there are few differences between expression levels of AK2, PKLR, and PKM in $CD4^+$ cells and $CD4^-$ cells.

Understanding which enzymes are responsible for the activation of these drugs in which tissues sets the groundwork for a pharmacogenomically-sensitive approach to understanding HIV and HBV treatment. Single nucleotide polymorphisms and other mutations that cause decreased enzyme function or expression have been identified for AK2 [32], PKLR [33], and CKB [34] and correlated to human disorders. Patients with one of these mutations may not efficiently activate NRTIs in the targeted cell types, and thus treatment with these drugs would not only be unsuccessful, but may also facilitate the spread of drug resistant virions or result in other undesirable side effects. There is clear precedent for using genetic information for selection (or avoidance) of certain drugs for which an individual patient has an increased sensitivity on a genetic basis. For example, it is standard practice to genotype patients for HLA-B*5701 before prescribing an abacavir containing regimen, and there is ongoing work studying the association of TFV induced renal toxicity with SNPs in drug transport proteins [35].

In contrast to the data presented here showing that the efflux proteins MRP1, MRP3, and MRP4 could not be detected in PBMCs, a previous study showed using the known substrate carobxy-2',7'-dichlorofluorescein that MRP is active in these cells [36, 37]. MDR1 activity was also demonstrated in PBMCs via a rhodamine 123 efflux assay, corroborating the findings of MDR1 mRNA expression in PBMCs in this study and mRNA expression and activity in a separate study [37]. Expression of BCRP on the mRNA level was also shown in PBMCs, which is in line with the present findings although we did not detect BCRP on the protein level [37]. To our knowledge, no work has been done examining the expression of OAT1, OAT3, ENT1, OCT1, and OCT2 in PBMCs on the mRNA or protein level, nor on BCRP at the protein level. Colorectal tissues have been shown to express MDR1, MRP1/3/4/5, BCRP, and OCT1 on the mRNA level, with no evidence of OCT2, OAT1, and OAT3 [38]. Protein expression of MRP4 and OAT1 has also been detected [39]. The current study was able to detect MRP4 and OAT1 mRNA in colorectal tissues; however, protein expression was not seen. Vaginal tissues have been shown to express MDR1, MRP1, MRP4, MRP7, BCRP, OAT1, and OAT3 on the mRNA level and MDR1 and MRP4 expression on the protein level [39, 40]. The mRNA expression data is corroborated in the present study whereas the protein expression data are not. Observed discrepancies in transporter expression between the present data and previously published studies are likely due to inter-individual variability; the present study is hampered by the limited number of donors. Nevertheless, while PBMCs, colorectal tissues, and vaginal tissues express various transporters capable of TFV efflux, potential TFV influx pathways are yet unclear. The

only transporters known to be capable TFV uptake, OAT1 and OAT3, have so far not been detected on the protein level in these cell/tissue types.

In summary, the present study demonstrates that AK2, PKM, and PKLR are responsible for activating TFV in PBMCs and vaginal tissues whereas AK2 and CKM are responsible for activating TFV in colorectal tissues. It also examines the protein expression of nucleotide kinases proposed to activate TFV in vitro in PBMCs, circulating $CD4^+$ cells, colon tissue, vagina tissue, and liver tissue and investigates expression of transporters predicted to mediate the influx or efflux of TFV. Protein activity and expression results from this study and previously published studies are summarized in Figure 9. We anticipate that these data can be leveraged in future studies to facilitate a rational in depth approach to optimal use of these drugs for treatment and prevention of HIV and HBV infection.

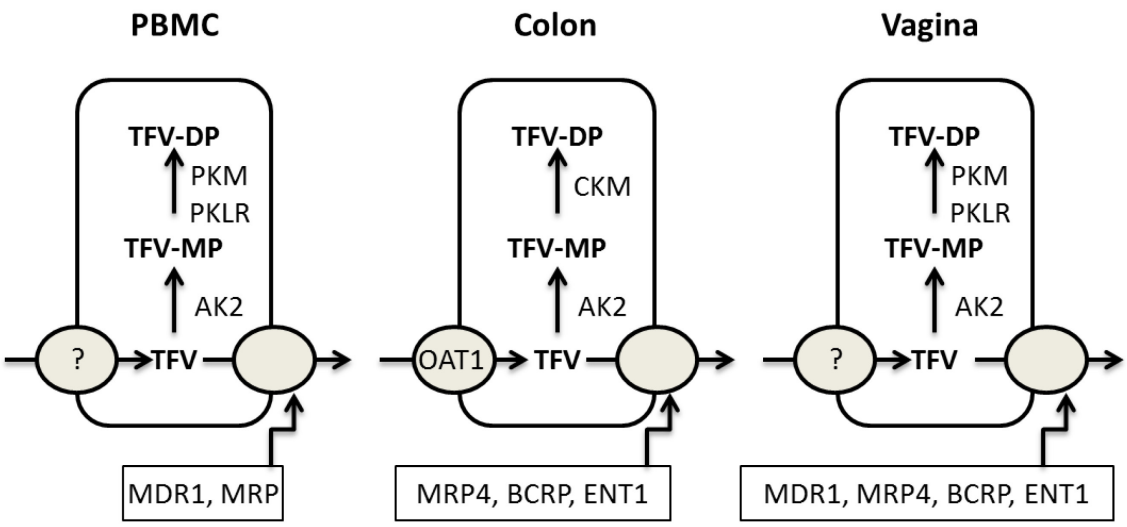

Figure 9. Proposed metabolism scheme of TFV in PBMCs, colorectal tissue, and vaginal tissue. Scheme is based off of protein expression and activity studies performed in both the current study and previously published studies.

References

1. Mendes-Correa M, Nunez M. Management of HIV and hepatitis virus coinfection. Expert Opin Pharmacother **2010**; 11:2497-516.

2. Cihlar T, Ray AS. Nucleoside and nucleotide HIV reverse transcriptase inhibitors: 25 years after zidovudine. Antiviral Res **2010**; 85:39-58.

3. Baeten J, Celum C. Systemic and topical drugs for the prevention of HIV infection: antiretroviral pre-exposure prophylaxis. Annu Rev Med **2013**; 64:219-32.

4. Anderson PL, Kakuda TN, Lichtenstein KA. The cellular pharmacology of nucleoside- and nucleotide-analogue reverse-transcriptase inhibitors and its relationship to clinical toxicities. Clin Infect Dis **2004**; 38:743-53.

5. Kearney BP, Flaherty JF, Shah J. Tenofovir disoproxil fumarate: clinical pharmacology and pharmacokinetics. Clin Pharmacokinet **2004**; 43:595-612.

6. Anderson PL, Kiser JJ, Gardner EM, et al. Pharmacological considerations for tenofovir and emtricitabine to prevent HIV infection. J Antimicrob Chemother **2011**; 66:240-50.

7. Delaney WEt, Ray AS, Yang H, et al. Intracellular metabolism and in vitro activity of tenofovir against hepatitis B virus. Antimicrob Agents Chemother **2006**; 50:2471-7.

8. Robbins BL, Srinivas RV, Kim C, et al. Anti-human immunodeficiency virus activity and cellular metabolism of a potential prodrug of the acyclic nucleoside phosphonate 9-R-(2-phosphonomethoxypropyl)adenine (PMPA), Bis(isopropyloxymethylcarbonyl)PMPA. Antimicrob Agents Chemother **1998**; 42:612-7.

9. Robbins BL, Greenhaw J, Connelly MC, et al. Metabolic pathways for activation of the antiviral agent 9-(2-phosphonylmethoxyethyl)adenine in human lymphoid cells. Antimicrob Agents Chemother **1995**; 39:2304-8.

10. Koch K, Chen Y, Feng JY, et al. Nucleoside diphosphate kinase and the activation of antiviral phosphonate analogs of nucleotides: binding mode and phosphorylation of tenofovir derivatives. Nucleosides Nucleotides Nucleic Acids **2009**; 28:776-92.

11. Varga A, Graczer E, Chaloin L, et al. Selectivity of kinases on the activation of tenofovir, an anti-HIV agent. Eur J Pharm Sci **2013**; 48:307-15.

12. Feng JY, Parker WB, Krajewski ML, et al. Anabolism of amdoxovir: phosphorylation of dioxolane guanosine and its 5'-phosphates by mammalian phosphotransferases. Biochem Pharmacol **2004**; 68:1879-88.

13. Cihlar T, Ho ES, Lin DC, et al. Human renal organic anion transporter 1 (hOAT1) and its role in the nephrotoxicity of antiviral nucleotide analogs. Nucleosides Nucleotides Nucleic Acids **2001**; 20:641-8.

14. Uwai Y, Ida H, Tsuji Y, et al. Renal transport of adefovir, cidofovir, and tenofovir by SLC22A family members (hOAT1, hOAT3, and hOCT2). Pharm Res **2007**; 24:811-5.

15. Minuesa G, Volk C, Molina-Arcas M, et al. Transport of lamivudine [(-)-beta-L-2',3'-dideoxy-3'-thiacytidine] and high-affinity interaction of nucleoside reverse transcriptase inhibitors with human organic cation transporters 1, 2, and 3. J Pharmacol Exp Ther **2009**; 329:252-61.

16. Ray AS, Cihlar T, Robinson KL, et al. Mechanism of active renal tubular efflux of tenofovir. Antimicrob Agents Chemother **2006**; 50:3297-304.

17. Imaoka T, Kusuhara H, Adachi M, et al. Functional involvement of multidrug resistance-associated protein 4 (MRP4/ABCC4) in the renal elimination of the antiviral drugs adefovir and tenofovir. Mol Pharmacol **2007**; 71:619-27.

18. Podgorska M, Kocbuch K, Pawelczyk T. Recent advances in studies on biochemical and structural properties of equilibrative and concentrative nucleoside transporters. Acta Biochim Pol **2005**; 52:749-58.

19. Koczor CA, Torres RA, Lewis W. The role of transporters in the toxicity of nucleoside and nucleotide analogs. Expert Opin Drug Metab Toxicol **2012**; 8:665-76.

20. de Wolf C, Jansen R, Yamaguchi H, et al. Contribution of the drug transporter ABCG2 (breast cancer resistance protein) to resistance against anticancer nucleosides. Mol Cancer Ther **2008**; 7:3092-102.

21. Louissaint NA, Cao YJ, Skipper PL, et al. Single dose pharmacokinetics of oral tenofovir in plasma, peripheral blood mononuclear cells, colonic tissue, and vaginal tissue. AIDS Res Hum Retroviruses **2013**; 29:1443-50.

22. To EE, Hendrix CW, Bumpus NN. Dissimilarities in the metabolism of antiretroviral drugs used in HIV pre-exposure prophylaxis in colon and vagina tissues. Biochem Pharmacol **2013**; 86:979-90.

23. Asif AR, Steffgen J, Metten M, et al. Presence of organic anion transporters 3 (OAT3) and 4 (OAT4) in human adrenocortical cells. Pflugers Arch **2005**; 450:88-95.

24. Update on activities at the Universal Protein Resource (UniProt) in 2013. Nucleic Acids Res **2013**; 41:D43-7.

25. Jansen RS, Rosing H, Kromdijk W, et al. Simultaneous quantification of emtricitabine and tenofovir nucleotides in peripheral blood mononuclear cells using weak

anion-exchange liquid chromatography coupled with tandem mass spectrometry. J Chromatogr B Analyt Technol Biomed Life Sci **2010**; 878:621-7.

26. Fromentin E, Gavegnano C, Obikhod A, et al. Simultaneous quantification of intracellular natural and antiretroviral nucleosides and nucleotides by liquid chromatography-tandem mass spectrometry. Anal Chem **2010**; 82:1982-9.

27. Patterson KB, Prince HA, Kraft E, et al. Penetration of tenofovir and emtricitabine in mucosal tissues: implications for prevention of HIV-1 transmission. Sci Transl Med **2011**; 3:112re4.

28. Haase AT. Perils at mucosal front lines for HIV and SIV and their hosts. Nat Rev Immunol **2005**; 5:783-92.

29. Van Damme L, Corneli A, Ahmed K, et al. Preexposure prophylaxis for HIV infection among African women. N Engl J Med **2012**; 367:411-22.

30. Grant RM, Lama JR, Anderson PL, et al. Preexposure chemoprophylaxis for HIV prevention in men who have sex with men. N Engl J Med **2010**; 363:2587-99.

31. Marrazzo J, Ramjee G, Nair G, et al. Pre-exposure prophylaxis for HIV in women: daily oral tenofovir, oral tenofovir/emtricitabine, or vaginal tenofovir gel in the VOICE study (MTN 003). In: 20th Conference on Retroviruses and Opportunistic Infections. (Atlanta).Abstract # 26LB.

32. Lagresle-Peyrou C, Six EM, Picard C, et al. Human adenylate kinase 2 deficiency causes a profound hematopoietic defect associated with sensorineural deafness. Nat Genet **2009**; 41:106-11.

33. Warang P, Kedar P, Ghosh K, et al. Molecular and clinical heterogeneity in pyruvate kinase deficiency in India. Blood Cells Mol Dis **2013**; 51:133-7.

34. Li C, Zhang Q, Hu WJ, et al. Effect of SNPs on creatine kinase structure and function: identifying potential molecular mechanisms for possible creatine kinase deficiency diseases. PLoS One **2012**; 7:e45949.

35. Tozzi V. Pharmacogenetics of antiretrovirals. Antiviral Res **2010**; 85:190-200.

36. Laupeze B, Amiot L, Payen L, et al. Multidrug resistance protein (MRP) activity in normal mature leukocytes and CD34-positive hematopoietic cells from peripheral blood. Life Sci **2001**; 68:1323-31.

37. Albermann N, Schmitz-Winnenthal FH, Z'Graggen K, et al. Expression of the drug transporters MDR1/ABCB1, MRP1/ABCC1, MRP2/ABCC2, BCRP/ABCG2, and PXR in peripheral blood mononuclear cells and their relationship with the expression in intestine and liver. Biochem Pharmacol **2005**; 70:949-58.

38. Hilgendorf C, Ahlin G, Seithel A, et al. Expression of thirty-six drug transporter genes in human intestine, liver, kidney, and organotypic cell lines. Drug Metab Dispos **2007**; 35:1333-40.

39. Nicol MR, Fedoriw Y, Mathews M, et al. Expression of six drug transporters in vaginal, cervical, and colorectal tissues: Implications for drug disposition in HIV prevention. J Clin Pharmacol **2013**.

40. Zhou T, Hu M, Cost M, et al. Short communication: expression of transporters and metabolizing enzymes in the female lower genital tract: implications for microbicide research. AIDS Res Hum Retroviruses **2013**; 29:1496-503.

Chapter 4: Final Conclusions

Drugs that are not given orally may never encounter the liver, which is the primary organ associated with drug metabolism. Antiretroviral drugs such as dapivirine and tenofovir are being developed for topical use in the colorectal and vaginal areas to prevent the establishment of HIV infection. As such, the metabolism of these drugs must be understood in these tissues to ensure optimal drug use. The studies presented here investigate the ability of the colorectal and vaginal tissue to metabolize these antiretrovirals, thus informing not only HIV PrEP, but also all further drugs that will be administered in these tissues.

Previous studies of P450 expression in the vaginal and colorectal areas were not comprehensive and sometimes looked only at mRNA levels without checking protein levels. Additionally, evidence of P450 activity has never been shown. In Chapter 1, the P450 and UGT mediated metabolism of dapivirine was determined by use of in vitro enzyme assays and uHPLC-MS. Armed with this knowledge, dapivirine was then used as a small molecule probe to investigate enzymatic activity in colorectal and vaginal tissues obtained from healthy human donors. Colorectal tissues were shown to produce both P450 and UGT mediated metabolites of dapivirine, whereas vaginal tissues only produced P450 mediated metabolites. This is the first direct evidence for such enzymatic activity in these tissues, and the first evidence that metabolism differs in the two areas. The lack of UGT activity also differentiates vaginal tissue metabolism from hepatic metabolism. Due to the difficulty of isolating microsomes from the limited colorectal tissue available from healthy donors, however, a direct comparison of relative metabolism activity between colorectal tissues and hepatocytes could not be performed.

The fact that not all of the P450 nor UGT mediated metabolites produced by human liver microsomes were produced by the colorectal biopsies may indicate lower metabolizing activity in the colorectal tissues, but there is nothing to normalize between the two systems.

The work in Chapter 2 also touched upon possible dapivirine mediated changes in the transcriptional regulation of CYP3A4. Because P450 induction or inhibition is the mechanism behind many drug-drug interactions, it is important to investigate potential drug dependent changes in P450 activity. Two other diarylpyrimidine drugs, etravirine and rilpivirine, were shown to induce CYP3A4 mRNA levels in a pregnane-X-receptor dependent manner [1, 2]. However, while etravirine and rilpivirine consistently induce CYP3A4 mRNA, dapivirine only does so in two out of three colorectal donors and in one out of three hepatocyte donors. The colorectal induction was shown in one donor to be PXR mediated by use of sulforaphane, a known PXR inhibitor. It is also interesting that etravirine and rilpivirine are orally bioavailable while dapivirine is not. Possible causes for these trends may be worth exploring, especially to discern whether the PXR dependent CYP3A4 induction and oral bioavailability of etravirine and rilpivirine may be related. One possibility may be the presence of two cyano groups in both etravirine and rilpivirine, but only one in dapivirine. Nevertheless, this work combined with the work done on etravirine and rilpivirine serve to establish the CYP3A enzymes as consistent metabolizers of diarylpyrimidine drugs.

Chapter 3 investigates the metabolism of tenofovir, a drug that not only is known to be activated through its metabolism, but is also known to be unaffected by P450s. Because tenofovir is administered in oral formulation for HIV and HBV treatment and

HIV PrEP, its metabolism must be understood in white blood cells and hepatocytes in addition to the colorectal and vaginal tissues. The active metabolite of tenofovir is tenofovir diphosphate, which is produced via two intracellular phosphorylation events by nucleotide kinases. While many candidate kinases have been proposed and examined via in vitro enzyme assays, the metabolism pathway for tenofovir in the various tissues is not well-defined. Expression profiling of candidate nucleotide kinases reveals that adenylate kinases and creatine kinases are expressed at much higher levels in colorectal tissues versus vaginal tissues and PBMCs whereas pyruvate kinases show the opposite trend. This is another example of differential drug metabolism in the colorectal and vaginal areas. Additionally, only expression of CKM, AK2, GUK1, PKM, and PKLR were detected in human liver tissues and primary human hepatocytes. This is further support for the difference in hepatic, colorectal, and vaginal drug metabolism. Interestingly, the nucleotide kinase expression in PBMCs seems to match that of vaginal tissues. The difference becomes evident upon examination of equilibrative nucleotide transporter 1 and breast cancer resistance protein expression, which are detected in colorectal and vaginal tissues but not in PBMCs.

A previously published ion pairing uHPLC-MS/MS assay was used, after minimizing in source fragmentation, to determine which nucleotide kinases responsible for activating TFV in PBMCs, colorectal tissues, and vaginal tissues. Data from expression profiling informed the rational knockdown of AK2 and GUK1 in all three cell/tissue types, PKM and PKLR in PBMCs and vaginal tissues, and CKM in colorectal tissues. Subsequent to siRNA treatment, the cell/tissue samples were incubated with TFV and intracellular metabolites detected via uHPLC-MS/MS. It was concluded that AK2

carries out the first phosphorylation step of TFV in all three cell/tissue types. In PBMCs and vaginal tissues PKM carries out the second step with PKLR contributing to a lesser extent, and CKM performs the majority of the second step in colorectal tissues. The previously published *in vitro* evidence that CKs are much more active towards TFV than PKs, combined with the present *in situ* data, provide a mechanistic explanation for the observed phenomenon that TFV-DP is produced in greater quantities in colorectal versus vaginal tissues.

Collectively, these data represent a fundamental shift in the current understanding of drug metabolism. Not only do the colorectal and vaginal tissues metabolize drugs, but metabolism also differs between the two. Administration of drugs, including contraceptives and spermicides, to these tissues must first take P450 and UGT activity into consideration. The differential activation of tenofovir in colorectal versus vaginal tissues informs the future use of tenofovir and other NRTIs in these areas. Understanding which kinases activate tenofovir in which tissues also lays the groundwork for pharmacogenetic analyses to examine inter-individual differences in NRTI activation, which can be leveraged to optimize drug use for HIV treatment and prevention.

References

1. Yanakakis LJ, Bumpus NN. Biotransformation of the antiretroviral drug etravirine: metabolite identification, reaction phenotyping, and characterization of autoinduction of cytochrome P450-dependent metabolism. Drug Metab Dispos **2012**; 40:803-14.

2. Lade JM, Avery LB, Bumpus NN. Human biotransformation of the nonnucleoside reverse transcriptase inhibitor rilpivirine and a cross-species metabolism comparison. Antimicrob Agents Chemother **2013**; 57:5067-79.

Elaine E. To

Johns Hopkins University

to.elaine.e@gmail.com

Education

Ph. D. in Pharmacology and Molecular Sciences 2010-2014

Johns Hopkins University, Baltimore, MD.

Advisor: Dr. Namandjé N. Bumpus

Dissertation title: Metabolism of Antiretroviral Drugs Used in HIV Pre-Exposure Prophylaxis.

Thesis committee: Dr. Namandjé N. Bumpus, Dr. Craig W. Hendrix, Dr. Robert F. Siliciano, Dr. Heng Zhu, Dr. Susan H. Eshleman.

B. S. in Biology, California Institute of Technology, Pasadena, CA. 2006-2010

Research Experience

Ph. D. Candidate, Johns Hopkins University, Baltimore, MD 2010-present

Project: Differences in biotransformation of antiretroviral drugs dapivirine and maraviroc in colorectal and vaginal tissues.

Detected and characterized 11 novel metabolites of dapivirine using a novel LC-MS/MS assay.

Provided first evidence of cytochrome P450 activity in colorectal and vaginal tissues, but UDP- glucuronosyltransferase activity only in colorectal tissues.

Project: Expression of nucleotide kinases proposed to activate the antiretroviral drug tenofovir in liver cells, white blood cells, and mucosal tissues.

Showed that adenylate kinase and creatine kinases have greater expression in colorectal tissues, whereas pyruvate kinases have greater expression in white blood cells and vaginal tissues.

Determined that adenylate kinase 2 and pyruvate kinases activate tenofovir in white blood cells and vaginal tissues, whereas adenylate kinase 2 and creatine kinase muscle activate tenofovir in colorectal tissues.

Undergraduate Researcher, California Institute of Technology, Pasadena, CA 2008-2009

Project: Screening and isolation of single chain variable fragments (scFvs) to target proteins implicated in neurodegenerative disorders.

Identified and cloned two novel scFvs targeting DISC1 and two scFvs targeting amyloid beta peptide.

Teaching Experience

Teaching Assistant, California Institute of Technology, Pasadena, CA 2009-2010

Neuroscience course for Young Engineering and Science Scholars

Synthesis and Analysis of Organic and Inorganic Compounds (winter and spring quarters)

Experimental Procedures of Synthetic Chemistry

The Biology and Biophysics of Viruses

Publications

To, E. E., Hendrix, C. W., Bumpus, N. N. "Dissimilarities in the metabolism of antiretroviral drugs used in HIV pre-exposure prophylaxis in colon and vagina tissues." *Biochem. Pharmacol.* 2013; 86: 979-990.

Honors and Awards

Best Abstract Competition invitee (American Society for Pharmacology and Experimental Therapeutics, Drug Metabolism Division) at Experimental Biology, April 2013.

Rose Hills Foundation Summer Undergraduate Research Fellowship, California Institute of Technology, 2009.

Rachel F. Gray Summer Undergraduate Research Fellowship, California Institute of Technology, 2008.

Conference Presentations

To, E. E. and Bumpus, N. N. "Mucosal Expression of the Cytochromes P450 (CYP) and Nucleotide Kinases Involved in the Biotransformation of Drugs used in Human Immunodeficiency Virus (HIV) Pre-exposure Prophylaxis (PrEP)." Poster presentation at ASPET/British Pharmacological Society Annual Meeting at Experimental Biology, 04/2013.

To, E. E., Khoshnan. A, and Patterson, P. H. "Generation of Intrabodies as Molecular Tools to Dissect the Function of Disrupted in Schizophrenia 1 (DISC1)." Oral presentation at California Institute of Technology Summer Seminar Day, 08/2009.

To, E. E., Khoshnan, A., and Patterson, P. H. "Isolation and Characterization of ScFvs that Bind to the Amyloid Beta Pyro Peptide." Oral presentation at California Institute of Technology SURF Seminar Day, 10/2008.

Professional Societies

American Society for Pharmacology and Experimental Therapeutics (ASPET) 2012-present

Leadership, Management, & Outreach Experience

Enrollment Coordinator & Divisional Leader, Incentive Mentoring Program, Baltimore, MD

2010-present

Streamlined enrollment procedures enabling over 700 new volunteers to commit to the organization and guided team leaders of 4 individual teams in accomplishing short and long term goals in tutoring and mentoring a high school student.

Guest Blogger, Scizzle, Atlanta, GA 2013-present

Contributed bimonthly blog posts summarizing scientific publications for a general audience.